



# ***ALADIN NEWSLETTER 28***



*January-July 2005*



Copyright: ©ALADIN 2005

Scientific Editor: Dominique GIARD

Web Master: Patricia POTTIER & J-D GRIL

Lay out & Linguistic Advisor: J-A MAZIEJEWSKI

This paper has only a very limited circulation and permission to quote from it should be obtained from CNRM/GMAP/ALADIN

## CONTENTS

<b>1.EDITORIAL</b> .....	<b>5</b>
1.1. <u>EVENTS</u> .....	5
1.2. <u>ANNOUNCEMENTS</u> .....	7
1.3. <u>ALADIN 2</u> .....	9
1.4. <u>GOSSIP</u> .....	15
<b>2.OPERATIONS</b> .....	<b>16</b>
2.1. <u>INTRODUCTION</u> .....	16
2.2. <u>Changes in the Operational Version of ARPEGE</u> .....	23
2.3. <u>AUSTRIA</u> .....	24
2.4. <u>BELGIUM</u> .....	24
2.5. <u>BULGARIA</u> .....	24
2.6. <u>CROATIA</u> .....	24
2.7. <u>CZECH REPUBLIC</u> .....	26
2.8. <u>FRANCE</u> .....	27
2.9. <u>HUNGARY</u> .....	28
2.10. <u>MOROCCO</u> .....	28
2.11. <u>POLAND</u> .....	29
2.12. <u>PORTUGAL</u> .....	29
2.13. <u>ROMANIA</u> .....	29
2.14. <u>SLOVAKIA</u> .....	30
2.15. <u>SLOVENIA</u> .....	32
2.16. <u>TUNISIA</u> .....	32
<b>3.RSEARCH &amp; DEVELOPMENTS</b> .....	<b>33</b>
3.1. <u>AUSTRIA</u> .....	33
3.2. <u>BELGIUM</u> .....	35
3.3. <u>BULGARIA</u> .....	35
3.4. <u>CROATIA</u> .....	35
3.5. <u>CZECH REPUBLIC</u> .....	36
3.6. <u>FRANCE</u> .....	37
3.7. <u>HUNGARY</u> .....	37
3.8. <u>MOROCCO</u> .....	38
3.9. <u>POLAND</u> .....	38
3.10. <u>PORTUGAL</u> .....	38
3.11. <u>ROMANIA</u> .....	38
3.12. <u>SLOVAKIA</u> .....	46
3.13. <u>SLOVENIA</u> .....	46
3.14. <u>TUNISIA</u> .....	47
3.15. <u>HIRLAM</u> .....	48
<b>4.ALADIN PhD Studies</b> .....	<b>49</b>
4.1. <u>Radi AJAJI : Incrementality deficiency in ARPEGE 4d-var assimilation scheme</u> .....	49
4.2. <u>Steluta ALEXANDRU : Scientific strategy for the implementation of a 3D-Var data assimilation scheme for a double-nested limited-area model</u> .....	49
4.3. <u>Margarida BELO-PEREIRA : Estimation and study of forecast error covariances using an ensemble method in a global NWP model</u> .....	49
4.4. <u>Karim BERGAOUI : Further improvement of a simplified 2d variational soil water analysis</u> .....	49
4.5. <u>Vincent GUIDARD : Evaluation of assimilation cycles in a mesoscale limited area model</u> .....	49
4.6. <u>Jean-Marcel PIRIOU: Modelling convection for global and regional models: concepts, equations, case studies</u> .....	49
4.7. <u>Raluca RADU : Extensive study of the coupling problem for a high-resolution limited-area model</u> .....	49
4.8. <u>Wafaa SADIKI : A posteriori verification of analysis and assimilation algorithms and study of the statistical</u> .....	49

<a href="#">properties of the adjoint solutions</a> .....	49
4.9. <a href="#">Andre SIMON: Study of the relationship between turbulent fluxes in deeply stable PBL situations and cyclogenetic activity</a> .....	50
4.10. <a href="#">Klaus STADLBACHER: Systematic qualitative evaluation of high-resolution non-hydrostatic model</a> .....	50
4.11. <a href="#">Simona STEFANESCU: The modelling of the forecast error covariances for a 3D-Var data assimilation in an atmospheric limited-area model</a> .....	50
4.12. <a href="#">Malgorzata SZCZECH-GAJEWSKA : Use of IASI/AIRS observations over land</a> .....	50
4.13. <a href="#">Jozef VIVODA: Application of the predictor-corrector method to non-hydrostatic dynamics</a> .....	50
4.14. <a href="#">Fabrice VOITUS : A survey on well-posed and transparent lateral boundary conditions (LBCs) in spectral limited-area models</a> .....	50
<b>5. PAPERS and ARTICLES</b> .....	<b>54</b>
5.1. <a href="#">ARPEGE and ALADIN models coupling experiments: J. Barckicke, Y. Bouteloup, J.L. Ricard, K. Yessad</a> .....	54
5.2. <a href="#">Operational implementation of ALADIN 3DVAR at the Hungarian Meteorological Service : G. Bölöni</a> .....	60
5.3. <a href="#">Improvements of Lopez’s prognostic large scale cloud and precipitation scheme: Y. Bouteloup, F. Bouysse, P. Marquet</a> .....	66
5.4. <a href="#">Testing the new sub-grid scale orography representation on bura cases: D.Drvar, I.Stiperski, M.Tudor, V.Tutiš</a> .....	74
5.5. <a href="#">Dynamical downscaling of the ECMWF ERA-40 re-analyses with the ALADIN model: S. Kertész, G. Szépszó, E. Lábó, G. Radnóti, A. Horányi</a> .....	78
5.6. <a href="#">Mesoscale overview of Lothar storm (26 december 1999): D. Raspaud, P. Arbogast, G. Hello, D. Lambert</a> .....	84
5.7. <a href="#">The sensitivity of the AROME simulations on the Gard case to synoptic forcing : D. Raspaud, P. Arbogast, G. Hello</a> .....	88
5.8. <a href="#">Testing radiation and cloudiness parameterization: M. Tudor, I. Stiperski, D. Drvar</a> .....	93
5.9. <a href="#">Testing the New Semi-Lagrangian Horizontal Diffusion Scheme: Martina Tudor, Ivana Stiperski, Dunja Drvar, Vlasta Tutiš and Filip Vana</a> .....	98
5.10. <a href="#">High-resolution wind climatology from ERA-40: M. Žagar, N. Žagar, J. Cedilnik, G. Gregorič, J. Rakovec</a> .....	101
5.11. <a href="#">Latent heat nudging: J. Cedilnik</a> .....	105
5.12. <a href="#">ALADIN NORAF paralle suite based on 3D-VAR assimilation technique. Zahra SAHLAOUL</a> .....	111
<b>6. PUBLICATIONS</b> .....	<b>115</b>
6.1. <a href="#">Haiden T. and C. D. Whiteman: Katabatic Flow Mechanisms on a Low-Angle Slope: Vol. 44, No. 1, pp. 113–126. Journal of Applied Meteorology. <a href="http://www.ametsoc.org">http://www.ametsoc.org</a></a> .....	115
6.2. <a href="#">Whiteman C. D., T. Haiden, B. Pospichal, S. Eisenbach, and R. Steinacker: Minimum Temperatures, Diurnal Temperature Ranges, and Temperature Inversions in Limestone Sinkholes of Different Sizes and Shapes: Vol. 43, No. 8, pp. 1224–1236. Journal of Applied Meteorology. <a href="http://www.ametsoc.org">http://www.ametsoc.org</a></a> .....	115
6.3. <a href="#">Guidard V., C. Fischer, M. Nuret and A. Dziedzic</a> .....	115
6.4. <a href="#">Bénard P., J. Masek, and J. Vivoda</a> .....	115
6.5. <a href="#">Deckmyn A., and L. Berre</a> .....	115
6.6. <a href="#">Pailleux, J. et J.-F. Geleyn</a> .....	115
6.7. <a href="#">Geleyn J.-F., P. Bénard and R. Fournier</a> .....	115
6.8. <a href="#">Fischer C., T. Montmerle, L. Berre, L. Auger and S.E. Stefanescu</a> .....	115
6.9. <a href="#">Belo Pereira M. et L. Berre</a> .....	115
6.10. <a href="#">Berre, L., S. E. Sttefanescu and M. Belo Pereira</a> .....	116
6.11. <a href="#">Gérard, L. and J.-F. Geleyn</a> .....	116
6.12. <a href="#">Soci C. , C. Fischer and A. Horanyi</a> .....	116
6.13. <a href="#">Stefanescu, S. E., L. Berre and M. Belo Pereira</a> .....	116
6.14. <a href="#">Žagar N., M. Žagar, J. Cedilnik, G. Gregorič and J. Rakovec</a> .....	116

## **1. EDITORIAL**

This is the first trial to deport some of the editorial work of the Newsletter: András Horányi was asked to write the editorial part of the Newsletter. This is the reason for the slightly modified style and content of this part of the Newsletter.

### **1.1. EVENTS**

#### **1.1.1. ALADIN workshop**

A huge and successful ALADIN workshop was organised in Bratislava with the participation of 74 registered participants from 19 countries (is it a record?). Many-many thanks for the local organisers and especially to Maria Derkova and Michal Majek. The main sessions of the workshop were as follows:

- General presentations on projects and models
- Equations and interfaces
- STORMNET
- Dynamics and coupling
- Data assimilation
- Physics, case studies and diagnostics
- Verification and adaptation
- Technical issues
- SURFEX
- EPS and downscaling

The workshop was completed by final discussions (see details on the ALADIN website, <http://www.cnrm.meteo.fr/aladin/meetings/Wk2005/program.html> ). And it was preceded by the first HMG-CSSI meeting (see hereafter).

The host of the next venue is Sofia (Bulgaria).

#### **1.1.2. AROME project review**

On 30<sup>th</sup> of June an AROME project review was organised in Toulouse, where Eric Brun (head of research at Météo-France) had invited two researchers from the ALADIN community: Bart Catry and Andras Horanyi (with the condition of understanding French). The meeting was based on the presentation of Francois Bouttier and the discussions were focusing on the progress in modelling and data assimilation and then on the planning aspects. French summary of the meeting is available from Toulouse.

#### **1.1.3. STORMNET**

The STORMNET proposal was refused at the first evaluation step. After this failure it was decided to pursue our efforts for submitting a new proposal, and first discussion was realised during the ALADIN workshop in Bratislava. The new call is already published and the deadline is 28th of September, 2005.

The main highlights of the discussions in Bratislava are available on the STORMNET web site : <http://www.cnrm.meteo.fr/stormnet/v0.0/> and on the pages of the workshop.

#### **1.1.4. Other workshops**

##### **x HIRLAM All Staff Meeting**

The 2005 All Staff Meeting (ASM) was organized in Dublin by Met' Eireann on March 14-16.

It was the first one hold in the framework of an enhanced cooperation between the HIRLAM and ALADIN consortia. Presentations and discussions were marked by this partnership and the need to refine the strategy for going towards very high resolution.

The program was quite dense and presentations of high quality, but schedule was perfect with even more time than expected for working groups. Official and informal discussions have been very carefully prepared.

HIRLAM scientists did or want to start quickly working with the ALADIN/AROME code in an enlarged partnership, though they are afraid of loosing their identity ("being eaten by France"). However they felt more confident on this issue at the end of the meeting (there was no reason to worry so much).

A detailed report was sent by Dominique Giard to the "*coordala*" list, and the proceedings are available in HIRLAM Newsletter 48 :

<http://hirlam.knmi.nl/> ↗ "*Publications*" ↗ "*Newsletters*"

**x First SRNWP PEPS and second SRNWP short-range EPS workshop was organised in Bologna (Italy) at 6-8 April, 2005.**

More details on the SRNWP web site :

[http://srnwp.cscs.ch/Lead\\_Centres/2005Bologna/Agenda.htm](http://srnwp.cscs.ch/Lead_Centres/2005Bologna/Agenda.htm)

[http://srnwp.cscs.ch/Lead\\_Centres/2005Bologna/ReportFinalDiscussion.htm](http://srnwp.cscs.ch/Lead_Centres/2005Bologna/ReportFinalDiscussion.htm)

**x 4th WMO international symposium on "Assimilation of Observations in Meteorology and Oceanography"**

This huge event (around 100 presentations and 160 posters) was held on April 18-22, 2005, in Prague (Czech R.). Presentations are available on :

<http://www.chmi.cz/meteo/ok/dasympo/index.html>

A coordination meeting between ALADIN and HIRLAM scientists was held beside the meeting, to discuss research plans in data assimilation. The minutes will be available on the ALADIN web site.

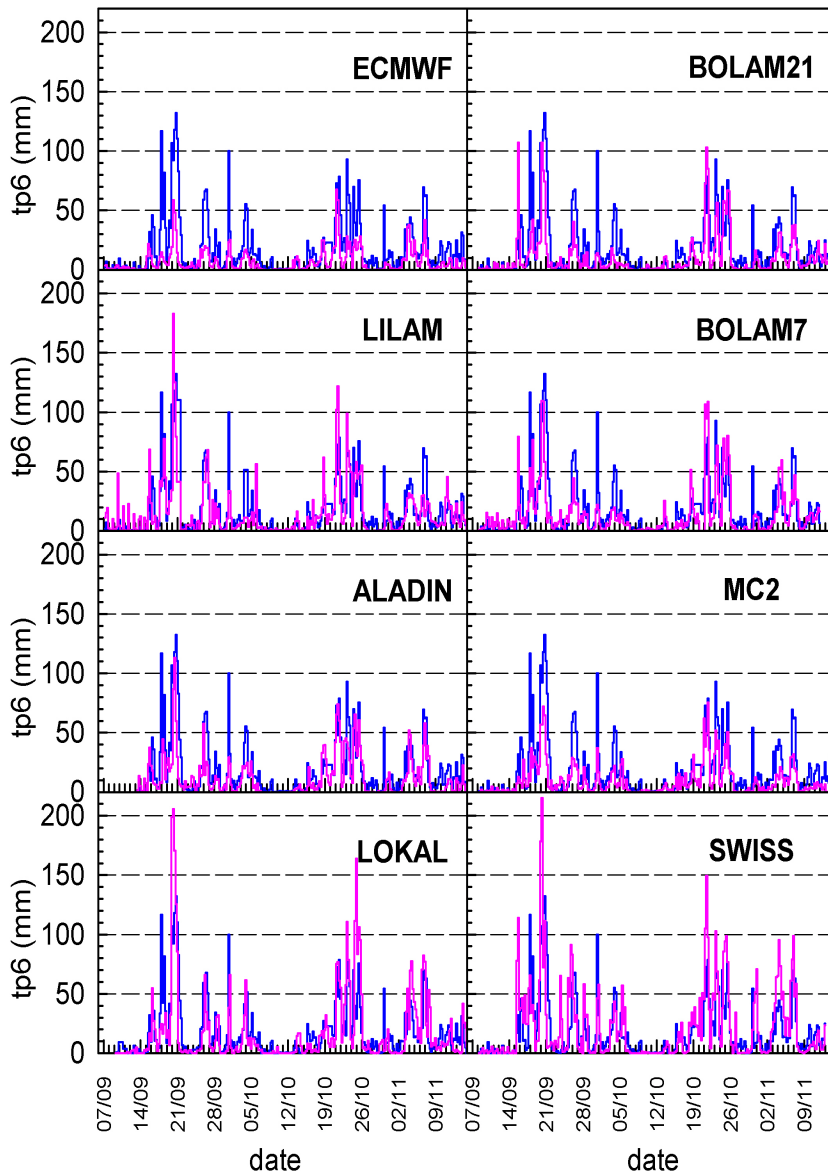
**x ICAM-MAP meeting**

The 28th International Conference on Alpine Meteorology (ICAM) and the Annual Scientific Meeting of the Mesoscale Alpine Programme (MAP) 2005 was held in Zadar (Croatia), from 23 to 27 of May. The proceedings will be published in Meteorologische Zeitschrift, Special Issue on ICAM/MAP2005, and presentations are available on :

<http://meteo.hr/ICAM2005/>

The performances of the different models available during the MAP field experiment were presented, with comforting results for ALADIN(-LACE) :

Performances of models along MAP : precipitations (from Pedemonte et al., E.Richard)



MESO-NH	+29%
MM5	+25%
MOLOCH	-21%
MC2	-30%
ALADIN	+17%
ARPEGE	+18%

Mean bias over the SOP period

Maximum TP for day 2 (MC2 day 1) – Rain gauge

x **Third SRNWP workshop on "Statistical and Dynamical Adaptation" was held in Vienna (Austria) at 1-3 June, 2005.**

More details on the SRNWP web site :

[http://srnwp.cscs.ch/Lead\\_Centres/2005-Vienna/Summaries\\_of\\_the\\_Presentations.htm](http://srnwp.cscs.ch/Lead_Centres/2005-Vienna/Summaries_of_the_Presentations.htm)

### 1.1.5. Bad news

The ALADIN project was touched by the death of Vladimir Ivanovici, Deputy Director of the Romanian National Institute for Meteorology and Hydrology and ALADINist of the first hour.

## 1.2. ANNOUNCEMENTS

### 1.2.1. EWGLAM/SRNWP meeting, Ljubljana (Slovenia), 3-5 October, 2005

Environmental Agency of the Republic of Slovenia, Meteorological office is organizing the

27th meeting of the European Working Group on Limited Area Modelling (EWGLAM) and the 12th meeting of the Short-Range Numerical Weather Prediction (SRNWP) Network, to be held in Ljubljana between the 3rd and 5th October 2005.

The special topic of this year's EWGLAM meeting is : Modelling in very high resolution, i.e. at a few kilometres scale.

Contributions concerning not only the models' accuracy in terms of predicted values, but also concerning their behavior at these scales, in comparison to observations with high temporal resolution, could be particularly interesting.

An informal ALADIN meeting will be organized beside the workshop, to discuss operational updates, the next research plan, etc ... A reduced HMG-CSSI meeting will be hold on Thursday, 6th, to discuss the common HIRLAM-ALADIN research issues.

More informations on the workshop pages : [http://www.arso.gov.si/ewglam\\_2005/](http://www.arso.gov.si/ewglam_2005/) !

### **1.2.2. 10th Assembly of ALADIN partners**

The next Assembly of ALADIN Partners will be organized on October 21<sup>st</sup> 2005, in Bratislava, Slovakia. It will have to deal with the new Memorandum of Understanding (with preliminary discussions in Heidelberg in September), the cooperation with HIRLAM, the next research plans, ...

### **1.2.3. AROME workshop, Brasov, (Romania), 21-25 November, 2005**

The location of the 1st AROME training course is now established: Poiana Brasov. It will focus on the most important points for running AROME in the forecast mode, considering both the theoretical and the practical aspects of :

- Méso-NH physics,
- ALADIN NH dynamics,
- AROME prototype, including the externalized surface module.

The registration deadline is September 30<sup>th</sup> 2005. Information is available on a dedicated page on the NMA web site : <http://www.inmh.ro/images/Arome2005/index.htm>

### **1.2.4. HIRLAM-ALADIN code maintenance and data assimilation workshop, Budapest (Hungary), 14-18 November, 2005**

After the successful training courses organized in Toulouse (mid-March) and the TCWGPDI workshop (in Prague) it was an idea to organize a working week on data assimilation between ALADIN and HIRLAM scientists. According to the original idea it was foreseen that all the HIRLAM activities in the field of data assimilation will be presented to the ALADIN researchers and at the same time HIRLAM people would learn about theoretical and practical aspects of the ALADIN data assimilation system. Later on the idea was oriented more on the training aspects and moreover the scope was also extended to the ALADIN code maintenance and merging issues. Finally the workshop will be organized in Budapest between 14-18 November having more code maintenance and phasing issues in the first two days and data assimilation practical concerns for the last three days. This organization will allow participants to participate either at the very beginning or the second part of the workshop. In the very preliminary program 2 days are devoted to code maintenance and merging issues, and 3 days to data assimilation practical issues. More details at : <http://www.cnrm.meteo.fr/aladin/meetings/budaNov2005.html>

### 1.2.5. And next ...

#### x 7th COSMO Meeting, Zürich (Switzerland), 19-23 September 2005

Representatives from other consortia are welcome. Among other issues, a new strategy for data assimilation and an enhanced cooperation between consortia will be discussed.

More details at the meeting web site: <http://cosmo-model.cscs.ch/public/agenda2005.htm>

#### x LC for Non-hydrostatic Modelling, Bad Orb (Germany), 31 October - 2 November 2005

Special topic for 2005 is : "Convection resolving models"

#### x HIRLAM workshop on mesoscale modelling, Norway, December 2005

#### x Early 2006 :

LC for Numerical Techniques (De Bilt, The Netherlands)

ALADIN-HIRLAM working week on predictability

etc ...

## 1.3. ALADIN 2

### 1.3.1. HIRLAM Council's resolution

---

#### **HIRLAM Resolution on the Collaboration with ALADIN** ( HIRLAM Council Meeting, Basel, Switzerland, 11 April 2005)

- NOTING:

- (1) That the HIRLAM Council at its meeting on 2 June 2004 agreed to a full code collaboration with ALADIN on meso- scale modelling and other agreed areas following the best suited approach across the IFS/ARPEGE/ALADIN/HIRLAM chain;
- (2) That the HAC Chairman and the Project Leader were invited as observers to the ALADIN General Assembly 29- 30 October 2004.

- CONSIDERING:

- (1) The Resolution on ALADIN- HIRLAM cooperation that was adopted by the ALADIN General Assembly;
- (2) The presentation on the ALADIN resolution and response to our informal contacts at the HIRLAM Council on 15 December 2004 by Mr. Ivan Cacic as Chairman of the ALADIN Assembly;
- (3) The reply to Mr Cacic by the HIRLAM Council on 23 December 2004;
- (4) The support by the HIRLAM Evaluation for code collaboration with ALADIN.

- ACKNOWLEDGING:

- (1) The strong and positive interest shown by ALADIN to engage in a full code collaboration with HIRLAM.

- BEARING IN MIND:

- (1) The support for this collaboration by individual HIRLAM Council members in response to the recent HIRLAM Evaluation.

- EMPHASISING:

- (1) That HIRLAM and ALADIN should have observer status at the Assembly and Council

meetings, respectively.

- DECIDES:

A. To commit itself to a full code collaboration with ALADIN ;

B. That HIRLAM will make fair and strong contributions in agreed areas of expertise to the common HIRLAM/ALADIN code in the agreed collaboration area;

C. That an Agreement (signed before the End of 2005) with ALADIN and Météo-France should be based on the following principles:

(1) Joint arrangements shall be made to coordinate scientific plans and in particular for the common elements agreed by HIRLAM and ALADIN;

(2) The HIRLAM Management Group and the ALADIN Committee for Scientific and Strategic Issues (CSSI) in their meeting in June 2005 shall address common issues that will appear in both the HIRLAM and ALADIN science plans;

(3) The content of the HIRLAM and ALADIN scientific strategies are in line in the collaboration areas;

(4) The cooperation between HIRLAM and ALADIN is included in a consistent way in the new Memoranda of Understanding for the respective organisations;

(5) The detailed conditions of the cooperation are further developed and formulated, including legal and commercial conditions for the HIRLAM and ALADIN members.

---

### 1.3.2. HMG-CSSI meeting

Here is the main body of the report sent to ALADIN Directors and coordinators. The full document is available on the ALADIN web site :

<http://www.cnrm.meteo.fr/aladin/concept/collaboration.html>

### Conclusions of the first HMG-CSSI coordination meeting

Bratislava, June 5th, 2005

According to the resolution accepted at the last ALADIN Assembly in Split the ALADIN Coordinators for Strategic and Scientific Issues (CSSI) and HIRLAM Management Group (HMG) have met (for list of participants see Appendix A) in order to plan and create a joint science plan between ALADIN and HIRLAM projects. Discussions along this first meeting focused on working practises (*How shall we work together?*) and common scientific planning (*What do we want to achieve together?*).

Before going to more details, more general and strategic questions were dealt with. First, the advantage of the IFS/ARPEGE software backbone was recognised: it outweighs the associated maintenance constraints since it allows building on the existing pieces without a need of a heavy re-development. Second, it was said that the joint code should encompass a NWP system suitable for scales from synoptic to meso-gamma, which is a quite ambitious goal. These two important points streamlined the following discussion.

#### Code management and maintenance

The principles of code collaboration were set as follows:

- IFS/ARPEGE software as a backbone, as has been the case for ALADIN
- Reference code releases (cycles) common with IFS once or twice a year, intermediate cycles for new developments and operations

- New developments must be carefully prepared and further maintained by the authors
- To begin with, selection of the modification likely to enter cycles through 3 successive steps:
  - control at "team" level, through transversal thematic scientific coordination
  - HIRLAM-ALADIN-ARPEGE coordination meeting
  - ARPEGE-IFS coordination meeting
- Solidarity: all should contribute to maintenance tasks, including phasing (creation and technical validation of new cycles by merging and checking contributions), with the possible emergence of a second phasing centre (beside Toulouse) in a longer term
- Evolution as soon as possible towards a HIRLAM-ALADIN-ARPEGE-IFS coordination

The maintenance tasks in the ALADIN organization roughly correspond to the duties of the system manager and the core group in the HIRLAM one. The involvement of HIRLAM will be a progressive one, as will be code collaboration and will start in autumn 2005. There was an agreement on the following steps:

- Training on the IFS-ARPEGE-ALADIN code via an extension of the planned common workshop on data assimilation (Budapest, 14-18/11/2005) to code maintenance aspects
- Participation of HIRLAM scientists to the next phasing actions in Toulouse: 2 stays of 1 to 1.5 month at the end of 2005 or the beginning of 2006
- Further sustained training of code experts within HIRLAM and ALADIN partners, to face the burden of maintenance brought by such a wide code collaboration
- HIRLAM commits to devote a 2 person-year effort (annually) to common code maintenance activities
- As first practical exercise, the introduction and interfacing of the HIRLAM physical package into IFS-ARPEGE-ALADIN is considered (modification ready)

#### Scientific coordination and planning

The following procedure was agreed for this first common planning exercise:

- This meeting (beginning of June):
  - identification of emerging topics of common interest
  - identification of relevant contact persons at each side (forming small subgroups)
- End of August:
  - detailed identification of common areas of interest for medium and short term (by the subgroups)
- Beginning of October (around EWGLAM meeting):
  - finalization of the common plans (detailed for 2006, main directions for the longer term), based on the proposals of the subgroups
- Before the end of the year:
  - presentation of the first plan on common scientific issues to the ALADIN Assembly and the HIRLAM Council

The following common research objectives were identified (for possible common subjects of interest see Appendix B), and drafting teams in charge of planning were nominated for each issue, as a first step towards a transversal cross-consortia coordination:

#### Dynamics and Lateral Boundary Coupling

Aim: keeping a top-level non-hydrostatic dynamical core and improving LBC treatment

Drafting team: Per Unden, Radmila Brozkova

#### (Atmospheric) Physics

There was an agreement on the bases of collaboration:

- For the start, keeping the present variety of options (i.e. adding HIRLAM physics to the ARPEGE/ALADIN and Meso-NH ones), letting further "friendly competition" decide on the best combinations;
- Design of a set of reference equations and a both clean and flexible physics-dynamics interface;
- Use of common validation tools.

Drafting team: Bent Hansen Sass, Laura Rontu, Jean-François Geleyn, Gwenaëlle Hello

#### Surface (physics, data assimilation, physiographic data)

Collaboration will go on as by the past, with objectives refined once the more technical "externalization" of surface schemes achieved.

Drafting team: Ernesto Rodriguez, Stefan Gollvik, Dominique Giard

#### (Variational) Data Assimilation

Objectives are more complementary than common as concerns algorithms: only 3D-Var is considered by ALADIN partners in the short term, at all scales, while HIRLAM will go on with 4D-Var assimilation at synoptic scales and considers both 3D-Var (for nowcasting) and 4D-Var for the mesoscale. But many common issues were identified in other domains.

Drafting team: Nils Gustafsson, Harald Schyberg, Claude Fischer

#### Predictability

- There is a strong need and interest at both sides, but science is not yet mature to define the right track. Basic research is needed for the start.

Drafting team : Ben Wichers Schreur, András Horányi

#### Verification and Diagnostics

This is essential. New methods and diagnostics, especially for the mesoscale and EPS, are to be designed through a close cooperation. Standard scores are clearly not enough.

Drafting team: Gerard Cats, Carl Fortelius, Joël Stein, Jean-Marcel Piriou

#### System

Aim: common design of simple, efficient and "free" code management tools, and friendly user interfaces

Drafting team: Gerard Cats, Jure Jerman, Eric Sevault

---

The next common meeting should be hold next spring, between the HIRLAM All Staff Meeting and the ALADIN workshop, provided it keeps consistent with organizations within the new MoUs, not yet known.

### **1.3.3. Next medium-term ALADIN research plan (2005-2008)**

Initial planning was produced before the ALADIN workshop for the HMG-CSSI meeting. Those plans were intensively discussed during the workshop. All the available draft plans can be found under <http://www.cnrm.meteo.fr/aladin/scientific/planscientif.html> (the temporary dedicated

site has been closed).

Dominique Giard is in charge of collecting all missing pieces and preparing an executive summary (for Directors) and if possible a complete version too with the next Assembly of Partners. It is still time to send her contributions (there were not so many up to now).

#### **1.3.4. Special project at ECMWF?**

During the last ALADIN workshop in Bratislava the question was raised, whether a special project at ECMWF can be initiated in order to access the ALADIN code put to the HPCF (High Performance Computing Facility) of ECMWF and moreover with the possible execution of simple pre-processing applications, while preparing IFS-based initial and lateral boundary conditions for the ALADIN model (for example ERA40 downscaling, study of the impact of IFS boundaries in ALADIN etc.). The idea was supported in Bratislava and András Horányi volunteered to ask the principle opinion of ECMWF about such project. After contacting Umberto Modigliani (User Support) a positive general answer was received and furthermore it was asked that such project should be initiated by Mété-France. Mété-France (François Bouttier) kindly accepted to write the special project proposal based on some inputs received from the ALADIN Partners (a circular about the project was submitted at the beginning of July for the coordinators of the Partners). The project was submitted mid-July with the following description:

---

#### **Coupling of ALADIN and AROME models to boundary conditions from ECMWF and ERA model data**

Météo-France and the other meteorological services of the ALADIN consortium (Algeria, Austria, Belgium, Bulgaria, Moldova, Croatia, Czech Republic, Hungary, Morocco, Poland, Portugal, Romania, Slovakia, Slovenia, Tunisia in 2005) have developed the ALADIN and AROME limited area models, with the help of the IFS/ARPEGE software cooperation agreement with ECMWF. Traditionally, ALADIN and AROME have been coupled to large scale boundary conditions provided by the French ARPEGE global model. The purpose of this project is the investigation of the option to couple ALADIN and AROME to large scale model data, namely, the IFS operational archive and the ERA archives on MARS. This is of scientific and technical interest to all ALADIN participants, as well as to the HIRLAM consortium (Denmark, Ireland, Finland, Iceland, The Netherlands, Norway, Spain, Sweden) who plans to test the ALADIN/AROME software coupled to the ECMWF boundary conditions data products.

HIRLAM and Météo-France have already set up a simplified technical environment, called hiral, on the HPCF in order to facilitate joint work on the ALADIN software. The COSMO-LEPS and HIRLAM projects have shown the usefulness of coupling LAMs to the ECMWF model data, but there is very little experience in this area within the ALADIN consortium. Some pilot experiments (e.g. climatological rain and wind downscaling in Austria, Hungary and Slovenia from ERA-40) have recently demonstrated that coupling ALADIN to ECMWF is feasible and yields interesting results, but some technical and scientific issues deserve further investigation. This project plans to explore the following questions:

- technical issues when coupling ALADIN/AROME to ECMWF model data: file preparation, data compression and telecommunication issues
- relative merits of coupling ALADIN/AROME to IFS vs ARPEGE models for NWP, using various geographical domains (the ARPEGE variable resolution grid is optimized for Southwestern Europe only, so using IFS output may be particularly interesting for more distant applications)
- impact of the large-scale model resolution on the quality of limited-area modelling

- desirable resolution and archiving policy of future reanalysis datasets for downscaling using ALADIN and/or AROME
- coupling issues linked to the representation of the surfaces
- coupling issues linked to the differences in physical packages, e.g. cloud physics
- optimisation of an intermediate coupling model for running at kilometric scales using AROME

These questions are related to the distinct LAM-EPS project lead by the Austrian Meteorological Service (ZAMG). Here, the intention is (1) to allow scientists from some selected (Cooperating and Non-Member) States access to resources on the HPCF, in order to perform boundary condition file preparation at ECMWF before sending it to their own sites for running the LAMs, and (2) to offer a unified software environment for preparing ALADIN and AROME boundary conditions to all interested States, for experimentation. The planned activities of this project are:

1. installation and maintenance of the ARPEGE/ALADIN scripts (IFS configurations 901/923) on the HPCF to convert IFS non real time model data on MARS into ALADIN/AROME coupling files
2. development and testing of new software to resolve model inconsistencies e.g. related to the surface initialization. An important aim of this project is to provide a unified, well-maintained environment for preparing LAM experiments.
3. preparation, by the Special Project participants, on the HPCF, and storage on ECFS of ALADIN/AROME coupling files for chosen test periods and geographical domains. This item is dimensioning for the Special Project, as it requires HPCF access for all listed participants, and some HPCF and storage resources.
4. local LAM experimentation to investigate model performance sensitivity to the coupling technique. Some LAM runs may be performed on the HPCF as well for testing purposes. This is where the scientific evaluation of the boundary condition quality will be performed.

This project will be used for scientific experimentation only. The real-time sending of ECMWF boundary conditions, or the routine execution of LAM applications on the HPCF, are explicitly outside its scope. The list of scientists involved in the project may be extended to other scientists from ALADIN cooperating services during the lifetime of the project.

## 1.4. GOSSIP



Many thanks to marvellous Mariska and her colleagues for a very successfull workshop despite an apalling weather.

A Reminder: Whenever using MF-KIT, don't forget to send me all receipts, flights coupons etc..

Another Reminder: If no one is picking you up at the airport, once at the main gate, don't forget to ask for the envelope bearing your name.

## **2. OPERATIONS**

### **2.1. INTRODUCTION**

#### **2.1.1. Scheduled changes in climate and coupling files( D. GIARD, M. DERKOVA & R. EL KHATIB)**

##### **x New climate files**

According to several mails and as presented at the 15th ALADIN workshop, a major coordinated update of climate files and "telecom" files is scheduled for the beginning of the autumn (end of October ?).

ALADIN climate files must be anyway recomputed because the climatological snow cover was not computed consistently in e923 and c923 till the most recent version, leading to spurious snow melting in E927. Furthermore, a few ones are very very old, with still anything in the extension zone, and some partners anyway already scheduled domain changes.

Besides, new databases have been used in the ARPEGE parallel suite launched on June 30th, and expected to move to operations at the end of October : finer GTOPT030 data for the definition of orography, new, finer and more sensible, databases for climatological/ relaxation surface fields. The same must be done for ALADIN models, in order to avoid initialization problems : the distance to climatology is usually interpolated in configuration 927 for surface fields.

New scripts for configuration 923 are now available, thanks to Francoise Taillefer, and some more documentation has been sent. Most of the work can be performed by the Toulouse team, provided partners do send the required information.

##### **x New "telecom" files**

The additional proposed changes in "telecom"/coupling files are the following (answers are also needed):

1. change or not in vertical resolution? which vertical grid?  
*ARPEGE will switch to 46 levels in October; if nothing is done, the same 46 levels will be used for telecom files.*
2. keeping or not "constant" fields in telecom files ?
3. *Most of them are not used at all, since read in model clim files by EE927. The required modset should be soon ready. It will allow sending 22 less 2d gridpoint fields. This will also prepare the move to SURFEX.*
4. which new fields in telecom and coupling files ?  
warning index (*1 diagnostic 2d spectral field*) ?  
new snow scheme (*2 constant, 2 prognostic and 1 diagnostic 2d gridpoint fields*) ?  
ozone and aerosols (*7 constant 2d gridpoint fields*) ?  
Lopez' micro-physics (*3 prognostic and 1 diagnostic 3d gridpoint fields*) ?

##### **x Contact points : Dominique Giard and Maria Derkova**

#### **2.1.2. Operational applications**

##### **x Notes**

"hrda" stands for high-resolution dynamical adaptation hereafter; the frequency along each forecast is mentioned instead of the number of runs per day. Lagged coupling is used only for ALADIN-NORAF and ALADIN-BG. Plans are detailed in national reports, when available.

### 2.1.3. Table

Partners	Models	Coupling	Applications	per day	Details	Libraries	Computer
Austria	"Austria"	ARPEGE every 3 h	DFI + 48 h forecasts	2	$\Delta t = 415$ s post-processing every 1 h	25T2	SGI
Belgium	"large"	"France"+ARP every 3 h	DFI + 60 h forecasts	2	$\Delta t = 300$ s post-processing every 1 h	28T3	SGI
Bulgaria	"BG"	ARPEGE every 6 h	DFI + 48 h forecasts	2	$\Delta t = 514$ s post-processing every 3 h	25T1 (28T3) (29T2)	Linux PC
Croatia	"LACE"	ARPEGE every 3 h	DFI + 48 h forecasts	2	$\Delta t = 514$ s post-processing every 3 h	25T1 (28T3)	SGI
	"Croatia"	"LACE" every 3 h	48 h forecasts	2	$\Delta t = 327$ s post-processing every 3 h		
	7 domains	"Croatia"	hrda for wind	3 h	$\Delta t = 60$ s		
Czech R.	"CE"	ARPEGE every 3 h	DFI spectral + surface blending IDFI + 54/24 h forecasts diagnostic analyses	4 2 2+2 24	$\Delta t = 360$ s post-processing every 1 h	28T3	NEC
	"MFSTEP"	" "	spectral+surface blending DFI + 120 h forecasts	4 1/week	$\Delta t = 400$ s post-processing every 1 h		
France	"France"	ARPEGE every 3 h	3d-var assimilation DFI + 36-54 h forecasts diagnostic analyses	4 4	$\Delta t = 415$ s post-processing every 1 h	29T1 (29T2)	Fujitsu
Hungary	"HU"	ARPEGE every 3 h	3d-var assimilation DFI + 48 h forecasts diagnostic analyses	4 2	$\Delta t = 300$ s post-processing every 1 h	28T3	IBM
	1 domain	"HU"	hrda for wind	2	$\Delta t = 60$ s		
Morocco	"NORAF"	ARPEGE every 6 h	DFI + 72 h forecasts	2	$\Delta t = 900$ s post-processing every 6 h	25T1 (28T3)	IBM
	"Maroc"	"NORAF" every 3 h	DFI + 72 h forecasts	2	$\Delta t = 675$ s post-processing every 3 h		
Poland		ARPEGE every 6 h	DFI + 48 h forecasts	2	$\Delta t =$ s post-processing every 3 h	15	SGI
	1 domain	"Poland"	hrda for wind		$\Delta t =$ s		
Portugal		ARPEGE every 6 h	DFI + 48 h forecasts	2	$\Delta t = 600$ s post-processing every 1 h	12	DEC
Romania	"SELAM"	ARPEGE every 6 h	DFI + 60 h forecasts	2	$\Delta t = 900$ s post-processing every 6 h	28T3	SUN
	"Romania"	ARPEGE every 6 h	DFI + 48 h forecasts	2	$\Delta t = 450$ s post-processing every 3 h		
	2 domains	"Romania"	hrda for wind	2	$\Delta t = 60$ s		
Slovakia	"SHMU"	ARPEGE every 3h	DFI + 54 h forecasts	3	$\Delta t = 400$ s post-processing every 1h	28T3	IBM
	1 domain	"SHMU"	hrda for wind	3 h	$\Delta t = 120$ s		
Slovenia	"SI"	ARPEGE every 3h	DFI + 54 h forecasts	2	$\Delta t = 400$ s post-processing every 1 h	25T1	Linux cluster
	1 domain	"SI"	hrda for wind+precipit.	3 h	$\Delta t = 60$ s		
Tunisia		ARPEGE every 3h	DFI + 48 h forecasts	2	$\Delta t = 568$ s post-processing every 3 h	26T1 (28T3)	IBM

### 2.1.4. Main model characteristics

#### x Warning

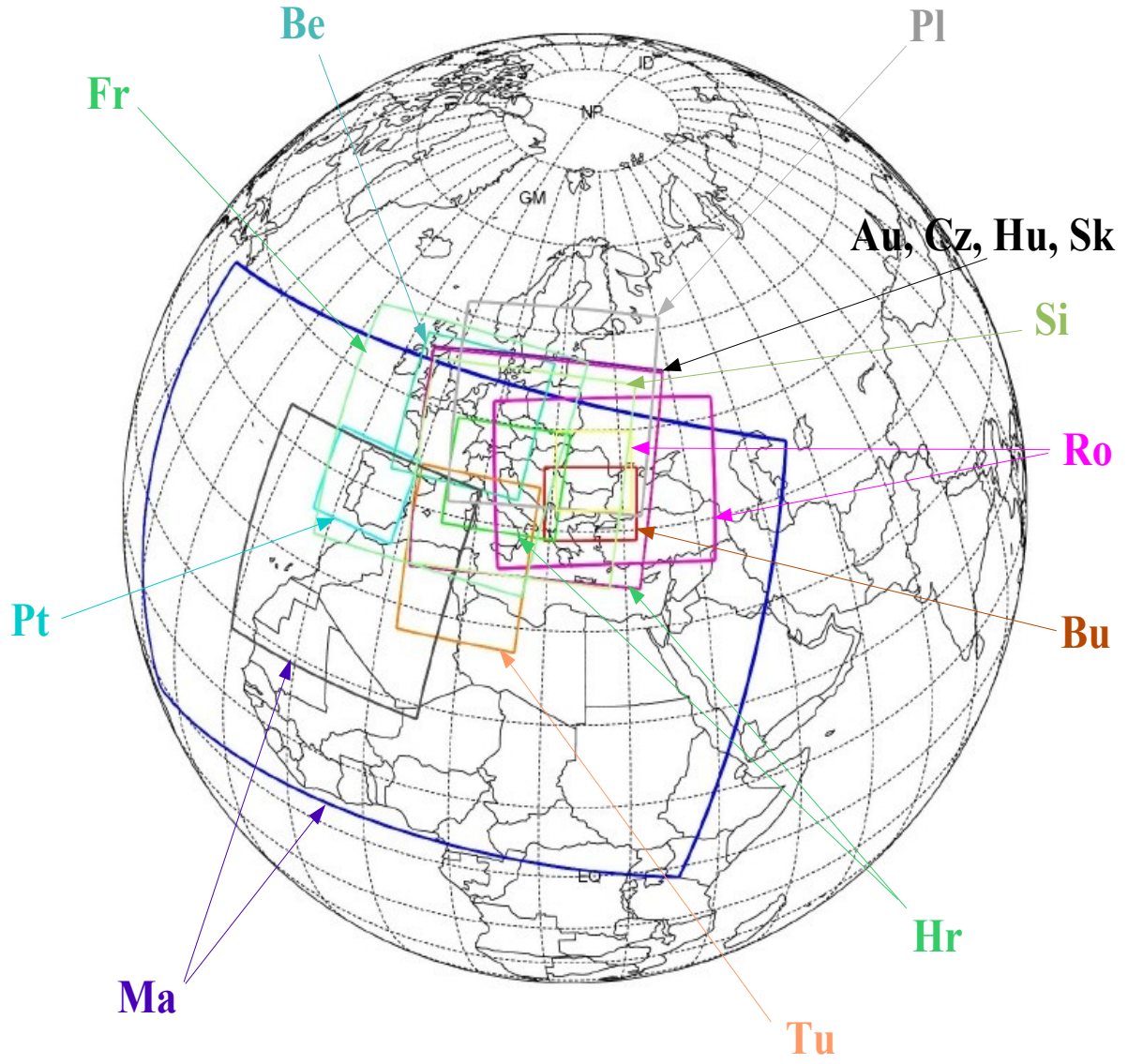
Horizontal characteristics are in latitude  $\times$  longitude (or y  $\times$  x) ordering here.

For telecom domains, all grids (or truncations) are quadratic ones.

When changes are scheduled, the new domains are described in *italics*.

LACE : Au, Cz, Hr, Hu, Si, Sk

SELAM : Bu, Ro  
2.1.5. Main forecast domains



Partner	L	$\Delta x$ (km)	Number of gridpoints	Centre of domain	spectral trunc.	Grid type
Austria	45	9.64	259;289 (270;300)	46.26°N;17.00°E	89; 99	quadratic
Belgium	41	6.97	229;229 (240;240)	50.21°N; 5.62°E	79; 79	quadratic
Bulgaria	41	12.00	69; 91 ( 80;108)	42.75°N;25.50°E	39; 53	linear
Croatia	37	12.18	205;229 (216;240)	46.24°N;17.00°E	71; 79	quadratic
	37	8.00	149;169 (160;180)	44.60°N;13.00°E	53; 59	quadratic
	37	8.00	205;229 (216;240)	46.00°N;15.00°E	71; 79	quadratic
Czech R.	43	9.00	277;309 (288;320)	46.24°N;17.00°E	143;159	linear
	37	9.53	189;245 (200;256)	38.77°N; 9.00°E	99;127	linear
France	41	9.51	289;289 (300;300)	46.47°N; 2.58°E	149;149	linear
Hungary	49	7.96	309;349 (320;360)	46.10°N;17.00°E	159;179	linear
Morocco	37	31.14	189;289 (200;300)	29.00°N; 0.00°E	66; 99	quadratic
	37	16.70	169;169 (180;180)	31.56°N;-7.00°E	59; 59	quadratic
Poland	31	13.5	169;169 (180;180)	52.50°N;19.00°E	59; 59	quadratic
Portugal	31	12.7	89; 79 (100; 90)	40.10°N;-7.00°E	33; 29	quadratic
Romania	41	24.03	79;109 ( 90;120)	45.01°N;27.75°E	29; 39	quadratic
	41	10.00	89; 89 (100;100)	46.0°N,26.0°E	33; 33	quadratic
Slovakia	37	9.00	277;309 (288;320)	46.24°N;17.00°E	95;106	quadratic
Slovenia	37	9.50	244;258 (256;270)	45.44°N;14.86°E	84; 89	quadratic
Tunisia	41	12.50	151;117 (162;128)	36.06°N; 9.36°E	80; 63	quadratic

### 2.1.6. Telecom domains

Name	L	$\Delta x$ (km)	Number of gridpoints C+I (C+I+E)	Centre of the domain	Spectral truncation	Extension (km)
Belgique	41	9.49	181;181 (192;192)	50.76°N; 3.90°E	63;63	1718;1718
LACE	37	20.68	124;139 (135;150)	46.24°N;17.00°E	44;49	2564;2874
MFSTEP	37	28.96	109;205 (120;216)	41.95°N; 9.81°E	39;71	3157;5937
NORAF	41	42.23	149;229 (160;240)	29.50°N; 0.35°E	53;79	6292;9670
Pologne	31	21.44	109;109 (120;120)	52.50°N;19.00°E	39;39	2337;2337
Portugal	31	21.30	85; 85 ( 96; 96)	39.99°N;-9.05°E	31;31	1810;1810
SELAM	41	24.03	79;109 ( 90;120)	45.01°N;27.75°E	29;39	1898;2619
Tunisie	41	24.00	97; 97 (108;108)	36.18°N; 6.00°E	35;35	2328;2328
MFSTEP	37	23.97	85;109 ( 96;120)	38.77°N; 9.00°E	31;39	2037;2612

### 2.1.7. Post-processing domains

Partner	Grid type	Resolution (° / km)	Size	Centre	Note
<b>Austria</b>	latlon model grid	0.072;0.110 <i>see above</i>	243;273 -	46.70°N;17.20°E -	without clim
<b>Belgium</b>	latlon " " "	0.117;0.165 0.060;0.091 0.122;0.184 0.244;0.368	115;115 97; 97 48; 48 25; 25	50.60°N; 3.90°E 50.53°N; 4.53°E " "	big domain small domain " "
<b>Bulgaria</b>	latlon	0.100;0.100	70;121	42.65°N;25.50°E	
<b>Croatia</b>	latlon	0.080;0.120	126;126	44.60°N;13.00°E	without clim
<b>Czech R.</b>	latlon latlon Lambert latlon	0.100;0.167 0.100;0.167 25.00 km 0.100;0.100	91; 91 116;175 65; 75 151;241	49.50°N;15.50°E 49.75°N;15.50°E 49.00°N;15.00°E 38.50°N; 9.00°E	CE " " MFSTEP
<b>France</b>	latlon	0.100;0.100	221;281	46.00°N; 3.00°E	
<b>Hungary</b>	latlon	0.100;0.100	191;291	46.50°N;16.50°E	
<b>Morocco</b>	latlon latlon	0.217;0.244 0.142;0.153	189;289 169;169	24.31°N; 0.00°E 31.09°N;-7.00°E	without clim
<b>Poland</b>	model grid Lambert latlon	<i>see above</i> 10.13 km 0.094;0.149	120;120 180;180	52.50°N;19.00°E 52.50°N;19.00°E	
<b>Portugal</b>	latlon	0.110;0.135	89;79	39.95°N;-6.95°E	
<b>Romania</b>	latlon model grid	0.125;0.100 <i>see above</i>	78;86	45.95°N;26.01°E	without clim
<b>Slovakia</b>	model grid	<i>see above</i>	-	-	
<b>Slovenia</b>	latlon model grid	0.085;0.120 <i>see above</i>	211;217 -	45.00°N;15.00°E -	without clim
<b>Tunisia</b>	model grid	<i>see above</i>			

### 2.1.8. Post-processing on a new grid : with or without "clim" files ?

During the horizontal interpolations the usage of auxiliary climatology datasets improves the accuracy of the resulting upperair fields (when interpolated on surface-dependent levels, like height or model levels), and of many surface fields.

The minimal option (NFPCLI=1) is to provide a climatology file on the geometry of the post-processing files, containing the orography and the land-sea mask. Then this orography will be taken into account to compute more precisely the post-processed surface pressure. Consequently the upperair fields on height and model levels, when close to the surface, will be more accurate. The land-sea mask is used to compute the weights used for the interpolation of physical surface fields (for a given post-processing point, only the neighbouring point on the model grid which are of the same nature - land or sea - are used for interpolation). When the climatology land-sea mask is not provided, the program has to create the post-processing land-sea mask by interpolating the model land-sea mask.

More complete option (NFPCLI=3) is recommended to improve as well the interpolation of most physical surface fields : in that case all, instead of a straightforward interpolation of the model fields, post-processed "climatology constants" (like albedo, emissivity ...) are copied from the climatology file ; "pseudo-historical" variables (like roughness length) are copied as well from the climatology file. Prognostic fields (like surface temperature, water contents, snow depth) are interpolated considering their departure from the climatology.

To do all that, it is then necessary to provide monthly climatology datasets of both the post-processing domain and the model one.

Note that computation of post-processed PBL fields would benefit from the improved computation of surface temperature, water contents, etc.

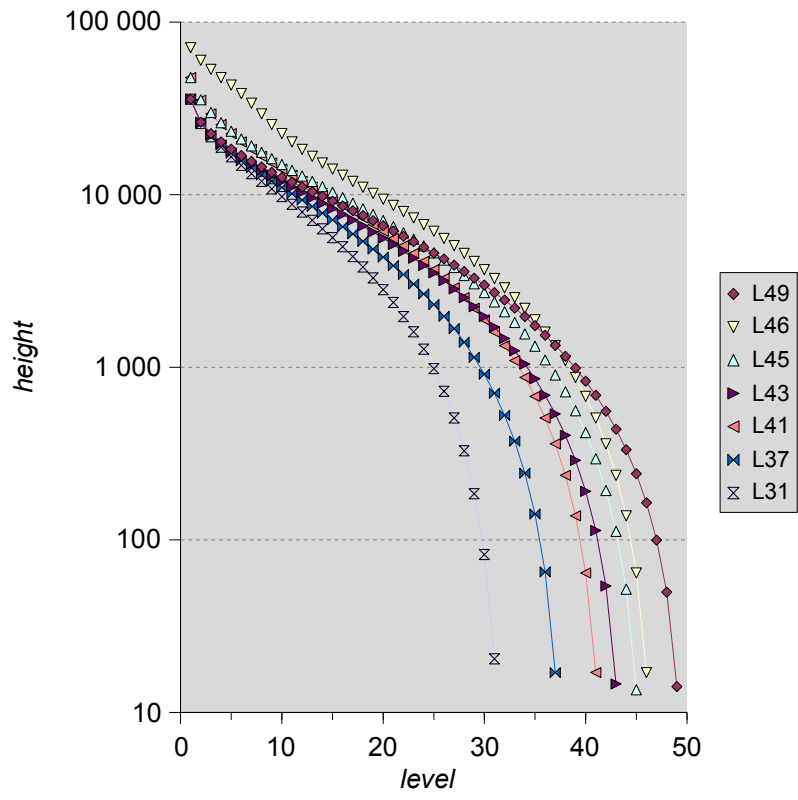
### 2.1.9. Other local domains

Partner	Application	Name	Gridpoint resolution	Number of gridpoints	Centre of domain	Trunc.
<b>Belgium</b>	research	small lin.	6.97 km	97;97 (108;108)	50.47°N; 4.86°E	53;53
	"	small quad.	"	"	"	35;35
<b>Croatia</b>	HR dyn. adapt.	Senj	2.00 km	72;72 (80;80)	45.10°N;14.20°E	26;26
	"	Maslenica	"	"	44.20°N;15.50°E	"
	"	Split	"	"	43.30°N;16.70°E	"
	"	Dubrovnik	"	"	42.70°N;18.00°E	"
	"	Karlovac	"	"	45.40°N;15.70°E	"
	"	Osijek	"	"	45.50°N;18.90°E	"
	"	Dart	"	97;72 (108;80)	41.75°N;16.00°E	35;26
<b>Czech R.</b>	blending	CE	9.00 km	277;309 (288;320)	46.24°N;17.00°E	42;47
	"	MFSTEP	9.53 km	189;245 (200;256)	38.77°N; 9.00°E	22;28
<b>Hungary</b>	parallel suite		12.18 km	205;229 (216;240)	46.24°N;17.00°E	71;79
	HR dyn. adapt.	DADA	2.37 km	169;239 (180;250)	47.35°N;19.12°E	59;83
	DADA post-p.		0.021°	161;337	47.27°N;19.50°E	
<b>Poland</b>	HR dyn. adapt.		2.78 km	169;169 (180;180)	50.00°N;20.00°E	59;59
<b>Romania</b>	HR dyn. adapt.	MARE	2.50 km	89;109 (120;100)	44.70°N;29.50°E	39;33
	"	VALE	"	89; 89 (100;100)	45.50°N;25.00°E	33;33
<b>Slovakia</b>	HR dyn. adapt.	sk25	2.50 km	189;289 (200;300)	48.70°N;19.70°E	66;99
<b>Slovenia</b>	HR dyn. adapt.	SIDA	2.50 km	108;148 (120;160)	45.80°N;14.50°E	39;49

### 2.1.10. Vertical discretization

Six different vertical grids are used in operations and another one (L46) is under test for ALADIN-France. The repartition of vertical levels with height for a standard atmosphere is described the figure hereafter.

The lowest level lies between 14 m (L45, 49) and 20 m (L31), while the highest one is between 13.6 hPa (L31, 37, 43, 49) and 0.1 hPa (L46).



## 2.2. Changes in the Operational Version of ARPEGE

(more details joel.stein@meteo.fr)

### 2.2.1. 8th March: modification of the mixing lengths of the turbulence scheme and use of the AMSU-A radiances of the AQUA satellite

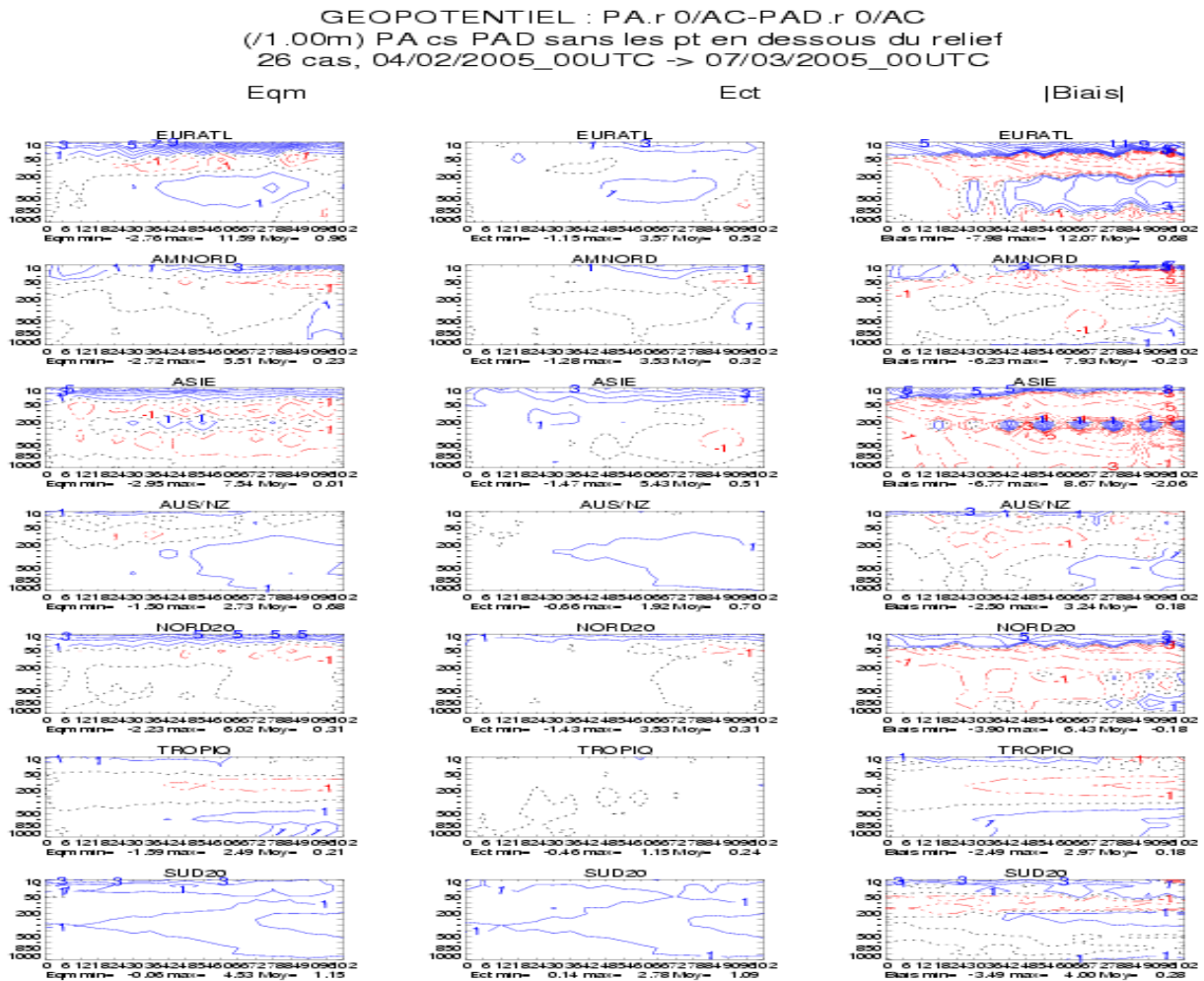


Figure 1: First parallel suite in 2005 : comparison of the operational forecast and the new version against the TEMP observations. The isolines of the geopotential are plotted every meter. The blue isolines correspond to an improvement and the red ones to a deterioration.

A new formulation of the mixing lengths has been proposed by Eric Bazile (Météo-France) and tested against the GABLS data set (see the previous Newsletter). This modification has been tested together with an increase of the thermal inertia of the vegetation. This second modification was necessary because the diurnal variation of the bias of the temperature was increased by 20 % when only the modification of the mixing length was taken into account. Thus, the thermal inertia of the vegetation returned to the value operational before the last change, operated the 19 October 2004. This new turbulence scheme was tested over Europe during a particularly cold winter and provides improved forecasts for the geopotential height and wind over this region but also in the southern hemisphere (Figure 1).

#### 2.2.2. 31st May: technical change (cycle 29T1)

This is a technical change which leads to a neutral impact for the quality of the forecasts. Among the technical changes, we can mention that the cycle 8 of the RTTOV library, necessary for the assimilation of the satellite radiances, is now operational. And, as an unexpected by-product, a small increase in the size of the coupling files, by about 3 %, has been noticed.

### 2.3. AUSTRIA

(more details thomas.haiden@zamg.ac.at)

There have been no changes in ALADIN-AUSTRIA since the last Newsletter

### 2.4. BELGIUM

(more details olivier.latinne@oma.be)

We actually run ALADIN on cycle 28T3 with a patch of low cloudiness developed by the Prague group.

We are planning to make two important modifications for the beginning of October, we will:

- 1) start to run ALADIN version 29 in a parallel chain on a new Silicon Graphics (SGI) parallel computer with 56 Itanium2 processors, 112 GB RAM and 2 x 1168 local disk.
- 2) make 4 runs by day.

### 2.5. BULGARIA

(more details andrey.bogatchev@meteo.bg)

No news.

### 2.6. CROATIA

(more details tudor@cirus.dhz.hr,ivateks@cirus.dhz.hr)

#### 2.6.1. Summary

The operational suite has suffered from numerous problems with hardware. The operational ALADIN forecast did run as scheduled, only the time it finished was delayed by up to one hour.

#### 2.6.2. Operational suite

##### x Status

ALADIN is operationally run twice a day, for 00 and 12 UTC. Coupling files are retrieved from ARPEGE ( Mété-France global model) via internet and RETIM2000. Model resolutions are 12.2 km for LACE domain, 8 km for Croatian and 2 km for the high-resolution dynamical adaptation domains. The execution of the suite is controlled by OpenPBS (Portable Batch System) as queuing system.

Initialisation of ALADIN on LACE domain is provided by Digital Filter Initialisation (DFI). Coupling frequency and frequency of output files for the LACE and Croatian domains are 3 hours. When the 48 hours forecast on the LACE domain is finished, 48 hours forecast for Croatian domain starts without initialisation, with coupling files from LACE.

Visualisation of numerous meteorological fields are done on LINUX PC. Comparison of forecasts with SYNOP data are done hourly for today's and yesterday's forecasts. The products are available on Intranet & Internet. Internet address with some of the ALADIN products, like total precipitation and 10 m wind : [http://prognoza.hr/aladin\\_prognoza\\_e.html](http://prognoza.hr/aladin_prognoza_e.html) .

##### x Domains

Horizontal resolution of the LACE domain is 12.2 km, with 37 levels in the vertical, time-step 514 sec, 229x205 grid points (240x216 with extension zone). Corners: SW (34.00N,2.18E), NE (55.62N,39.08E).

Horizontal resolution of Croatian domains is 8 km, with 37 levels in the vertical, time-step 327 sec, 169x149 grid points (180x160). Corners: SW (39.00N,5.25E), NE (49.57N,22.30E).

6 domains are used for the dynamical adaptation of the wind field in the lower troposphere to 2-km resolution orography for mountainous parts of Croatia. Dynamical adaptation is run sequentially for each output file, with 3 hour interval. In the dynamical adaptation meteorological fields are first interpolated from input 8-km resolution to the dynamical adaptation 2-km resolution. The same file is used as initial and as coupling file.

### x Operational model version

The operational model version is AL25T1 export version.

### x Problems

4th May 2005, 4 disks of the RAID5 system collapsed, machine was re-established by the end of May, all data connected to research and a part of operationally stored data (1.5 Tb) were lost.

12th May 2005, 4 processors on the SGI became useless due to a broken switch that was repaired the next day, and lost again the day after. 18th May 2005, 2 processors became permanently gone and got replaced on 31st May 2005.

### x Plans

Switch to a configuration of AL28T3 without envelope, new gravity wave drag, cloudiness and radiation packages and semi-Lagrangian horizontal diffusion. The new snow scheme will be used after the required fields become available in the coupling files.

Switch to a single big domain with 8 km resolution in the place of the LACE and the current operational Croatian domain and prolongate the forecast range to 54 hours. The increase of the vertical resolution is being considered.

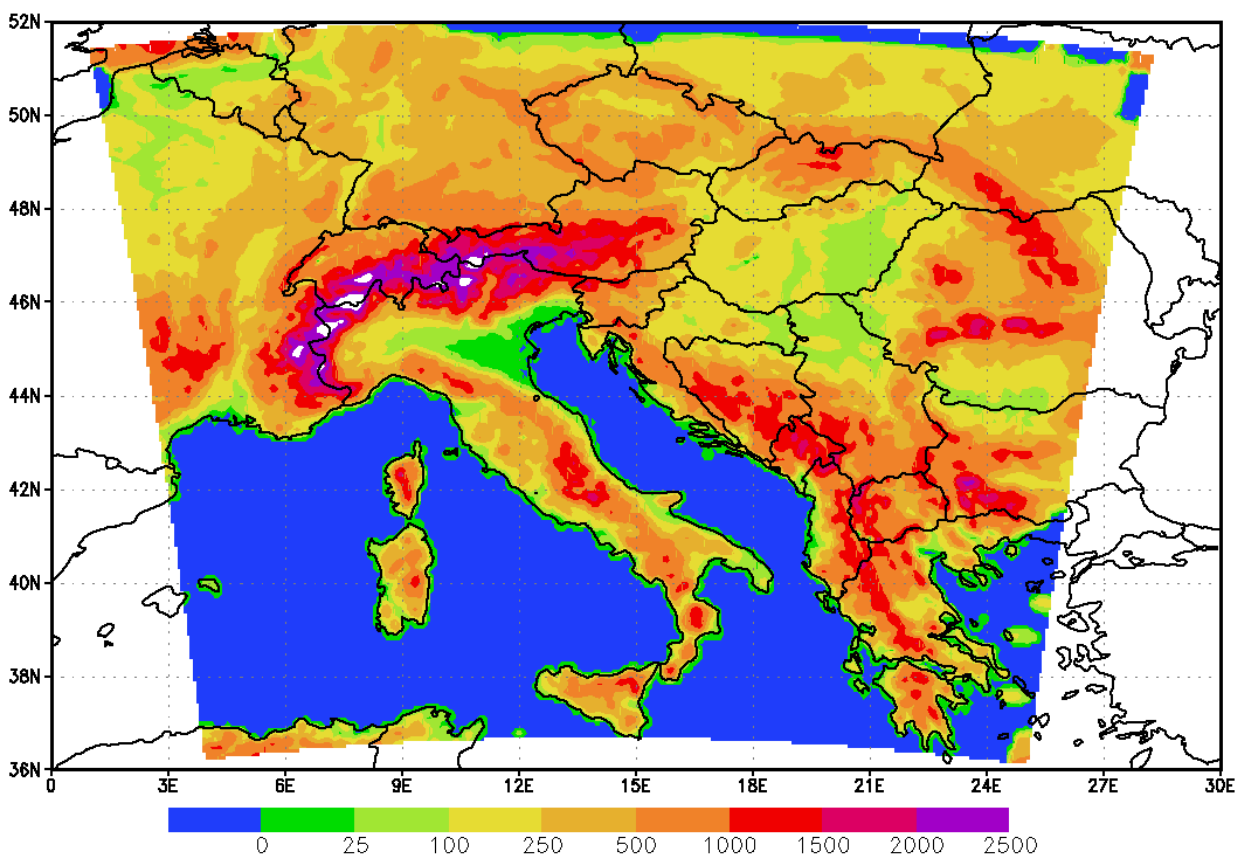


Figure 1. Planned new Croatian domain.

## 2.7. CZECH REPUBLIC

### 2.7.1. Operations

The ALADIN/CE suite was switched to the cycle **28T3** on:

**31/03/2005** at 12 UTC network time for the production run and at 06 UTC network time for the assimilation cycle.

This switch was technical; new cycle was validated to give the same meteorological results as the operational branch developed on the cycle 25T4. For the adiabatic model the norms were bit identical between the two cycles. When validating the code with physics, we noticed that some routines (namely *accvimp* and *accvimpd*) were changing results more significantly pending the release of compiler. Therefore we could not move on to higher compiler releases until this problem was fixed with help of NEC analyst: it turned out it was enough to add a compilation option to treat the occurrence of negative zeros. Then the entire library was recompiled, using the latest compiler release. The bit identical norms were not obtained either for the code with physics but a parallel suite (ADZ) gave neutral scores.

The operational suite was switched to the library compiled with the compiler release 305 on:

**14/06/2005** at 12 UTC network time for the production run and at 06 UTC network time for the assimilation cycle.

### 2.7.2. Parallel Suites & Maintenance

In spring a family of parallel suites tested the spline interpolators used together with SLHD (suites ADU, ADV, ADW and ADY), following Váňa, 2005 (article in Newsletter 27). As expected, the use of spline interpolators improved the bias of surface pressure. On the other hand, biases worsened in mid troposphere. One plausible explanation is that these interpolators counter the 3D effect of SLHD (cf suite ADY). Unfortunately it was not possible to get a combination of interpolators keeping the improvement of surface pressure bias alone.

Another family of parallel suites gives as well mitigate results but is promising for the future (set of tests from AEB to AEG). It tests a new computation of the mixing length according to Ayotte-Tudor, including the tunings. This modification changes the results only when we have typical winter situations with the blocking effects of the mountains. In such situations we obtain a nice improvement of temperature and wind scores at the top of PBL (at 850 hPa), see Figure 1. Unfortunately at the same time the already cold bias of the screen-level temperature gets even cooler (Figure 2). This fact disables for the time being the operational use of this type of mixing length, till we combine it with the improved radiation scheme allowing for more surface heating under the winter sun. This improvement is already under development in the framework of ALARO streams.

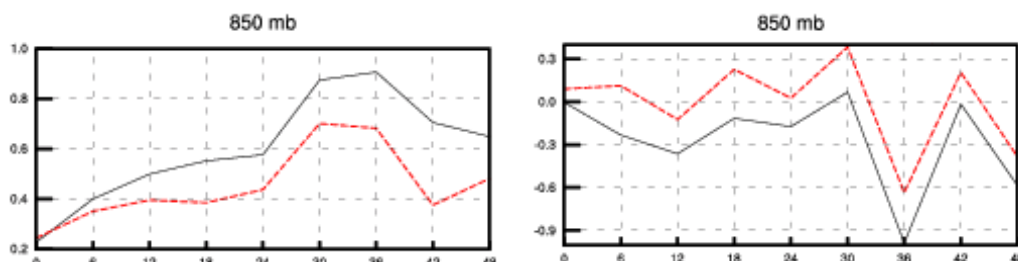


Figure 1: AEE suite scores (red dashed lines) compared to the reference (black solid lines) for the winter testing period. 850 hPa temperature bias is on the left panel, wind speed bias is on the right panel.

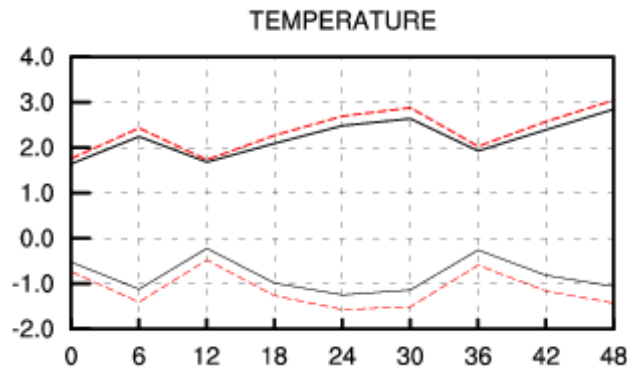


Figure 2: AEE suite scores (red dashed lines) compared to the reference (black solid lines) for the winter testing period. Screen-level temperature RMSE (upper curves) and bias (lower curves).

Finally, surface assimilation using CANARI is tested instead of surface blending (suite ADX). In this configuration the surface analysis is made first, prior to spectral blending; this configuration is called as CANSBLEND. However the existing tools for surface blending are still used in order to impose the ARPEGE analysis of sea surface temperature; the sea analysis in ALADIN is switched off. The analysis uses a dense network of SYNOP stations and is tuned as such. Results of this suite are rather encouraging: we can observe improved scores for the screen-level temperature, in bias, visible for the whole forecasting length (48 h in parallel suites), see Figure 3. The ADX test runs continuously since 18 May 2005 and shall continue longer, namely to observe the switch from summer to winter conditions.

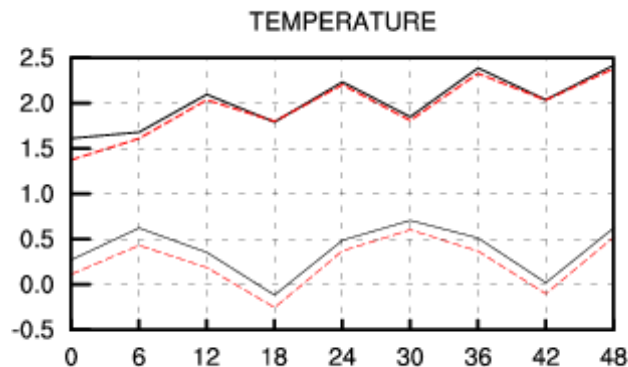


Figure 3 : ADX suite scores (red dashed lines) compared to the reference (black solid lines) for the month of June 2005. Screen-level temperature RMSE (upper curves) and bias (lower curves).

## 2.8. FRANCE

(more details joel.stein@meteo.fr)

No specific changes in the operational version of the ALADIN-France model.

It should be mentioned that a test of the 3d-var assimilation scheme for this model has been tested together with the move to cycle 29T1. This was the first step of the work performed in Météo-France to render operational an assimilation scheme for the LAM ALADIN-France (see the Bratislava presentation of Stein et al., 2005). A second version of the 3d-var assimilation scheme has been implemented and tested during summer 2005 and has led to a final approval of this version and a passage as operational model, on the 25th of July 2005. This will be documented in the next ALADIN Newsletter.

## 2.9. HUNGARY

(more details kerteszs@met.hu)

Significant changes were realised as far as the operational suite is concerned at the Hungarian Meteorological Service. After the full validation of cy28, this cycle is to be used for operations. The modifications of the operational suite were carried out in two consecutive steps:

a) The horizontal and vertical resolutions of the model were modified in dynamical adaptation mode (at the beginning of the year). The new characteristics of the model were as follows:

- Horizontal resolution: 8 km
- Vertical resolution: 49 levels
- Grid: linear

b) The dynamical adaptation was replaced by the three-dimensional data assimilation (3d-var) system (on 17th of May, 2005). The observations used are : SYNOP, TEMP, ATOVS: AMSU-A, AMDAR

(More details about the basic evaluation of the 3d-var system can be found in a separate article of this Newsletter)

Parallel suites are still kept alive, which are as follows at the moment:

- ALADIN dynamical adaptation in 8 km resolution (49 levels)
- ALADIN dynamical adaptation in 12 km resolution (37 levels)

The monitoring of all operational and parallel suites are based on web technology and comprises the following main aspects:

- Monitoring of operational and parallel suites (the data for the last two days can be retrieved through the control of file production during the execution,
- Observation monitoring system linked to the 3d-var data assimilation scheme (available observations, obs-guess statistics etc.).

The different model versions are inter-compared objectively and subjectively (a new interactive web-based verification software is also under development: easy-to-use verification of all the available NWP models at the Hungarian Meteorological Service).

Additionally there are some short-range ensemble products available for the forecasters through web-interfaces:

- COSMO-LEPS products received through ftp from Reading,
- SRNWP PEPS products received from DWD.

All these experimental products are monitored and compared to ALADIN/LAMEPS outputs for case studies.

## 2.10. MOROCCO

(more details jidane@marocmeteo.ma)

Nothing new.

## 2.11. POLAND

(more details [zijerczy@cyf-kr.edu.pl](mailto:zijerczy@cyf-kr.edu.pl))

Two major changes were introduced in first half of 2005 year. These are exchange of software for fetching coupling files from Météo-France servers and usage of doubled computational resources for some operational works.

New flexible software have replaced the old one being used since 1999 year for coupling files fetching. The developed set of Bourne scripts is accompanied by *pscan* port scanner written in Perl and available under GPL licence. *Nmap* scanner also can be applied if available.

ALADIN Group was granted at last with 16 processors and 8 GB of memory. Currently changes of operational suite make possible usage of mentioned computational resources for ee927 configuration purposes.

## 2.12. PORTUGAL

(more details [manuel.lopes@meteo.pt](mailto:manuel.lopes@meteo.pt))

No news.

## 2.13. ROMANIA

(more details [doina.banciu@meteo.inmh.ro](mailto:doina.banciu@meteo.inmh.ro))

The changes in the operational suite concern the ALADIN model version (cy28t3) and an additional integration of the model for the SELAM domain, mainly for Black Sea related applications (wave and marine circulation models).

## 2.14. SLOVAKIA

### 2.14.1. Summary

The current status and the evolution of the ALADIN/SHMU operational application during the first half of the year 2005 is described together with the other ALADIN-related activities at the Slovak Hydro-Meteorological Institute.

### 2.14.2. Operational ALADIN/SHMU system

There were no changes in the ALADIN/SHMU domain or computer characteristics during the described period.

Since 01/01/2005 the operational suite is non-stop (24/7) human monitored. Five persons are responsible for this monitoring, working on weekly shifts. The on-line monitoring and documentation system is used, accessible also via pocket communicator (PDA, see Fig. 1). PDA enables remote login to the computer system and necessary fixing of the aborted jobs in the emergency cases.

Within the last 6 months there were 11 serious crashes or substantial delays of our operational suite (end of suite delayed by more than 2 hours) and about 30 minor problems mainly in the products distribution to final users. The failures were originated by the following occasions (ordered by frequency):

1. Data distribution problems due to LAN/NFS crashes and remote servers connection errors.
2. Problem with LBC fetching because of weak internet connection, Local Area Network problems at SHMI, RETIM disfunctionality, Meteo-France HW/SW problems. (This problem is partly solved by sophisticated parallel LBC fetching via RETIM (usually fully available at 03:45 and 15:45 UTC) and INTERNET (usually fully available at 03:00 and 14:55 UTC)).
3. Problems with model output visualization (the visualisation software is sometimes not capable to contour too complicated fields – it is usually good indicator of severe weather conditions such as high precipitation rates:
4. HW/SW problems on SHMI HPC and other workstations (LoadLeveler queueing system bugs, storage problems, UPS weakness (one of the biggest crashes ever) => inevitable UPS upgrade for IBM HPC on 22/03/2005), insufficiently tested suite modifications.

The switch to +54h integration happened on the 12/01/2005.

The export versions of CY28T1 and T3 were ported. CY28T3 was validated in parallel suite, with non-satisfactory results, mainly in the cloudiness forecast. Later the so-called "\_czphys" package was implemented and tested (but without SLHD and still using the old version of the gravity wave-drag parametrisation with envelope orography, so, basically, cloudiness and radiation were changed). Good results were found both in the parallel suite and in the case studies (see Fig. 2). The CY28T3\_czphys version became operational on 31/03/2005 12 UTC.

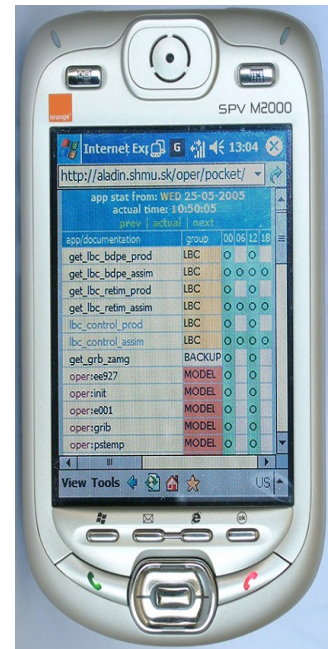


Figure 1 The PDA used to monitor the ALADIN/SHMU operational suite displaying its current status

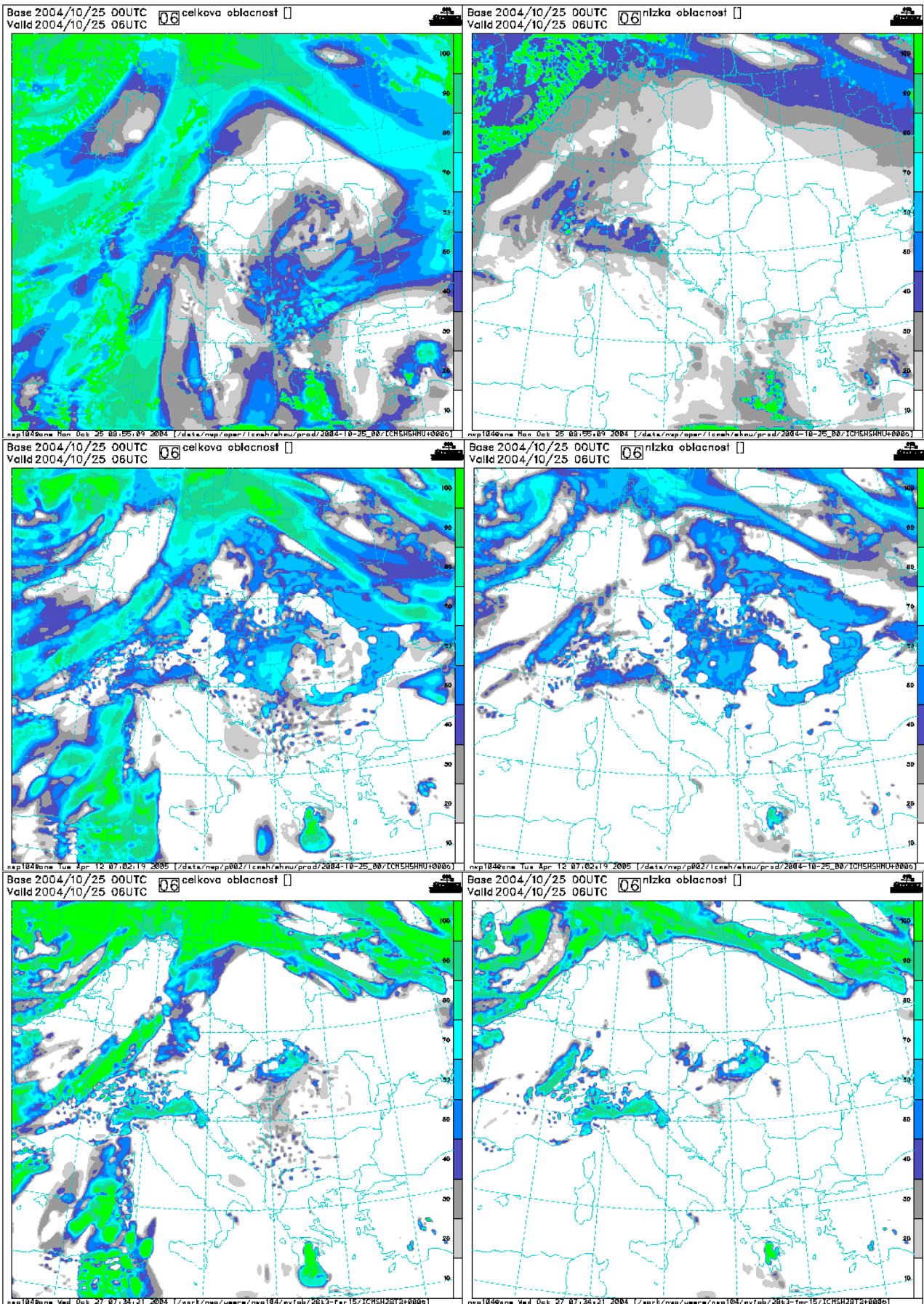


Figure 2 The total (left) and the low (right) cloudiness for the CY25T2 (top), the export version of CY28T3 (middle) and the "\_czphys" modifications (bottom)

On the 10/05/2005 the backup jobs ("fullposes") for ZAMG were activated.

On the 29/06/2005, a new automatically generated product - the meteogram based on the ALADIN/SHMU forecast, was introduced .

### **2.14.3. Other ALADIN-related activities**

The 15th ALADIN workshop "Quo vadis, ALADIN?" was organized in Bratislava, 6-10/06/2005.

Some tests with the Lopez microphysics scheme were made.

The feasibility study of the application of the MOS technique was performed.

### **2.14.4. Future plans**

The archiving machine IBM Tivoli (IBM TotalStorage 3584 Tape Library with 8TB LTO Data Cartridge and IBM Tivoli Storage Manager 5.3 software) shall be operational during this summer. Once ready, 4 runs per day will be introduced (these were already experimentally tested). The prolongation of the forecast range up to +72h is scheduled when the LBC data are available from Mété-France. Testing of the linear grid and of the mean orography are planned together with the porting of the ODB software and consequent testing of the assimilation tools like VERAL, Diag-Pack and DFI blending.

## **2.15. SLOVENIA**

(more details neva.pristov@rzs-hm.si )

The operational suite is monitored regularly and some small script improvements were done (earlier start of coupling file transfer, available number of processors for integration detected, supervision of SCORE). On the request of forecasters, forecast length was increased up to 54h (20/07/2005). The cluster system is still having some problems with stability, but with the help of automatic supervision system (SMS) and high availability (HA) functionality of SCORE cluster operational ALADIN products are (mostly) available on time. Since end of July the whole cluster system and operational suite is controlled by NAGIOS supervision system and failures are reported to e-mails and via SMS messages to mobile phones.

In April the coupling files from the ARPEGE model (transferred only via Internet from Toulouse) in the afternoon were quite often delayed because of the slow transfer rate (10kB/s). On the first of April the available bandwidth for the default ftp traffic in Météo-France was reduced. Situation improved after our IP address was declared in Météo-France.

The ALADIN cycle in operational suite is still cy25T1. When the code cy29 was available we decided to move on and forget cy28t3 (unresolved problems with xrd library manifesting in the configuration ee927). Some of the problems appear again in the new cycle in configuration ee927, but 001 configuration runs fine and it is running already in double suite. There are some unresolved problems with OpenMP configuration of ALADIN (001), but the early results are promising concerning timing and memory usage on 2 way Xeon systems. Initial efforts were done in porting AROME to the cluster but so far without success.

## **2.16. TUNISIA**

(more details nmiri@meteo.tn)

Nothing new.

### 3. RESEARCH & DEVELOPMENTS

#### 3.1. AUSTRIA

##### 3.1.1. Orographic precipitation (operational scheme vs. Lopez-scheme)

For a strong precipitation event in the Southern Alpine area in Austria during November 2000 a comparison between the operational precipitation scheme and Lopez-scheme was made. As shown in other case studies, there are several regions in the south of Austria (especially in Carinthia) which show a significant high percentage of cases where ALADIN (operational) tends to underestimate the precipitation amounts during southerly flows.

AVI00 PREC [mm/24h] valid: 20001106 00 UTC + 30

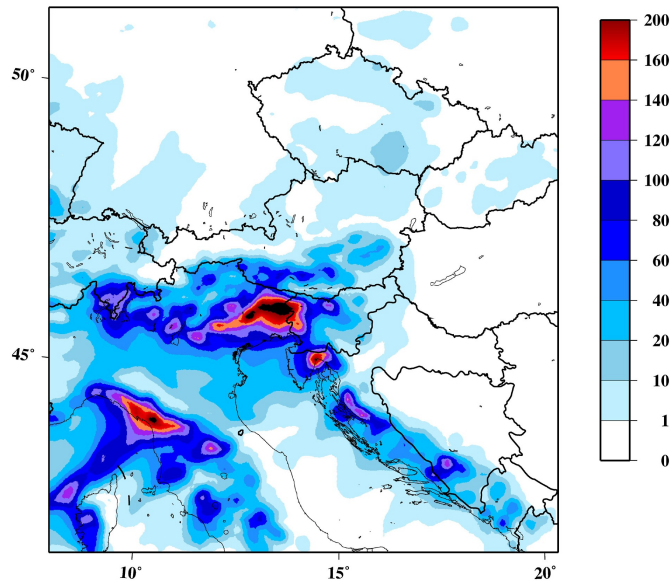


Figure 1 : ALADIN 24h precipitation forecast 20001106 06 – 20001107 06 UTC (operational scheme).

In comparison with the observed pattern (Figure 2) it can be seen that the operational scheme (Figure 1) shows a rather unrealistic precipitation pattern in some downwind areas, creating over-pronounced upslope precipitation amounts and significantly underestimated amounts on the lee side (Gail valley, Drau valley and the Klagenfurt basin).

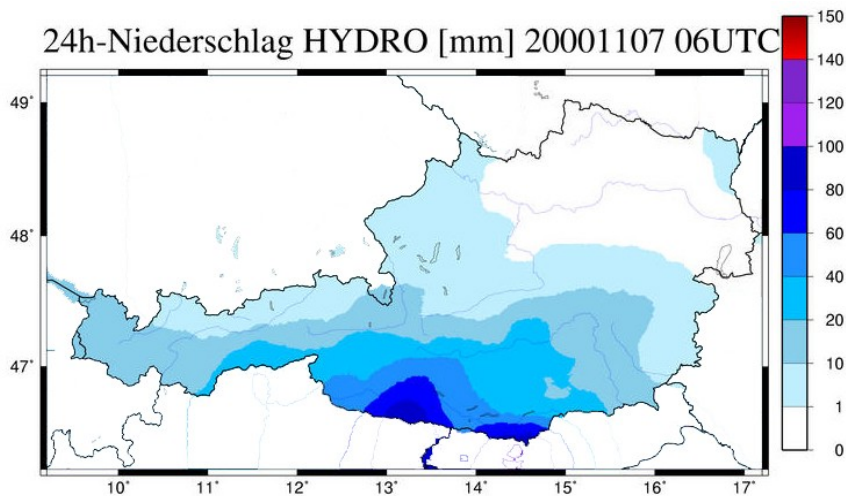


Figure 2: Observed 24h precipitation for the period 20001106 06 – 20001107 06 UTC (interpolated hydrological station data).

In Figure 3, the pattern obtained with Lopez scheme is shown. Apart from the fact that the peak values in the upslope areas in Italy and Slovenia are reduced, it is particularly striking that the precipitation fields in the named regions on the down-wind side get closer to reality. So, for this present case, the advection of cloud water (and precipitable water) to lee side can be handled in a more realistic way with Lopez scheme, whereas the diagnostic scheme produces an overestimated and unrealistic downwind/upwind precipitation contrast.

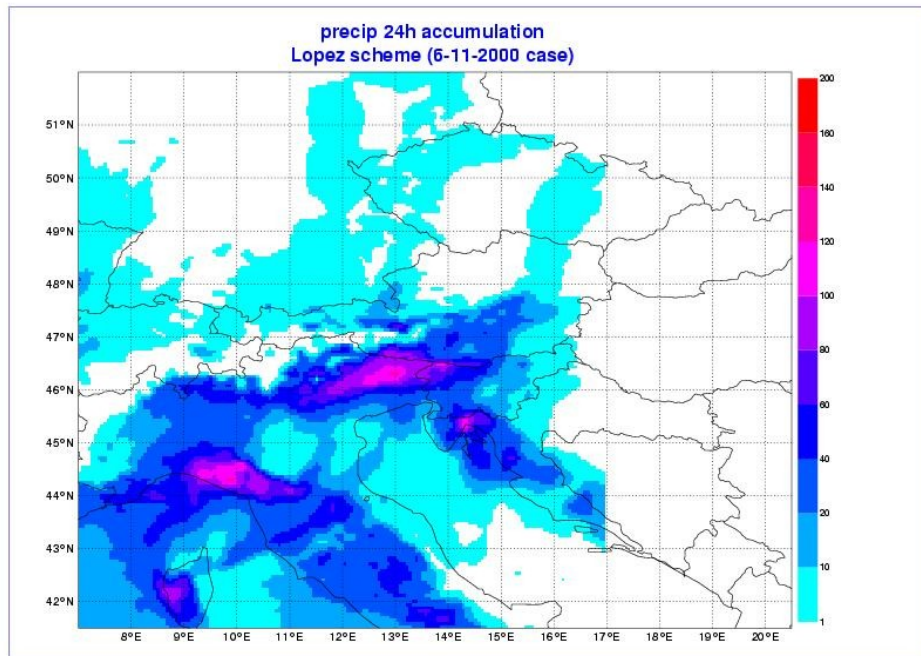


Figure 3: 24h precipitation forecast for the period 20001106 06 – 20001107 06 UTC (Lopez-scheme). By Yves Bouteloup, Météo-France.

*More information: christoph.wittmann @zamg.ac.at*

### 3.1.2. Development of the ALADIN Limited Area Ensemble Forecasting system LAEF

Efforts have been put on the development of different initial perturbation techniques, like breeding, ETKF (Ensemble Transform Kalman Filter) and ET (Ensemble Transform). Several experiments with breeding, coupled with control forecast as LBC (lateral boundary condition) and with ARPEGE EPS members as LBCs, and directly downscaling the ARPEGE EPS forecast have been carried out. The performance of the different methods and different LBCs has been investigated for the 2 weeks period of the Lothar Storm. Some results are encouraging. The above mentioned ETKF and ET methods have been implemented at ZAMG. The first results of ETKF and ET are being studied.

*More information: wang@zamg.ac.at*

### 3.1.3. Study on ALADIN physical parametrization over complex topography

Several physical parametrization schemes in ALADIN have been tested over mountainous area, which are Lopez microphysics scheme, modified Kann-Fritsch deep/shallow convection, prognostic TKE scheme. The focus has been put on the precipitation forecast. One of the most intense rainfall episodes during the Mesoscale Alpine Programme, MAP IOP2b (19-20 Sept. 1999) was used for all the experiments. The preliminary conclusion of this case study are summarized in the following:

- (1) In general, all the simulations have recognized the major features of the mesoscale structure, but many disagreements with the observations exist, especially in the region with complex topography.
- (2) The statistical verification scores of the experiments show that the Lopez microphysics

scheme together with the modified Kann-Fritsch deep convection scheme bring the most benefits on the ALADIN precipitation forecasts over complex mountainous area.

- (3) Some spurious strong precipitation on the wind ward side of the mountain has been removed by the Lopez scheme. There are also some signs for improvement of the rainfall forecast on the lee side of the mountain.
- (4) In the valley region, like Po valley, it is difficult to find any improvement. In the regions of steep mountain like Lago Maggiore area, all the schemes generalize the rainfall well compared with the observations.
- (5) The modified Kann-Fritsch convection scheme alone doesn't improve the forecast, but it makes the convection more organized than the Bougeault scheme.
- (6) The prognostic TKE parametrization has little impact on the precipitations for the MAP IOP2b case.
- (7) Longer time step lets less interaction between dynamics and physics in the model, which impacts on the precipitation forecast.

*More information: wang@zamg.ac.at*

#### **3.1.4. Development of the ALADIN-based nowcasting system INCA**

The analysis and nowcasting system INCA uses ALADIN forecasts (00 Z, 12 Z) as a basis for improved forecasts issued on a high temporal frequency (15 min for precipitation, 1 hour for other fields) and high spatial resolution (dx=1km, dz=100m). For temperature, humidity, and wind, 3D ALADIN forecast fields serve as a background on which corrections derived from comparison with observations are superimposed. In the case of precipitation and cloudiness, the forecast obtained by extrapolation methods is merged asymptotically with the ALADIN precipitation forecast. Major developments during the first half-year of 2005 include the kinematic downscaling of the ALADIN wind field from 9.6 to 1 km, using a relaxation algorithm under the constraint that wind observations at stations are (nearly) reproduced. The downscaling procedure is operationally producing a 3D wind field analysis and forecast every hour. Also under development is a visibility routine based on ALADIN humidity and cloudiness forecasts combined with MSG satellite data (fog product).

*More information: thomas.haiden@zamg.ac.at*

### **3.2. BELGIUM**

Informations in the next Newsletter

### **3.3. BULGARIA**

No news.

### **3.4. CROATIA**

#### **3.4.1. Semi-Lagrangian horizontal diffusion**

Semi-Lagrangian Horizontal Diffusion (SLHD) shows beneficial impact on the reduction of the overestimated cyclone intensity, correction of cyclone position while not altering a good intensity prediction and improvement of fog forecast in the valleys in an anticyclone.

#### **3.4.2. Radiation and cloudiness**

Unsatisfactory model forecast in fog has encouraged a study of alternative radiation and cloudiness schemes combined with different cloud overlap assumptions.

#### **3.4.3. Envelope or not?**

Removal of envelope and changes in gravity wave drag parametrization result in stronger winds on the windward and generally weaker winds on the leeward side of the obstacles, as well as mountain wave amplitude reduction and smoothing.

### 3.4.4. Vertical structure of bura flow

ALADIN 8 km and 2 km resolution dynamical adaptation forecasts and COAMPS-NH 3 km resolution forecast are compared to the aircraft measurements showing that ALADIN is able to reproduce the structure of PV banners, especially the 2 km resolution run.

### 3.4.5. Sensitivity to the initial conditions

Different initial and boundary conditions were used to run the ALADIN forecast: operational ARPEGE form 1999, ECMWF reanalysis from 2003 and a mixture of ECMWF upper-air and ARPEGE surface fields. Results of the numerical experiments show the higher sensitivity to the initial conditions for the MAP IOP 5 heavy precipitation case. Looking only on the wind field forecast during the MAP IOP 15, different initial conditions do not have a significant influence.

## 3.5. CZECH REPUBLIC

### 3.5.1. ALADIN/MFSTEP configuration

Since ALADIN/MFSTEP has been a very costly application, we explored ways to reduce it once the Target Observation Period was accomplished. Since the atmospheric forcing from ALADIN was used exclusively by oceanographers' groups working on the Western part of the Mediterranean basin, we negotiated limits of a new post-processing domain called West Sea. These limits turned out to be still out of reach, in case we would like to merge the MFSTEP and CE domains (it was seriously considered an option and discussed within LACE, due to its impact on the common telecommunication domain). For this reason we had to keep the two applications separated. First the post-processing domain was switched to the West Sea on 29 June 2005, while the change of the integration domain should happen in early July 2005.

Thanks to the validation of surface fluxes we have discovered a problem with ALADIN latent heat flux over the sea surface, where ALADIN had a non-negligible bias. Thus we retuned the Charnock formulae gustiness term to get rid of the latent heat flux bias (the saturation of moisture and heat flux is reached earlier). Now the values are fine both for weak and strong winds.

### 3.5.2. Optimisation and cleaning of ALADIN NH

The pseudo vertical divergence denoted as  $d_4$  represents till now the most stable option for the vertical-velocity based prognostic variable choice in the ALADIN NH dynamical core. It is defined as:

$$d_4 = d_3 + X$$

where  $d_3$  is the vertical part (corresponding to  $\partial w/\partial z$ ) and  $X$  is the horizontal wind-shear part of the total 3D divergence as computed in the  $\eta$ -coordinate system:

$$X = \frac{\partial V}{\partial \Phi} \cdot \nabla \Phi$$

While the evolution of  $d_3$  is computed as usual, the evolution of  $X$  is approximated by a first-order scheme (see the documentation on ALADIN NH for more details). When the  $d_4$  variable was implemented into ALADIN NH for the first time, it was convenient to explore several plausible solutions as regards the treatment of the  $X$  part (ND4SYS option in the code). It was also decided to bi-periodicise  $X$  tendency at every time-step. These solutions were suitable for research but costly. In addition, the ND4SYS variants were not respecting the exact diagnostic relationship  $d_4 = d_3 + X$  at every  $(x, y, \eta, t)$  and were re-using the first-order explicit estimates of  $X$  in the following time-step. This had an impact on the stability, pending which option of ND4SYS was used for which domain and meteorological situation. Therefore it was decided to retain the exact diagnostics of  $X$  whenever possible and to optimise the code of  $d_4$ . We established a plan of this

work in three steps: i) removal of option ND4SYS while respecting the diagnostic definition of  $X$ , ii) to include the spectral transforms of  $X$  in the same call as for the rest of prognostic variables while iii) removing the bi-periodic extension of  $X$  at every time-step and ensuring it by the lateral coupling.

Work on the recoding of the  $X$  pseudo-variable as part of  $d_4$  started in June and is supposed to be completed by the end of July 2005 and should enter cycle 30T1.

### 3.5.3. Set-up of SLHD

Although the SLHD scheme is implemented successfully in ALADIN/CE operational suite, its general setup for any horizontal resolution and domain size was not yet ready. In the late spring this missing piece of work was completed by Filip Váňa. Therefore we have now the setup rules and tunings for the SLHD scheme. The technical note explaining the basic properties of the SLHD as well as the recommended tunings as functions of the resolution and wave-length is under redaction and should be completed before the end of summer holidays.

### 3.6. FRANCE

A lot of phasing, plug-in, retuning and validations ... and not enough time to write a report.

More details in the presentations for the 15th ALADIN workshop and in the next Newsletter.

### 3.7. HUNGARY

The main orientation of the Hungarian Meteorological Service as far as ALADIN-related research and development is concerned is data assimilation, short range ensemble prediction and high resolution meso-gamma scale modelling (AROME model).

The main scientific aspects tackled during the first half of 2005 are as follows:

1. The further refinement of the three-dimensional variational data assimilation scheme. All the scientific and technical work on 3d-var led to the successful operational implementation of the data assimilation scheme (see also separate article). It should be also noted that significant efforts were pursued in order to establish the framework necessary for impact studies with the ALADIN model (required by EUCOS) using boundary conditions from the ECMWF/IFS model. The impact studies will address the relative weight (importance) of space and terrestrial components of the observing system (the project will take two years, first results are to be expected until the end of this year). For further application of new data types the main emphasis was put on the application of SATOB (Atmospheric Motion Winds from METEOSAT-8) and AMSU-B data in the data assimilation process.

2. The LAMEPS-related research and development had been continued with special emphasis on the further assessment of the downscaling of PEACE system (now with increased resolution) together with the optimal choice of the target domain and target time-window for the global singular vector computation. A one-month visit of Richard Mladek was carried out for studying the LAMEPS system and demonstrate its efficiency for some cases during the Czech floods.

3. Laszlo Kullmann overtook a one-month stay in Toulouse for studying the details of the AROME prototype with special emphasis on its practical installation and execution. The received version of the AROME model is basically adapted in Budapest and already some interesting meso-gamma scale events were selected, where the capability of the model will be tested (soon).

4. The dynamical downscaling of the ECMWF ERA40 data was continued for a 10 years period (1992-2001) and relevant wind climatology was computed over Hungary for the planetary boundary layer. The details and the first results of this work is presented in the same Newsletter.

5. The ALADIN-Climate model (AL15) was adapted at HMS and a one-month integration was carried out for the past. The results are now being compared to a reference run available in Toulouse. As soon as the inter-comparison is finished experiments with longer integration times will be launched.

### 3.8. MOROCCO

No news.

### 3.9. POLAND

See the report on operations.

### 3.10. PORTUGAL

No news.

### 3.11. ROMANIA

#### 3.11.1. Spectral coupling (Raluca Radu)

The impact of spectral coupling in ALADIN version 15\_03 was studied against the operational one. A daily data base over almost a year was realized and the response of the forecast model to the proposed coupling method versus the classic grid-point coupling method was analysed.

Going further with the validation of the spectral coupling method for ALADIN, aspects concerning its behaviour at finer resolution are investigated on some cases. The aim is to determine the physical processes leading to the accurate representation of a fluid sub-domain at smaller scales through the spectral treatment of the lateral boundary forcing. Another objective treated here is to analyse how the proposed coupling scheme performs in the ALADIN-NH version.

#### Tornado case (7.05.2005)

Several experiments were conducted in order to study the coupling methods impact on a tornado event (around 11 UTC, May 7, 2005 at north-east of Bucharest, marked with a circle on the satellite image from figure 1).

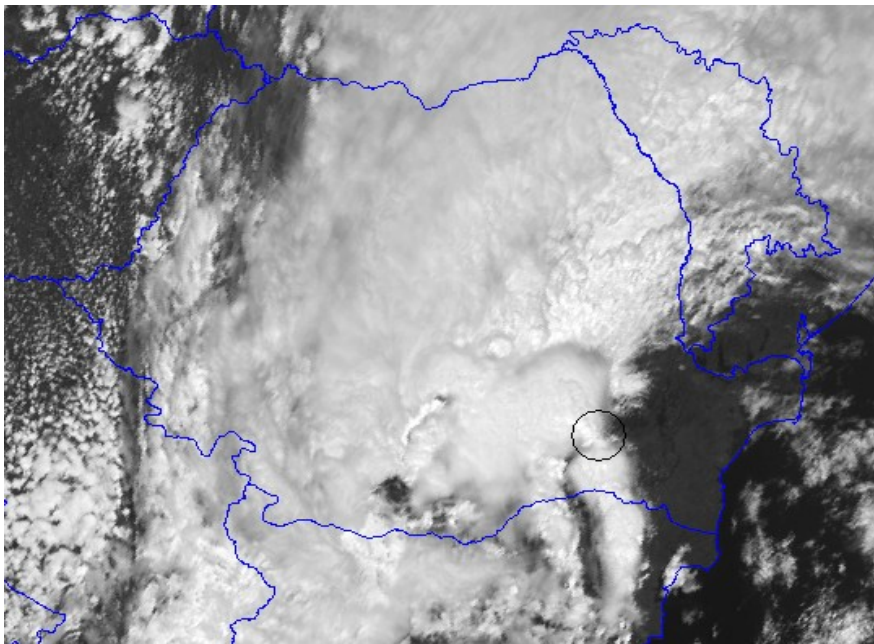


Fig. 1 : Satellite image (MSG, visible) – May 7, 2005, 11:00 GMT

The ALADIN (al15\_03 version) model was integrated for two domains : operational one (100x100 points, 10 km resolution) and a smaller one (50x50 points, 3.5 km resolution), using the classic and spectral coupling methods. The initial time of the numerical simulations is 6<sup>th</sup> of May 2005, 00 UTC.

For the 3.5 km resolution domain, experiments, using both hydrostatic (HH) and non-hydrostatic (NH) version, were performed in order to study the impact of coupling schemes correlated with non-hydrostatic dynamics. The main differences among different simulations made are presented in Table 1.

It is remarkable the way all experiments showed a good qualitative capacity to create the

correct, larger scale environment, leading to the strong frontogenesis at the right moment, corresponding to 35 hour forecast range).

	3.5 km (Bucharest domain)	10 km (Romania domain)
ALADIN-NH	OP SP (k0=0,k1=7) SP (k0=1,k1=7)	
ALADIN-HH	OP SP (k0=1,k1=7)	OP SP (k0=2,k1=10)

Table 1. Experiments with ALADIN-NH and ALADIN-HH: OP (operational grid point coupling), SP (spectral coupling, extended to all coupled variables in NH experiments), k0, k1- parameters for spectral relaxation.

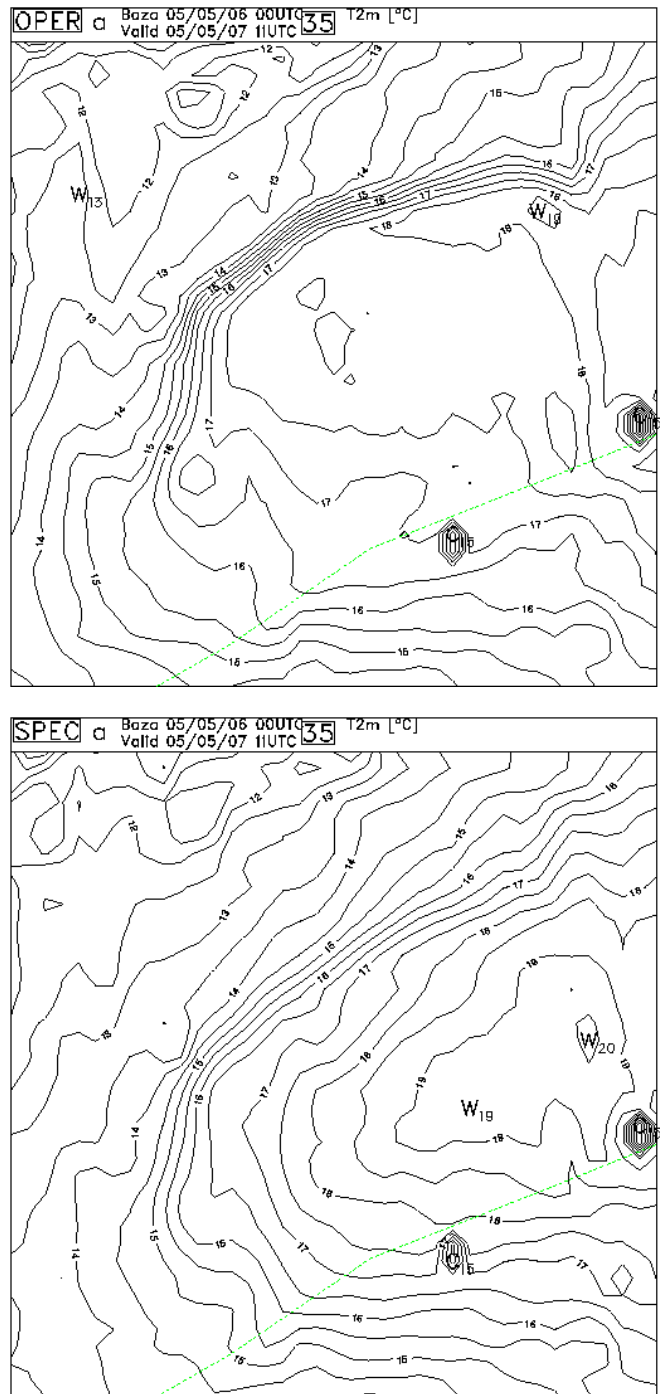


Fig. 2 : 2m temperature after 35 hours of integration : operational coupling (top) and spectral coupling (bottom)

The grid point coupling succeeds to better catch the local features (the strong temperature gradient see fig. 2; NB: the small cold nuclei correspond to some problems in the climatic file), while the spectral coupling seems to better represent the magnitude of the event.

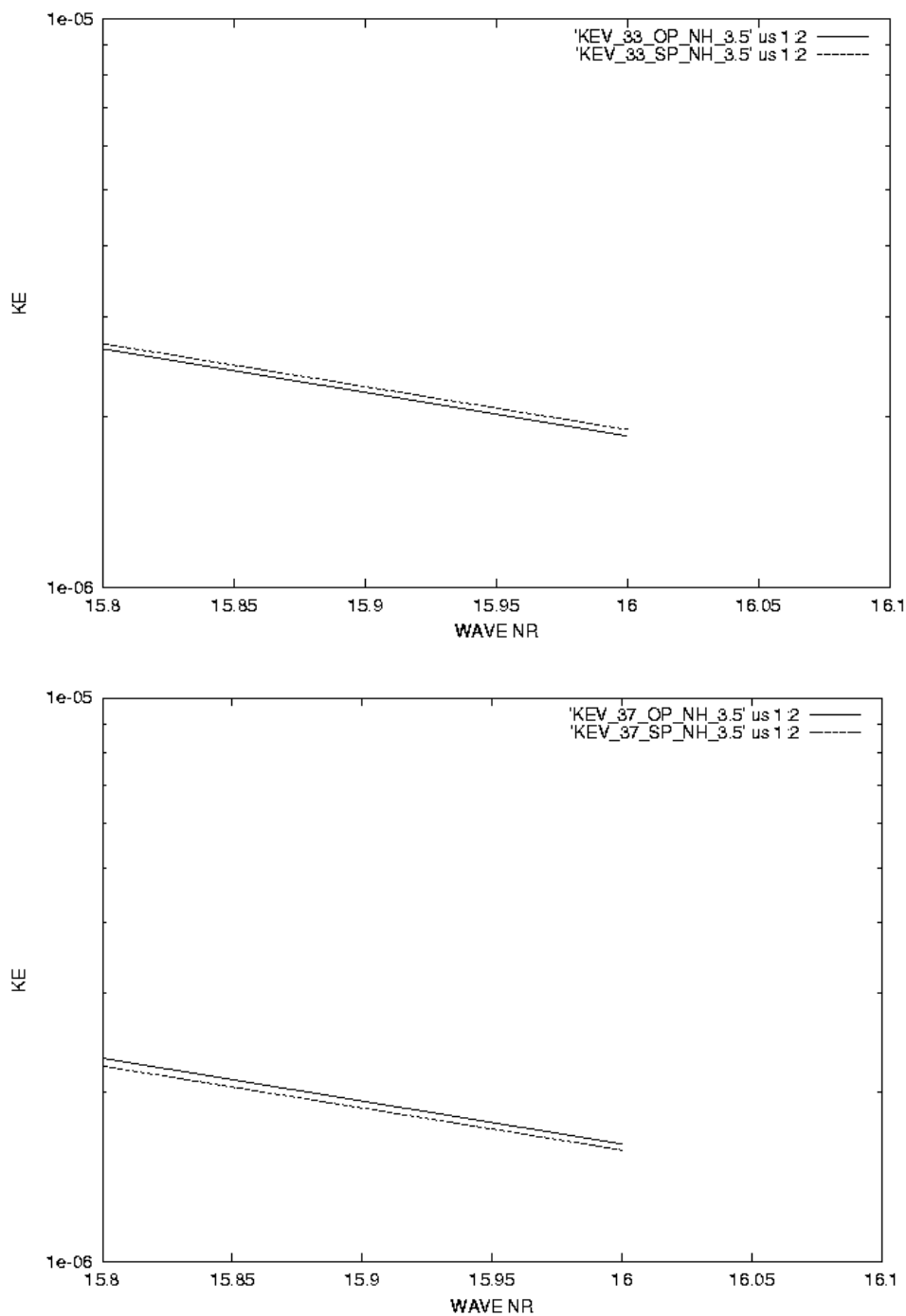


Fig. 3 : Kinetic energy spectra after 33 hours (top) and 37 hours (bottom); full line for operational coupling, dash line for spectral coupling

Spectra analysis shows a growth of the kinetic energy and relative vorticity for short waves during the event time, when the spectral coupling is used for both domains. For the 3.5 km resolution, the growth appears even with 2 hours anticipation (fig. 3, top part). In the next following hours, a sudden falling down of the kinetic energy was noticed (fig. 3 bottom part).

Further work will continue with analysis of simulated instability conditions.

### 3.11.2. New experiments with the high-resolution dynamical adaptation of the surface wind forecast using the hydrostatic and non-hydrostatic versions of the ALADIN/Romania model (Steluta Alexandru)

A five months period of evaluation (in terms of statistical measures) was realized by comparison with the real measurements, for the surface wind forecast obtained by the operational

model (at 10 km resolution) and using high-resolution dynamical adaptation method for the hydrostatic ALADIN/Romania model (at 2.5 km resolution). Also the forecasts of the 10 m wind field obtained with the hydrostatic and non-hydrostatic ALADIN/Romania models at high-resolution were illustrated during two snowstorms. All these results have been brought together into an article submitted to the "Romanian Journal of Meteorology", with the name "High-resolution dynamical adaptation of the ALADIN/Romania model's surface wind forecast".

### 3.11.3. ALADIN/Romania meteograms (Steluta Alexandru)

The meteogram format has been changed, including new fields: 2m relative humidity, convective precipitation, relative humidity field in altitude, 1000-500 hPa thickness, 2m dew point temperature. Also new towns have been added, covering each county of Romania. A meteogram's example for Resita city is presented below.

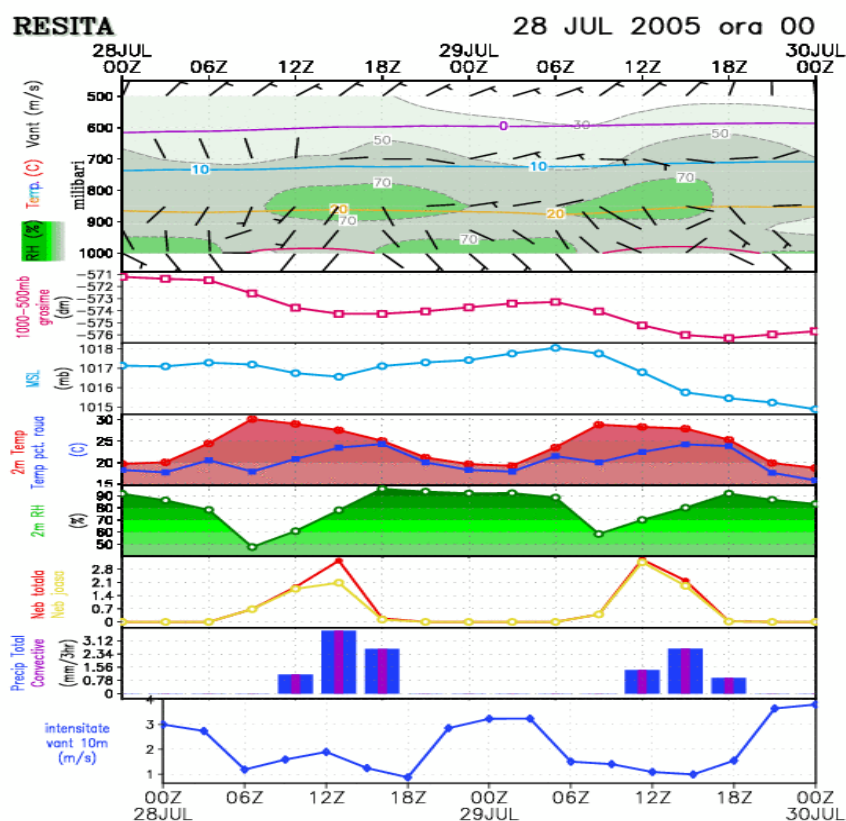


Fig. 4 : ALADIN meteogram

### 3.11.4. ALADIN diagnostic package (Simona Stefanescu)

The results of DIAGPACK, operationally implemented, are the basis of different diagnostics computations (CAPE, MOCON, stability indices) mainly used by the nowcasting department.

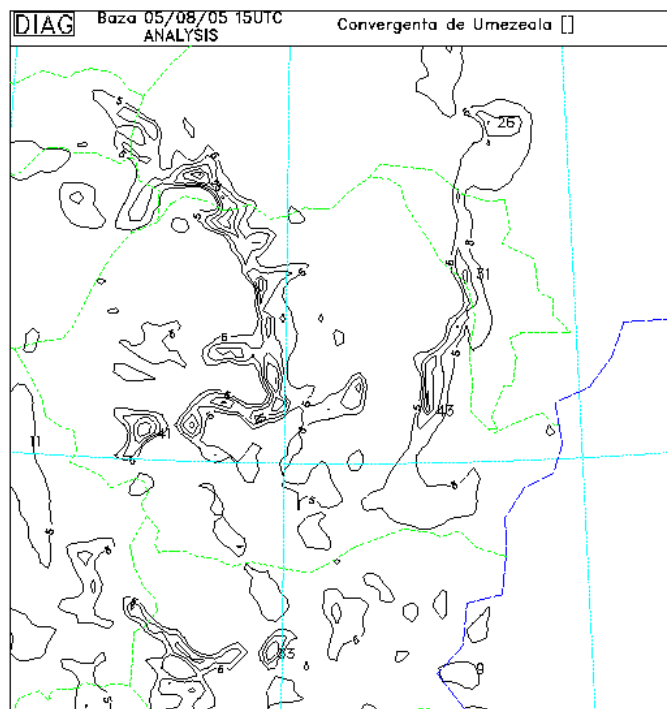
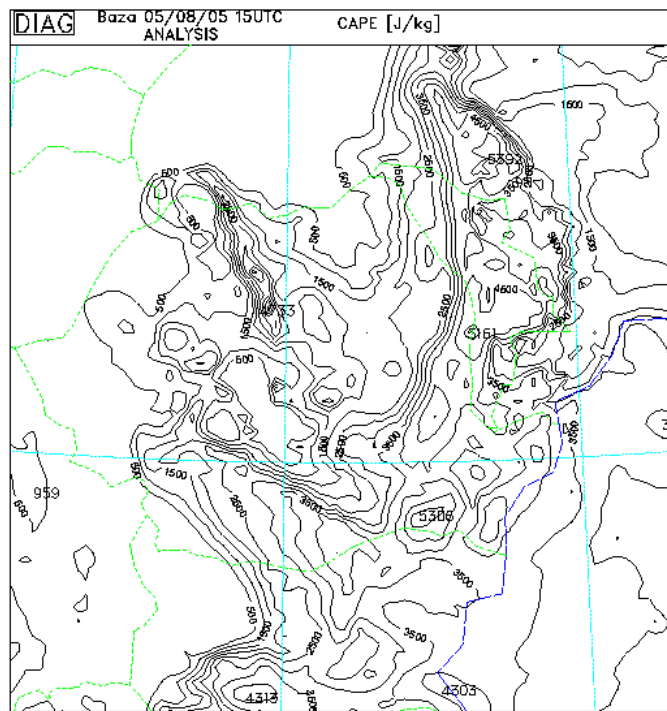


Fig. 5 : CAPE (top) and MOCON obtained by using DIAGPACK

### 3.11.5. A heavy precipitation case generated by short tropospheric waves (Forinela Popa, Doina Banciu, Viorica Dima)

The large amounts of precipitation registered in Romania in the last half of April were mainly generated by the fast evolution of short tropospheric waves, which evolved in the upper and medium levels of the troposphere. Between 13th and 27th of April, four such tropospheric waves crossed the Romanian territory, the second one (17th to 19th of April) being the most severe one and therefore being chosen for a detailed analysis. During this period, in the Banat area heavy rains have fallen in a relatively short time, inducing floods. The water-vapour satellite imagery and the outputs of the ALADIN model (especially the potential vorticity field), were extensively used. A

special attention was paid to the evolution in the upper half of the troposphere, at the tropopause level and in the low stratosphere.

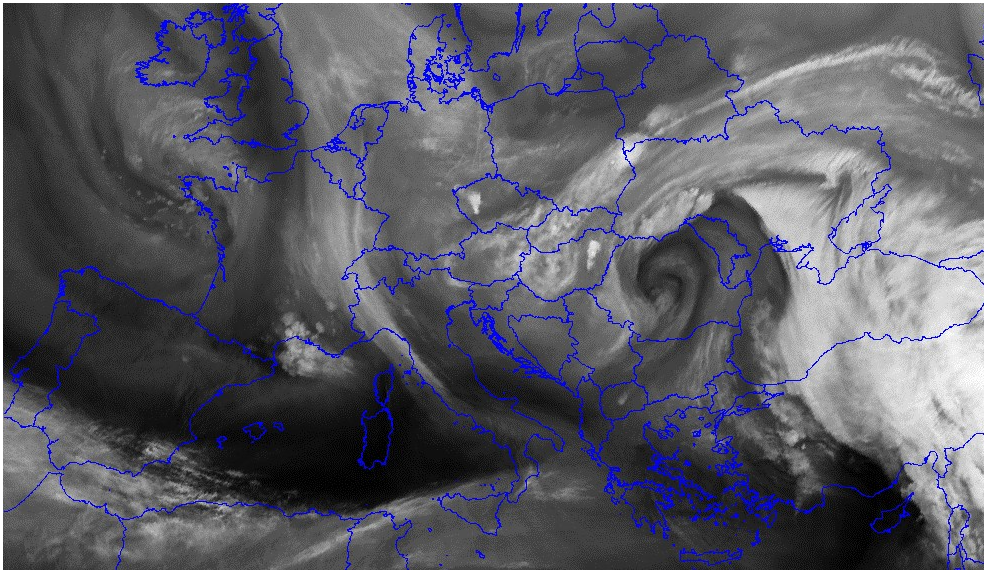


Fig. 6: Water vapour MSG image, April 18, 18:00 UTC

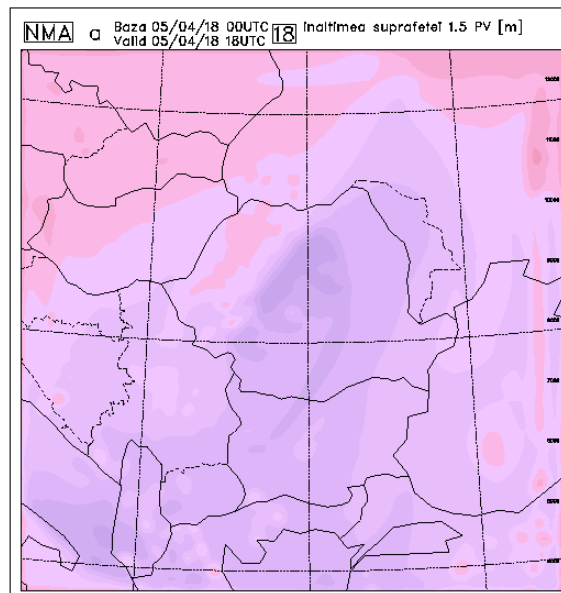


Fig. 7 : 1.5 PV height forecasted by the ALADIN model: April 18, 2005, 00 + 18 UTC

### 3.11.6. CONVEX experiment (Anca Barbu, Doina Banciu)

Between the 11–12-th of May 2005 in Romania took place an international exercise, CONVEX-3, when a nuclear accident at the power plant in Cernavoda has been simulated. The exercise has been coordinated by a Committee members from: IAEA, NEA/OECD (Nuclear Energy Agency/Organization for Economic Co-operation and Development), OCHA (United Nation Office for the Co-ordination of Humanitarian Affairs), WHO (World Health Organization) and WMO (World Meteorological Organization).

National Meteorological Administration (NMA) of Romania participated in the exercise with meteorological forecast provided by the ALADIN model, pollutant concentration forecast obtained by the coupled system ALADIN model – MEDIA model, 48 hours trajectories (issued from the trajectory model using ALADIN forecasted wind). The results – maps containing the distribution of the pollutant cloud and trajectories have been communicated to the decision factors and also stored

on the web page of the NMA.

The outputs of the models were, generally, in accordance with those provided from Météo-France and the Met Office. However, there were some differences with respect to the vertical and horizontal particle displacement.

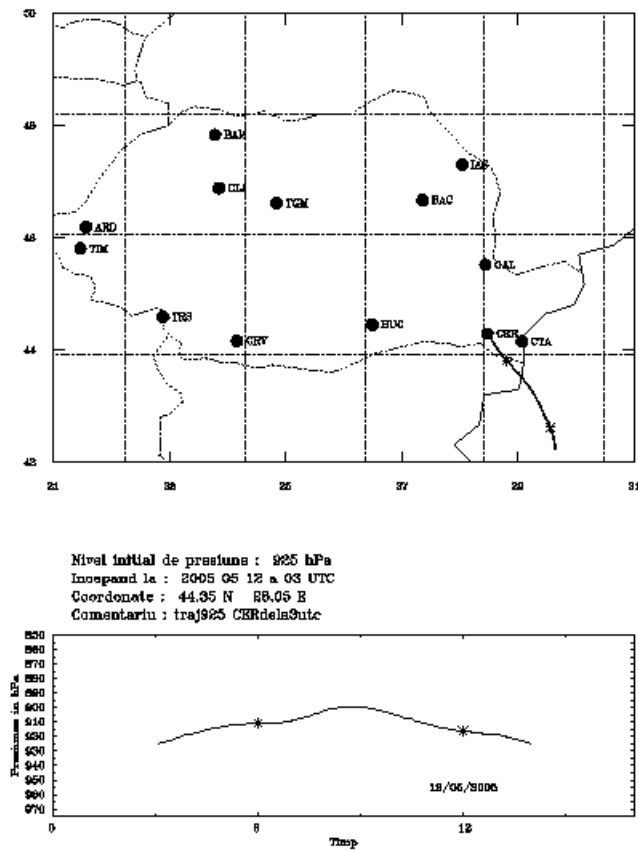


Fig. 8: 48 hours trajectory with the initial point at 925 hPa

Some differences appear also in the position of the pollutant cloud. In ARPEGE forecast, the highest concentration nucleus is focused in the area of the source while ALADIN splits this nucleus in two parts, equal in intensity, one, West of the source, and the other one, South of the source.

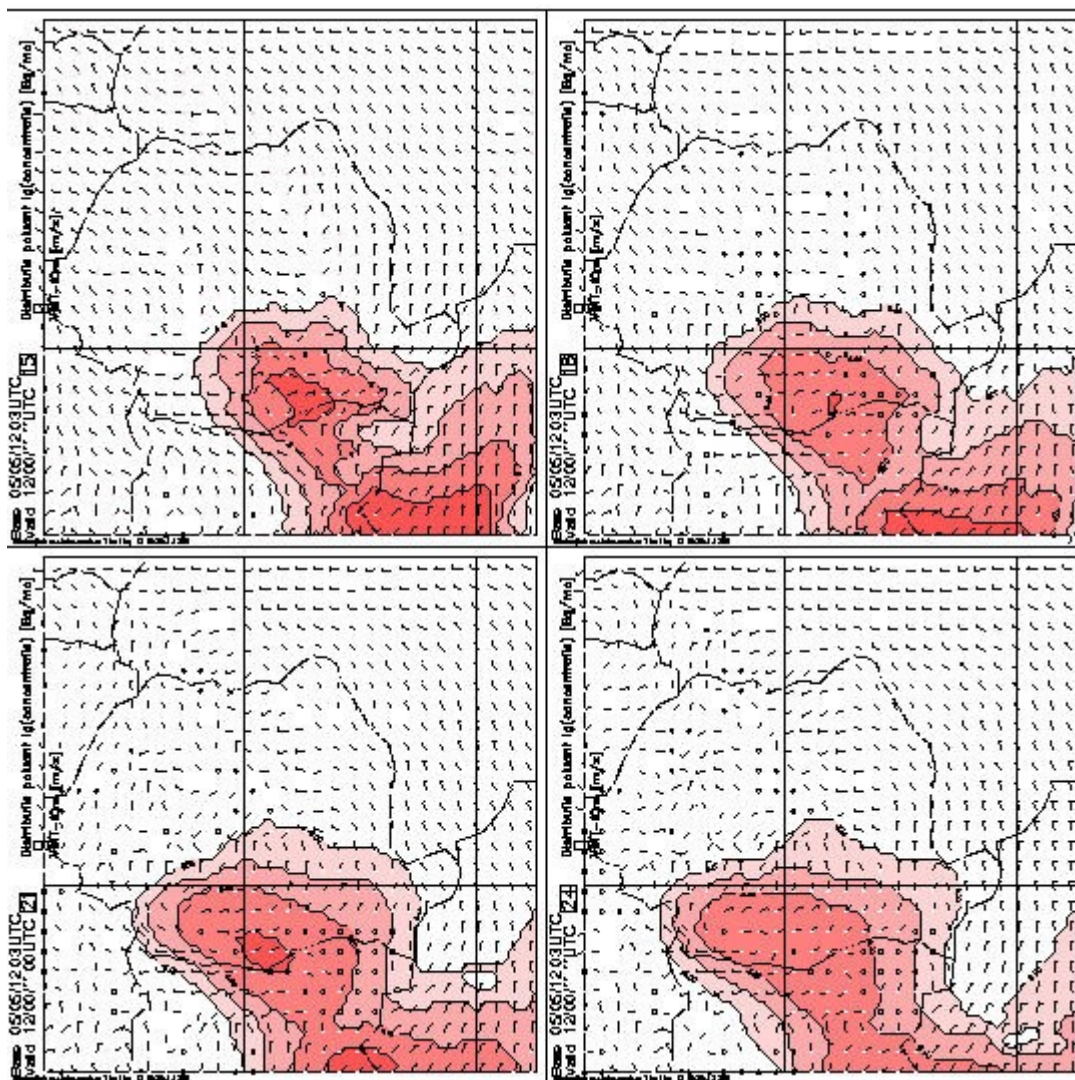


Fig. 9 : Pollutant concentration for 15, 18,21 and 24 hour forecast ranges

### 3.12. SLOVAKIA

See the general report on Operations.

Significant effort was also dedicated to PhD theses and to the organization of the ALADIN workshop.

### 3.13. SLOVENIA

(more details [neva.pristov@rzs-hm.si](mailto:neva.pristov@rzs-hm.si))

Report on «Latent heat nudging» and « High resolution wind climatology » can be found in the dedicated papers in this Newsletter.

#### Verification project

The web interface for verification is working, but is not very often used. Database is filled regularly with observations and model data from 8 countries (Austria, Croatia, Czech Republic, Hungary, Slovakia, Slovenia, Romania, Tunisia). Since mid-April, model data from Czech Republic and also upper air values from ARPEGE (calculated from coupling files) are available. All centers send data from their operational application and some also from double suites, so there are up to 14 various models represented.

Statistical packet R was tested for calculation and displaying of the results. Fewer problems than in the current *php* calculation and *JPgraph* visualisation were detected, but developments stopped

because Miha Razinger has temporarily left for the ECMWF.

New dedicated 2-way Opteron server is available since June. Current application was ported to the new server and a detailed study of database performance is going on. First results are quite promising. When the testing phase will be over, the whole production will be moved to the new system. The improved web interface will be available at that time as well. With the help of other centers we would like to define and prepare automatic regular monthly production of verification reports.

### 3.14. TUNISIA

With the aim of improving quality of the temperature forecast and touching new users more demanding than general public as regards forecast precision, a procedure of type MOS (Model Output Statistics) was tested for the forecast of extreme temperatures (minimal and maximal) for the following day.

This was applied to the 26 synoptic stations by establishing during a "training" period (year 2003) a synchronous statistical link between the forecast of the dynamical model ALADIN and the maximal or minimal temperature.

The selected predictors are the temperature at the 8 closest gridpoints for each station, at 5 standard levels : 2 m, 1000 hPa, 950 hPa, 900 hPa and 850 hPa. One applies an ascending progressive selection followed by a multiple linear regression to deduce the best predictors and their coefficients of regression. The coefficients are then evaluated during a "test" period (year 2004). The quality standards selected are the rates of success and failure, they are defined as the percentages of the forecasts where the error is lower than 2 degrees and higher than 5 degrees, respectively.

Starting from this quality standard one distributes the synoptic stations according to 4 classes :

- Bad : If the annual rate of success of the station is lower than 50%
- Mixed : If the annual rate of success of the station lies between 50% and 65%.
- Good : If the annual rate of success of the station lies between 65% and 80%.
- Excellent : If the annual rate of success of the station is higher than 80% (target rate in the plan of development of the INM set up in 2003)

The quality of the model temperature forecast at the closest grid point is considered as being the minimal quality to reach by the statistical downscaling MOS. It is presented in the table below :

ALADIN	Bad	Mixed	Good	Excellent
T min	19.2%	38.5%	34.6%	7.7%
T max	19.3%	23.1%	53.8%	3.8%

The forecast skill after statistical downscaling is now the following :

MOS	Bad	Mixed	Good	Excellent
T min	0%	0%	26.9%	73.1%
T max	0%	0%	30.8%	69.2%

The total average rate of success is 83.2% for Tmin and 80.5% for Tmax.

These encouraging results enable us to begin setting in operations this procedure of downscaling MOS.

### **3.15. HIRLAM**

Significant work has been achieved for one year. ALADIN is running daily with initial and lateral boundary conditions from HIRLAM, with maps and scores available at: <http://www.smhi.se/sgn0106/if/hirald/WebgraF/OPER/index.html>

Experiments at very high resolution were also performed, and the interfacing of HIRLAM physics with ALADIN is nearly achieved.

More details on the hirald web site: <http://www.dmi.dk/science/index/hirald.htm>

#### **4. ALADIN PhD Studies**

##### **4.1. Radi AJJAJI : Incrementality deficiency in ARPEGE 4d-var assimilation scheme**

On temporary (?) leave from Maroc-Météo.

##### **4.2. Steluta ALEXANDRU : Scientific strategy for the implementation of a 3D-Var data assimilation scheme for a double-nested limited-area model**

Operational duties at home (see the Romania R&D report).

##### **4.3. Margarida BELO-PEREIRA : Estimation and study of forecast error covariances using an ensemble method in a global NWP model**

A paper has been written and accepted by *Monthly Weather Review* :

Belo Pereira, M., et L. Berre : The use of an Ensemble approach to study the background error covariance in a global NWP model.

And the PhD manuscript is now ready. See the presentation at the 15th ALADIN workshop for an overview.

##### **4.4. Karim BERGAOUI : Further improvement of a simplified 2d variational soil water analysis**

Operational duties at home.

##### **4.5. Vincent GUIDARD : Evaluation of assimilation cycles in a mesoscale limited area model**

The paper "Evaluation of the ALADIN 3D-VAR with observations of the MAP campaign", by V. Guidard, C. Fischer, M. Nuret and A. Dziejic, has been accepted for publication in *Meteorology and Atmospheric Physics*. The PhD manuscript is near completion.

##### **4.6. Jean-Marcel PIRIOU: Modelling convection for global and regional models: concepts, equations, case studies.**

PhD University Paul Sabatier, Toulouse. Successfully defended on 29 September 2005.

##### **4.7. Raluca RADU : Extensive study of the coupling problem for a high-resolution limited-area model**

See the Romanian contribution to research and developments : **RD\_Ro.sxw**. The PhD work should be completed by the end of 2005.

##### **4.8. Wafaa SADIKI : A posteriori verification of analysis and assimilation algorithms and study of the statistical properties of the adjoint solutions**

Successful defence on April 7th ! Here is a summary of the PhD work :

The theory of data assimilation consists of making a combination between a background state of the atmosphere and observations using "*constraints*". The formulation of any assimilation system requires the knowledge of the weights attributed to each source of information, namely the background errors and observational errors. These errors are specified implicitly or explicitly by appropriate error covariance matrices.

The system of interest is the limited area 3d-Var analysis of ALADIN. The aim is, on the one hand, to study the properties of background error covariances in a limited area model like ALADIN and, on the other hand, to apply the *a posteriori* diagnostics in a real data observation environment,

in order to calibrate the background and observational error standard deviation parameters for a mesoscale analysis.

Firstly, we show that, for the large scales, the background errors are controlled by the ARPEGE global model. Secondly, new results on the *a posteriori* diagnostics are obtained, namely an underestimation of the background error variance, and an overestimation of the observational error variance. Moreover, the *a posteriori* diagnostics are adapted to the frame of a limited amount of observations using *ergodic* properties of the signals.

These promising results suggest that the procedure should be tested on various other analysis systems, or on one given assimilation system when significant modifications are brought to it, such as new observations or new *a priori* background error statistics.

#### **4.9. Andre SIMON: Study of the relationship between turbulent fluxes in deeply stable PBL situations and cyclogenetic activity**

Latest steps here too, with a defence expected during the spring of 2006. The latest developments concern tests on the sensitivity of the scheme of turbulent fluxes on baroclinicity of the atmosphere, following a very recent work of Plant, Adamson, Belcher and Hoskins from Reading University.

#### **4.10. Klaus STADLBACHER: Systematic qualitative evaluation of high-resolution non-hydrostatic model**

Operational duties at home.

#### **4.11. Simona STEFANESCU: The modelling of the forecast error covariances for a 3D-Var data assimilation in an atmospheric limited-area model**

Contribution to a third paper, submitted to *Q.J.R.M.S.*

#### **4.12. Malgorzata SZCZECH-GAJEWSKA : Use of IASI/AIRS observations over land.**

Still on maternity leave.

#### **4.13. Jozef VIVODA: Application of the predictor-corrector method to non-hydrostatic dynamics.**

A paper published :

Bénard, P., J. Masek, and J. Vivoda, 2005: Stability of Leap-Frog Constant-Coefficients Semi-Implicit Schemes for the Fully Elastic System of Euler Equations. Case with Orography. *Mon. Wea. Rev.*, **133**, 5, 1065-1075. and a second one under completion.

#### **4.14. Fabrice VOITUS : A survey on well-posed and transparent lateral boundary conditions (LBCs) in spectral limited-area models.**

##### **4.14.1. Introduction**

A great effort is made in order to construct a well-posed transparent LBC scheme in the view of regional NWP systems. For the HIRLAM semi-implicit grid-point model, the study of a new coupling approach based upon the "characteristics" approach, has been recently performed by McDonald (2000) for finite-difference (FD) discretization and by Hostald and Lie (2001) for finite-element (FE) method, with promising results.

The challenge question is : Can such a strategy be applied in a full Fourier spectral discretization ? Indeed, how can a well-posed transparent boundary treatment be incorporated into the semi-implicit spectral discretization of ALADIN ?

#### 4.14.2. Model equation and time discretization

For well-posedness only a certain subset of variables has to be imposed at boundaries. The number of allowable conditions to be applied at a point on the boundary depends on whether there is inflow or outflow at this point. Olinger and Sundstrom (1978) have shown that because of their hyperbolic character, it is theoretically possible to obtain a well-posed continuous problem for both Euler equations and shallow-water equations. But knowing that a continuous problem is well-posed does not necessarily mean that it is obvious how to implement boundary conditions for the associated discrete problem in a satisfactory manner.

To test some alternatives of boundary treatment in Fourier spectral discretization, a one-dimensional linearized shallow-water model is used and numerically solved by a two-time-level semi-Lagrangian semi-implicit time-marching which writes symbolically :

$$u^+ - \frac{\Delta t}{2} f v^+ + \frac{\Delta t}{2} C^2 \left( \frac{\partial \Phi}{\partial x} \right)^+ = R_{u,d}^0 \quad (1)$$

$$v^+ + \frac{\Delta t}{2} f u^+ = R_{v,d}^0 \quad (2)$$

$$\Phi^+ + \frac{\Delta t}{2} \left( \frac{\partial u}{\partial x} \right)^+ = R_{\Phi,d}^0 \quad (3)$$

$R_u^0$ ,  $R_v^0$  and  $R_\Phi^0$  are the explicit RHS (right hand side) terms, the subscript  $d$  means that quantities are interpolated to the departure point  $\left( \frac{\partial \Phi}{\partial x} \right)^0$ . These fields are first computed at each grid point by :

$$R_v^0 = v^0 - \frac{\Delta t}{2} f u^0 \quad (5)$$

$$R_\Phi^0 = \Phi^0 - \frac{\Delta t}{2} \left( \frac{\partial u}{\partial x} \right)^0 \quad (6)$$

Exponents + and 0 denote respectively the variable state at  $t+\Delta t$  and  $t$ . The resolution of this implicit problem implies to invert the so-called Helmholtz equation. This inversion is trivially performed in spectral space provided that RHS fields fulfil periodicity condition. Therefore, E-zone extrapolation seems to be unavoidable.

The main difficulty comes from the global character of spectral computations, which introduces a loss of flexibility compared to finite-difference discretization. As a consequence, well-posed boundary treatment in spectral space at  $t+\Delta t$  is not obvious at all, the more natural way is to perform the coupling explicitly at  $t$ , i.e. at the beginning of the time step. The basic idea consists in constructing the well-posed boundary strategy in the RHS fields in the integration area and using the E-zone extrapolation as an alternative to direct Fourier transform.

#### 4.14.3. Explicit boundary treatment

At each grid-point on the lateral boundaries, for each inward pointing characteristic velocity, a field must be externally supplied. Let us assume a subsonic flow pattern, i.e. such that the wind speed is less than the typical gravity waves phase speed ( $C > U > 0$ ), which is usual in atmospheric context. In that case, well-posedness is achieved by imposing only two fields at the western boundary ( $x=0$ ) boundary and only one at the eastern one ( $x=L$ ), see Olinger and Sundstrom (1978). The imposed fields are incorporated in the boundary RHS, using a classical one-sided finite-difference scheme to evaluate the derivative at the edges. Afterwards, semi-Lagrangian cubic

interpolation is performed, then the E-zone extrapolation is applied for periodicity. Three options have tested, following the various boundary strategies proposed by McDonald :

Option (i) : *Imposing u-field*

One imposes  $u$  at both boundaries and  $v$  at the western boundary.

Option (ii) : *Characteristics boundary condition*

The fields corresponding to the ingoing characteristics  $u+C\Phi$  and  $u-C\Phi$  are imposed and the outgoing characteristics are extrapolated from the interior. In subsonic case,  $u+C\Phi$  and  $v$  must be externally supplied at western boundary, while  $u-C\Phi$  is extrapolated from inside. At the eastern boundary, only  $u-C\Phi$  is supplied, one extrapolates the other fields, see Elvius and Sundstrom (1979).

Option (iii) : *Semi-transparent boundary condition*

Semi-transparent boundary conditions are derived from the Engquist and Madja (1977) theory, see also McDonald (2002, 2003) for more details. These non-reflecting boundary conditions are more accurate than the characteristic one. Interestingly, they are non-local in space, and so rather well-matched with spectral computation. It can be expressed as following :

$$B_{\pm}^1 = C \left( \frac{\partial \Phi}{\partial x} \right) - \left( \frac{f}{C} \right) v^0 \pm \left( \frac{\partial \Phi}{\partial x} \right) \quad (7)$$

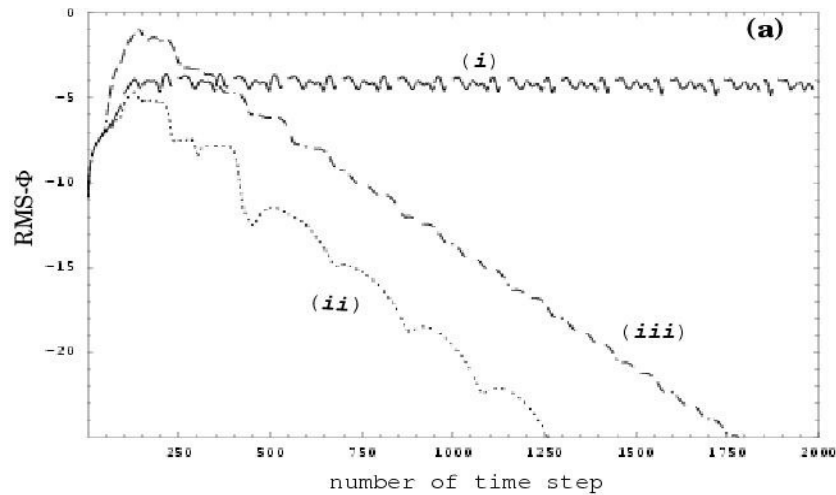
$B_+^1$  is imposed at western boundary and  $B_-^1$  at eastern boundary. Finite-difference evaluation of the derivative at boundaries is no longer necessary.  $v$  is subject to the same treatment as in (i) and (ii). It can be noticed that in a geostrophic pattern  $B_{\pm}^1 = 0$ .

#### 4.14.4. Numerical tests

We start with a geostrophically balanced bell-shape placed at the centre of the domain and moving in the positive direction at mean velocity  $U$  without changing shape. The settings for this experiment are :  $\Delta x = 10 \text{ km}$ ,  $U = 100 \text{ ms}^{-1}$ ,  $C = 300 \text{ ms}^{-1}$ ,  $f = 10^{-4} \text{ s}^{-1}$ .

This test has given some encouraging results for small time-steps,  $\Delta t = 50 \text{ s}$ , with option (i) : the bell-shape leaves the integration domain with some spurious unbalanced gravity waves, but a priori not large enough to be troublesome. Better results from the standpoint of transparency are obtained when imposing the characteristics fields (ii) and semi-transparent boundary (iii) conditions, see the figure below. But characteristics boundary conditions remains the best strategy. Unfortunately all these boundary explicit treatments are strongly unstable with larger time-steps, e.g.  $\Delta t = 400 \text{ s}$ .

The associated unstable mode corresponds to a large unbalanced disturbance with a  $2\Delta t$  time-frequency. It first appears at the eastern boundary then it extends to the other boundary through the E-zone, affecting the whole domain. It has been noticed that, the wider the E-zone is, the larger its influence over the integration area becomes.



It seems that the use of the E-zone extrapolation as an alternative to direct Fourier transform causes unbalanced waves (such as typical gravity waves) which spread out to the whole physical domain through the boundaries. This E-zone effect was previously pointed out by Haugen and Machenhauer (1993) for initialization issue. The Radnoti scheme (1995) avoids this difficulty by setting the E-zone perturbation values to zero. We must be careful, because what we do in the E-zone reveals of crucial importance.

An absorbing boundary zone has been added in the E-zone, to damp spurious waves. It works effectively well in reducing, but doesn't restore stability for large time-steps. Another technique was proposed by J-F Geleyn (during Bratislava's meeting), but is not implemented yet. It consists in applying an appropriate mapping factor in the E-zone in such a way that the spurious waves supported there are significantly vanished when arriving at boundaries.

#### 4.14.5. Concluding remarks and futur work

The proposed boundary scheme is unfortunately not able to control the growth of gravity wave disturbances at boundaries, Experiments show that the E-zone extrapolation is guilty. Therefore, the extension procedure has to be rebuilt in order to fulfil simultaneously stability and periodicity condition. Moreover, since efficient and robust boundary schemes are highly required in NWP system, some implicit boundary treatment should be investigated. Eventually, other coupling methods should be explored, provided that we succeed to solve the periodicity issue.

## **5. PAPERS and ARTICLES**

*5.1. ARPEGE and ALADIN models coupling experiments: J. Barckicke, Y. Bouteloup, J.L. Ricard, K. Yessad.*

### **5.1.1. Abstract**

A two-way coupling experiment between the operational models has been carried out. By using the existing software, the independence between the models is kept, and they are coupled through a full-duplex transfer of data. The comparison between the experiment and the operational ones shows an important noise due to the method. Reference uncoupled experiments which take into account this noise have then been done. With respect to these references, the impact of the coupling is strong and spreads far beyond the small scale model domain. The coupling experiment has been run on two winter and one summer situations. The objective scores are neutral for the winter situations. For the summer situation, we note a small degradation of the global scores, and a clear degradation of the scores over the domain of the small scale model. It is worth continuing the coupling experiment by improving the coupling technique and by using a better small scale model.

### **5.1.2. Introduction**

Météo-France uses a stretched global model and a limited-area model in order to obtain better results over its interest domain. But the results supplied by this method at small-scale are not as good as expected. Some improvements could occur by resolving the complicated problems due to the stretched grid. Another way is to use the information given by the small scale model in the global model. Our attempt will consist in simulating the grid-nesting technique, under the constraint to run experiments at an equivalent cost to the one of the current operational models.

Two kinds of improvements are expected. For the small-scale model, we hope that the fact to periodically inject its own data into the global-scale model will allow to especially improve the trajectory of the coupling area, and then to improve the boundary conditions which force the small-scale model. These boundary conditions would be closer to the small-scale model state, and by taking into account its characteristics, would allow a more soft evolution of this model. For the global-scale model, improvement are expected over the coupling area, but they could be transported beyond, improving more globally the large-scale results.

Part II describes the technique used, part III explains the tests over a first situation and part IV shows the experiments and the results. Part V gives the final interpretations and the perspectives.

### **5.1.3. The coupling method and the technical background**

#### **x General principles**

An ARPEGE forecast supplies results (historical files) and coupling files (called hereafter forcing files) every 3 hours. The ALADIN forecast uses these forcing files as initial and coupling files with a 3 hours interval. Once the ALADIN forecast done, an information which takes into account the small scale is available, and we wish to inject it into the state of the large-scale model before it runs toward the next steps. For example, the exchanges within the 6 h and 9 h forecast ranges are described in Figure 1.

The "bogussing" term used for the Full-Pos process which replaces, in a historical ARPEGE file, the ARPEGE data by ALADIN data, over the ALADIN domain. The historical ARPEGE file first is put in grid points. The difference between the ALADIN and ARPEGE historical files supplies increments which take into account the ALADIN contribution. These increments are interpolated over the ARPEGE grid-points and added to the data of the ARPEGE grid-point file built before. The ARPEGE file is put in spectral. This process is repeated every 3 hours in order to periodically refresh the ARPEGE state over the area where ALADIN data are available.

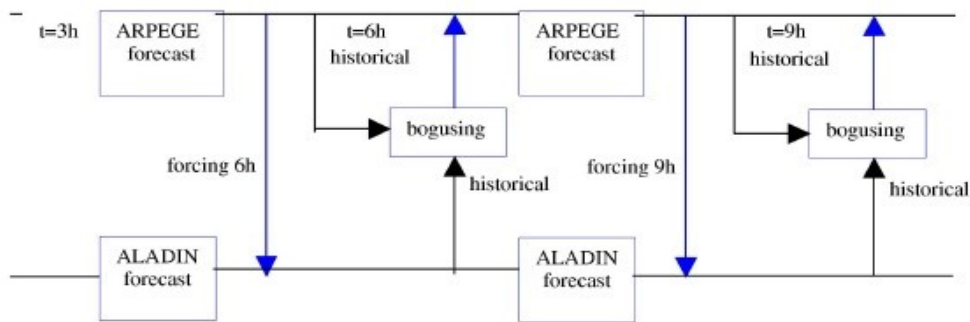


Figure 1 : bogussing procedure

## x The technical frame

This experiment consist in scheduling a lot of elementary tasks, work for which OLIVE is particularly adapted. After some modifications of the OLIVE software, updating and integration under OLIVE of the bogussing scripts, the tools were available. A new OLIVE configuration was created : bogussing.

### 5.1.4. Coupling test for a first situation

Three dates were selected for the experiments: 3d December 2003 (situation of winter blocking with a minimum centered over Spain), 13<sup>th</sup> January 2004 (winter situation with a westerly disturbed flow) and 6<sup>th</sup> August 2003 (extremely hot summer over France). Each forecast is run until 48 h with bogussing every 3 hours.

## x Coupling impact and comparison with the operational suite.

We worked on the first situation, and studied the results focussing on the following fields particularly: 200 hPa geopotential, 500 hPa geopotential, mean-sea-level pressure, 850 hPa temperature and humidity.

For about all fields, the comparison to the operational outputs shows very "noisy" fields, everywhere around the earth. Compared to the operational analysis, scores giving neither clear improvement or degradation (only some biases are clearly degraded) are obtained. More precisely, the "noise" presented the form of many well identified structures, but these structures were linked neither to physical phenomena nor to ALADIN domain properties. The noisy shapes and the degradation of biases warned us about a unphysical behavior of our system. The next experiments were carried out to understand the origin of the problem and to solve it.

## x Test of restart absence and of the bogussing technique

We try to quantify the noise due to the method itself. The sources of noise are the restart of the model from an historical ARPEGE file instead of a restart file, and the modification of the historical ARPEGE file by the bogussing technique.

It was easy to build two degraded configurations of the experiment under OLIVE. The first one only consists in restarting ARPEGE every 3 hours from the historical instead of the restart file (ALADIN is not used). Like that, the first source of noise is tested. The second one consists in doing the bogussing, but with the ALADIN forcing file instead of the ALADIN historical file as input. This version is a "go and back bogussing". It allows to test the impact of the absence of restart file and of the bogussing (but not the impact of the small-scale data).

By using the first degraded configuration, we obtained about a half of the so-called noisy structures, as they were visible on the maps discussed above in II.A. In that case, let us recall that the model restarts with information over one time-step only, and starts its run with a SL2TL scheme (equality of the values at  $t-dt$  and  $t$ ) instead of the two-steps scheme used with a restart file or during a run (no stop).

By using the second degraded configuration, we obtain the previously unexpected structures (the same as in discussed in II.A), but only the ones that were not supplied by the first degraded configuration. So the "mechanic" of the bogussing (spectral transforms and interpolations) produces the second half of the so-called noisy structures obtained in our coupling experiment. Only the structures present over or close to the ALADIN domain were not produced by the degraded configuration.

In conclusion we decided to test the impact of the ALADIN data on the ARPEGE/ALADIN system by using a reference experiment. This reference is obtained by using the ALADIN forcing file (that contains ARPEGE data) as input of the bogussing instead of the ALADIN historical file. Like that the only difference between the reference and the coupling experiment will stand in the "physical" ALADIN contribution.

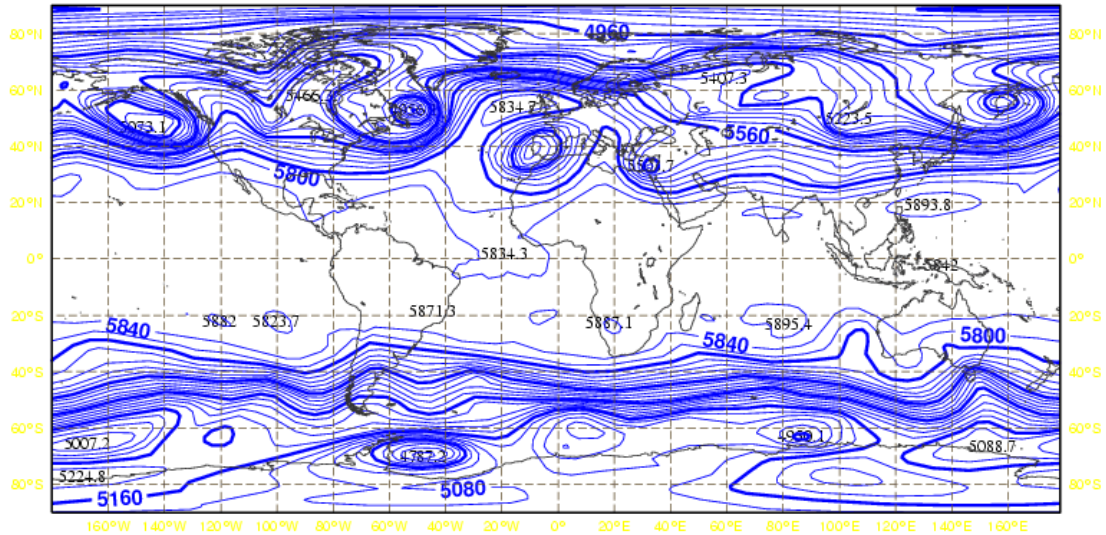
### **5.1.5. Coupling results**

#### **x Experiment of the 3 December 2003 with winter blocking.**

The first experiment, explained in III, is here compared to its reference.

- All structures that were not explained by a contribution of the small-scale model have disappeared. The impact starts always over the ALADIN domain, then spreads outside with time, depending on the flow.
- Transport and amplification of a departure to the reference (called "increment" hereafter) by the flow turning around the minimum centered over Spain. For the geopotential at 200 hPa, the increment is clear at 24 h (reaching 16 m) and centered over an area spreading from the Bay of Biscay to the Britain. At 42 h, it is centered over 20°W /40°N, still out of the ALADIN domain. At 48 h, it is 5° more towards the west. A second maximum of increment upstream the wind approaches Corogne. The one which appears over Persic gulf increases at 48 h (reaching 12 m) and fills the thalweg located over the north of Red Sea. Figure 2 shows this field at 500 hPa level where the rotation around the minimum is less clear, but the impact also strong.
- A negative increment goes northward upstream the flow and reaches at 48 h North America. It comes in phase with the thalweg located between USA and Greenland and digs it.
- These structures are present at 500 hPa. For the mean-sea-level pressure, a structure which fills by 3 hPa the low-pressure system centered over the Portugal is associated.
- The humidity is increased by 32 % in the perturbation located over Spain at 48 h.
- The impact of the small-scale data is clear, spreading outside the coupling area as expected. Moreover, it is remarkable that the impact goes upstream the wind too.

Reference PAT 20OG Ech 42 Z500hPa Zone [-90,-180,90,178.5] Validite 20031204 18heures  
 Minimum 4750.21/ Maximum 5895.14/ Moyenne 5642.36/ Ecart Type 278.717



PAT 20K2 Res 0 Ech 42 - PAT 20OG Res 0 Ech 42 Z500hPa Zone [-90,-180,90,178.5]  
 Minimum -18.0856/ Maximum 21.9382/ Moyenne -0.600876/ Ecart Type 1.79081 4

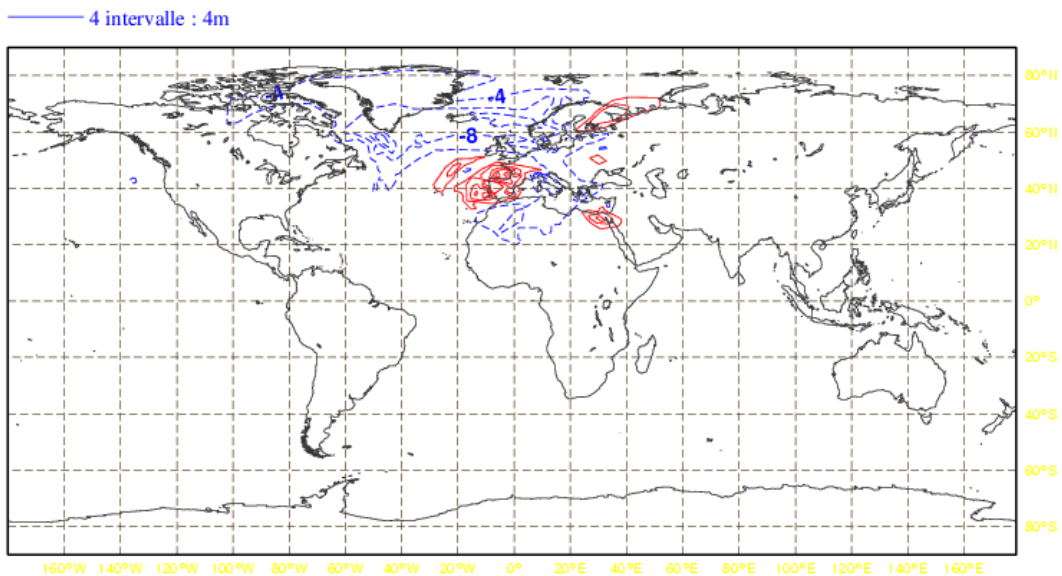


Figure 2 : Impact of the coupling by comparison to the reference experiment for the geopotential at 500 hPa at 42 h (Z500, the 20031203+42h).

Global scores have been computed by comparison to the operational analysis. Biases of the experiment are slightly worse than the reference ones, but nothing significant was found for the standard deviations. The same scores have been computed over the ALADIN domain, from the rather coarse EURAT5 grid. In both cases, no significant contribution due to the small scale data on the scores of the global model has been noted.

**x Situation of the 13 January 2004 with rapid westerly flow.**

Here too the experiment is compared to its reference.

- The impact always starts over the coupling area, then spreads following the flow, but only downstream.
- The geopotential departures created over the ALADIN domain are spread eastward as a plume. The increments reach the 60th east meridian at 48 hours.
- A negative increment goes downstream northward and is centered over Baltic sea at 48 h.
- Very strong humidity increments are obtained in the coupling area at 48 h.

The impact of the small-scale data is clear, spreading outside the coupling area mainly downstream as expected.

The global scores by comparison to the operational analysis show a small reduction of the mass fields biases but a small degradation of the humidity biases. The result is the opposite concerning the standard deviations. For the scores over EURAT5, the biases are strongly reduced in the coupling experiment, except concerning temperature at 850 hPa. The standard deviations are better only for the mean-sea-level pressure at 24 h and humidity at 850 hPa.

#### **x Situation of the 6 August 2003.**

The situation was anticyclonic over France.

- The coupling makes the fields smoother: it fills the minima located on Gibraltar and Caspienne Sea.
- The temperature modifications are clear, with a cooling over North Africa and West Europa, except over Morocco/Gibraltar and the center of Spain (increasing by 2.5 K).
- Note a bug over Antarctic, since strong increments appear from 12 h.

The differences between the global scores with respect to the operational analysis are not significant. The same scores computed over ALADIN domain (from EURAT5 grid) show a degradation of all scores.

#### **5.1.6. Conclusion and perspectives**

Three situations were selected for the experiments: 3d December 2003 (winter blocking with a minimum centered over Spain), 13<sup>th</sup> January 2004 (westerly disturbed flow) and 6<sup>th</sup> August 2003 (« killer summer » in France). Each run was a 48 h forecast with bogussing every 3 hours.

Once the sources of noise identified, due to the simple technique employed, reference experiments having the same noise have been built. A clear and logical impact of the contribution of the small scale model data has been observed. The magnitude of the increments cannot be neglected with respect to the concerned fields, and these increments are generally transported downstream, eventually far from the coupling area, impacting less and less significantly as we leave this area.

Concerning the objective scores, the results of both winter situations are neutral. But for the summer situation a clear negative impact is produced with the introduction of the small-scale model data. The reasons could be :

- An insufficient quality of the small scale model to improve the results of the large-scale model,
- A problem of the reference chosen to computed the objective scores. The analysis could be too close to ARPEGE or of insufficient characteristics,
- A too big noise due to the computing technique. To simplify the experiment, ARPEGE restarts every 3 hours on the basis of the historical file, which induces a noise whose impact has been discussed in III.B. The bogussing, that carries out the interpolations, produces a noise of the same magnitude (see III.B), which could warn us about an insufficient technique. Maybe the ALADIN data can improve the ARPEGE model state, but it is possible that the noises interacts in a negative way.

- A noise due to the numerical bogussing technique: the adding of the increments on the fields of the global model is done over a limited area, which could induce a physical, particularly thermodynamic, imbalance at the boundaries of this area. The temporal scheme of injection of the small-scale data into the large scale model is very simple too (adding of the increments every 3 hours). A grid-nesting scheme is generally more complex, with rather a recall toward the small scale model at each time step.

We point out that the two-way coupling idea is for us complementary to the stretched grid. We want to show the impact of the small scale on the large scale, and on the coupling conditions received by the small scale model. We hoped to show the interest of keeping a global model "modifiable by the small scale", instead of "bearing" an external global model and risking to limit the quality of our results at mesoscale. Being aware that the two-way coupling idea is founded on a solid basis, we deduce the following perspectives for next studies:

- This experiment should be pushed further, from a better small scale model, or from the same one but with improved initial states.
- Scores should be computed from a more objective or better quality reference.
- The noise induced by the absence of restart and the bogussing should be reduced. For example, to build real restart files would not be difficult and would allow to improve the objective scores.
- To reduce the method noise, it is possible to rerun the experiments (without big development) by modifying the historical ARPEGE in an incremental manner, using the difference between two "bogus" files (the one of this experiment – the one coming from the forcing ARPEGE file).

#### **5.1.7. Références**

- [1] Méso-NH: Scientific Documentation (<http://aeropc68.aero.obs-mip.fr/~mesonh/> Book 1)
- [2] Clark, T. L., and R. D. Farley, 1984: Severe Downslope Windstorm Calculations in Two and Three Spatial Dimensions Using Anelastic Interactive Grid Nesting: A Possible Mechanism for Gustiness, *J. Atmos. Sci.*, 41, 329-350.
- [3] J. P. Lafore et al., 2000: The Meso-NH Atmospheric Simulation System as a Research Tool at Mesoscale, Workshop Proceedings: Developments in Numerical Methods for Very High Resolution Global Model, ECMWF 1-14.

## 5.2. Operational implementation of ALADIN 3DVAR at the Hungarian Meteorological Service : G. Bölöni.

### 5.2.1. Introduction

ALADIN 3DVAR was first implemented at the Hungarian Meteorological Service (HMS) in June 2000 based on the cycle AL13. The first real time experimental assimilation cycle was then, set up during the summer 2001 on the former operational machine (SGI Origin 2000) of the service. That time the system was using only SYNOP and TEMP data over a small domain covering Hungary. As a next step the 3DVAR assimilation cycle was run as a quasi-operational application over the former ALADIN/LACE domain from November 2002 on an IBM p699 machine. At the same time, experimentations started in order to use satellite (ATOVS/AMSU-A) and aircraft (AMDAR) data. Since the end of May 2005, ALADIN 3DVAR is used operationally at HMS. This paper describes the operational assimilation system set up recently, and summarizes its results based on different verification methods and some case studies.

### 5.2.2. Main characteristics

The presently used operational domain (the same for assimilation and production) uses linear grid, 8km horizontal resolution and 49 vertical levels. The domain covers roughly the same area as the former LACE domain. The assimilation cycle is run with a 6 hour frequency which means 4 « long cut-off » analyses per day (00, 06, 12, 18 UTC) using all the actually available data and 2 « short cut-off » analyses at 00 and 12 UTC in addition to provide initial conditions for the 48 h production runs (figure 1.).

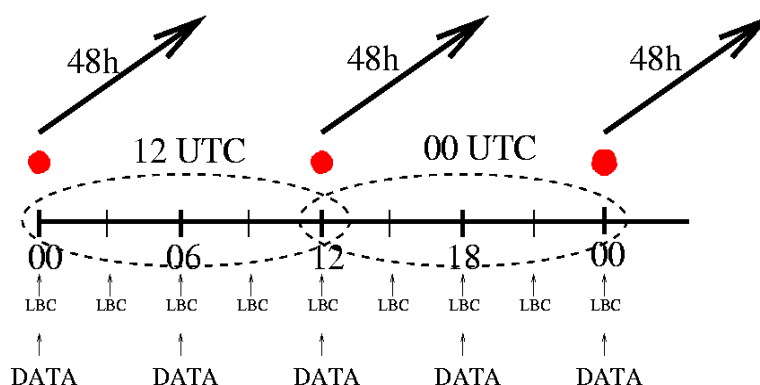


Figure 1 : The assimilation cycle

In every assimilation step, the surface (soil) analysis is taken from ARPEGE, more exactly the surface (soil) fields of the background are overwritten with those of the actual ARPEGE analysis interpolated on the ALADIN grid. The upper air fields are provided by the 3DVAR analysis. The presently used background error covariance matrix is computed following the standard NMC method. The background is a 6 hour forecast of the model which starts from the DFI initialized local analysis. During the integration a 3 hour coupling frequency is used. Namely, at 00, 06, 12, and 18 UTC the ARPEGE « long cut-off » analyses, at 03, 09, 15, and 21 UTC the 3 hour ARPEGE forecasts starting from the corresponding « long-cut off » ARPEGE analyses are used as coupling fields.

### 5.2.3. Observational data

The system presently uses surface, radiosonde, satellite and aircraft observations. The table below summarises all the observed parameters by observation type used in the system.

SYNOP surface reports	surface pressure
TEMP upper air reports	temperature, wind, geopotential, specific humidity
ATOVS satellite observations	AMSU-A radiances
AMDAR aircraft reports	temperature, wind

Table 1 : The observational data entering the assimilation system

It is important to mention, that all the observation types above are used in the ARPEGE 4DVAR assimilation system as well. However, the local assimilation system benefits from some useful additional observational input coming from local SYNOP reports (not disseminated through GTS), and due to weaker thinning of satellite (80 km for AMSU-A) and aircraft (25 km for AMDAR) data. Another remark which might be interesting is that a new procedure has been developed for the preprocessing of the AMDAR data, allowing a global quality control on the whole aircraft database in one go (the original screening of the data was done flight by flight) in order to avoid problems while using the aircraft data in a non-continuous way in time (3DVAR and not 4DVAR).

#### 5.2.4. Validation & Results

The validation of the assimilation system is done by plotting objective scores (observation minus model BIAS & RMSE) and performing a subjective verification procedure. The subjective verification consists of an everyday briefing comparing the different model versions (i.e. dynamical adaptation and the data assimilation system) performance for the actual situation. Finally, a note (a number from 1 to 5) is given to each model version by the members of the verification team that includes forecasters and modellers as well. According to the objective scores the impact of local data assimilation compared to dynamical adaptation can be summarized as follows (some selected figures are shown for illustration from the period 22.03.2005 – 05.04.2005):

- improvement on temperature and wind on all vertical levels (figure 2)
- improvement on geopotential on high levels (figure 3)
- small negative impact for mean-sea-level pressure (negative BIAS) (figure 3)
- mixed impact on humidity depending on forecast range (figure 4)
- negative impact on high-level humidity

The conclusions drawn according to the subjective verification, i.e. the daily comparison of the forecasted weather parameters, are listed below. For illustration the scores are plotted for a half-year period on figure 5.

- improvement in the 2m temperature forecast (0 – 24 h)
- improvement in the precipitation forecast (0 – 48 h)
- degradation (0 – 24 h) / neutral impact (24 – 48 h) in cloudiness
- neutral impact on wind

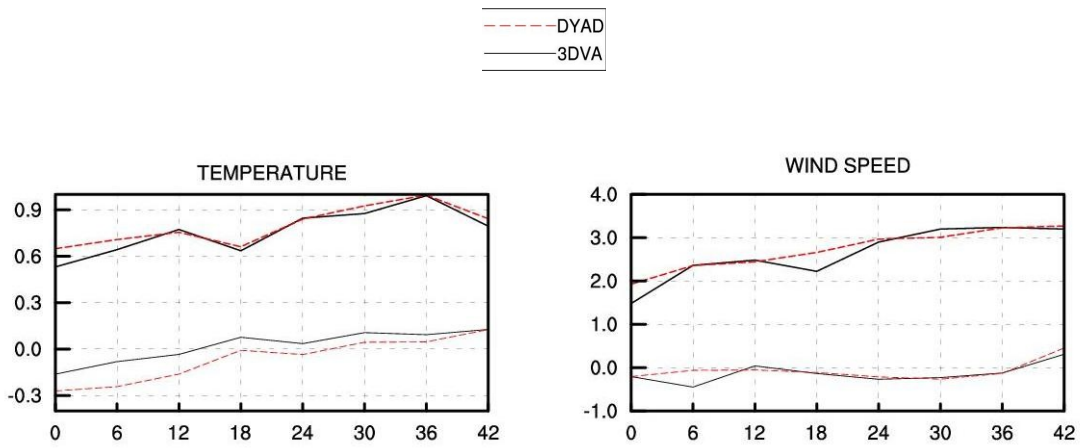


Figure 2 : RMSE and BIAS of the temperature and wind forecasts on 500 hPa

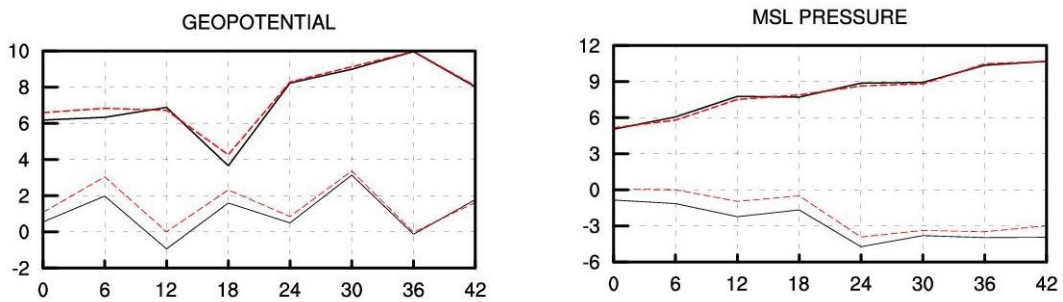


Figure 3 : RMSE and BIAS of geopotential on 700 hPa (left) and mean sea level pressure (right)

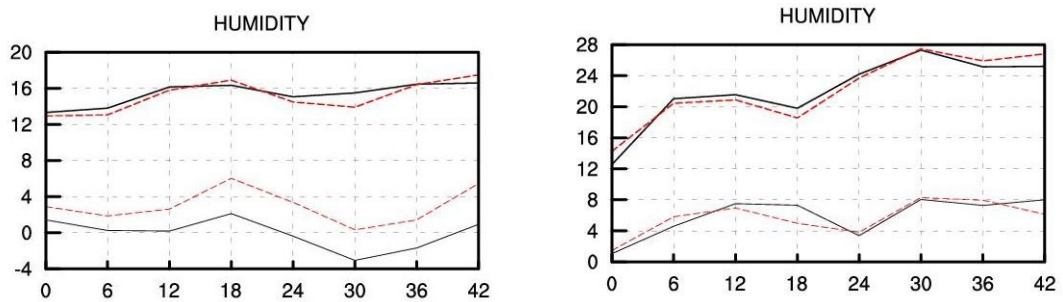


Figure 4 : RMSE and BIAS of humidity on the surface (left) and on 500 hPa (right)

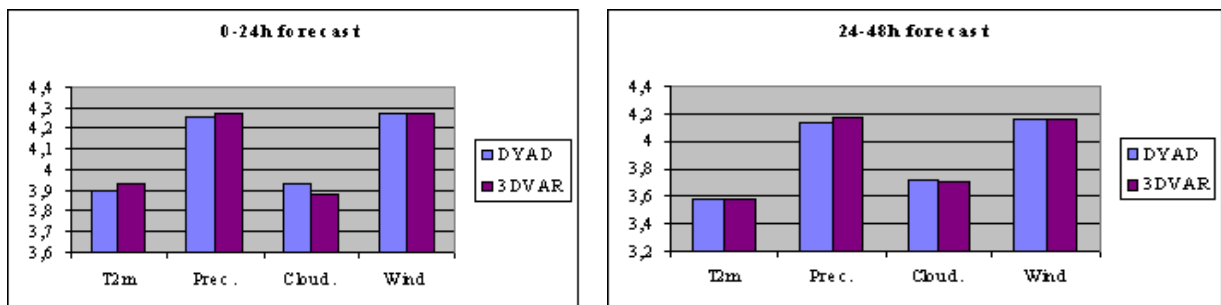


Figure 5 : Subjective scores of the dynamical adaptation (DYAD) and the assimilation system (3DVAR) for the first (left) and the second (right) day of the forecast (period: 01.07.2004 – 31.12.2004)

To close the presentation of the performance we show a case study. On the 18th of May 2005 a fast moving cold front was passing over Hungary, which was linked to a Mediterranean cyclone. It induced thunderstorms, strong wind gusts ( $> 100$  km/h) and heavy precipitation ( $\sim 45$  mm/ 24 h) in several places over the country.

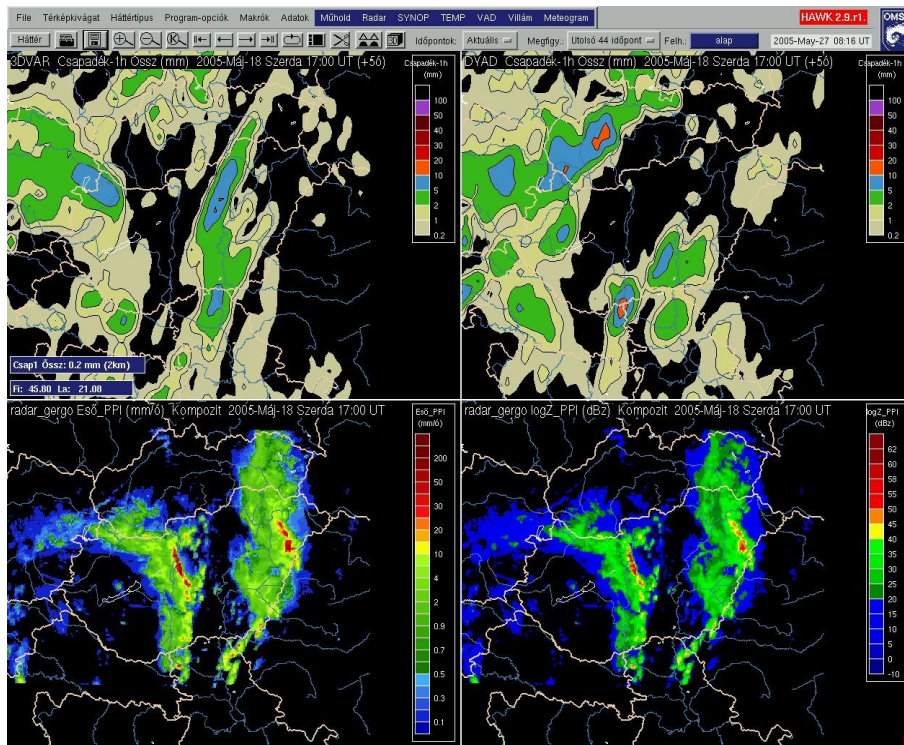


Figure 6 : Forecasted (top left: 3DVAR, top right: dynamical adaptation) precipitations (+5h) and observed reflectivities (bottom left: precipitable water, bottom right:  $\log Z$ )

Considering the precipitation forecast, the 3DVAR assimilation system performed much better than the dynamical adaptation as we illustrate on figure 6. There we show the radar reflectivities at an important moment of the event and the corresponding precipitation forecasts. On the figure we try to illustrate, that the structure of the precipitation patterns were better predicted by the assimilation, catching both band of precipitations being present in reality, during the whole integration up to +18 h, when system left Hungary and decayed. The comparison of observed and forecasted 6 h cumulated precipitations also indicated a better performance of the assimilation system (not shown).

### 5.2.5. Monitoring of the system

In order to be able to follow the operation of the system a web interface has been developed which makes it possible to follow the different steps of the assimilation procedure and model forecast as well as the used observational data base. We put the emphasis on the presentation of the latter as it was a necessary development connected specially to data assimilation. The observation monitoring system is based on the ODB mandalay viewer, which provides ascii dump of the ODB data base, then space and time statistics are computed on the ascii data (obs – guess, obs – analysis, observation quality flags) in order to represent the quality and availability of the data. Some examples are shown below.

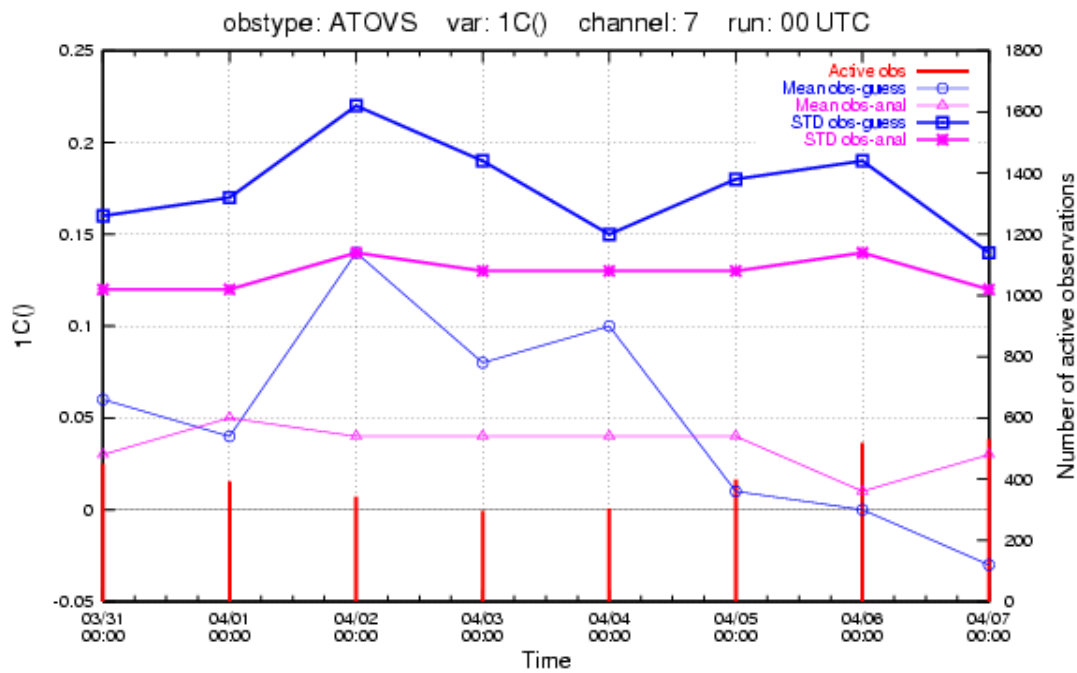


Figure 7: Time evolution of the different properties (mean and standard deviation of obs – guess and obs - analysis, number of active observations) of the ATOVS/AMSU-A data (channel 7)

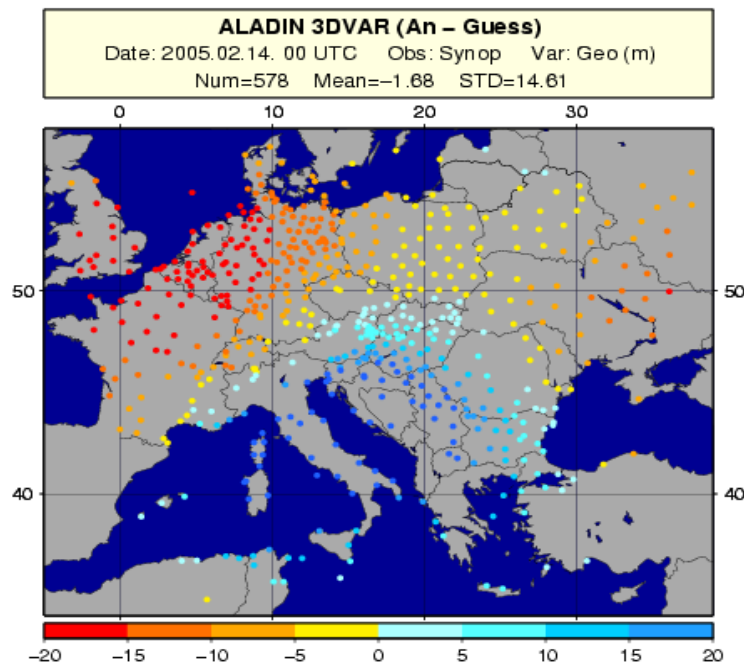


Figure 8: Horizontal map of the mean-sea-level pressure analysis – guess differences at the location of SYNOP observations, which shows the increments caused by the used observations (in the north-west the guess was corrected by the observation of a low-pressure system, in the south-east the guess was corrected by the observation of a high pressure system)

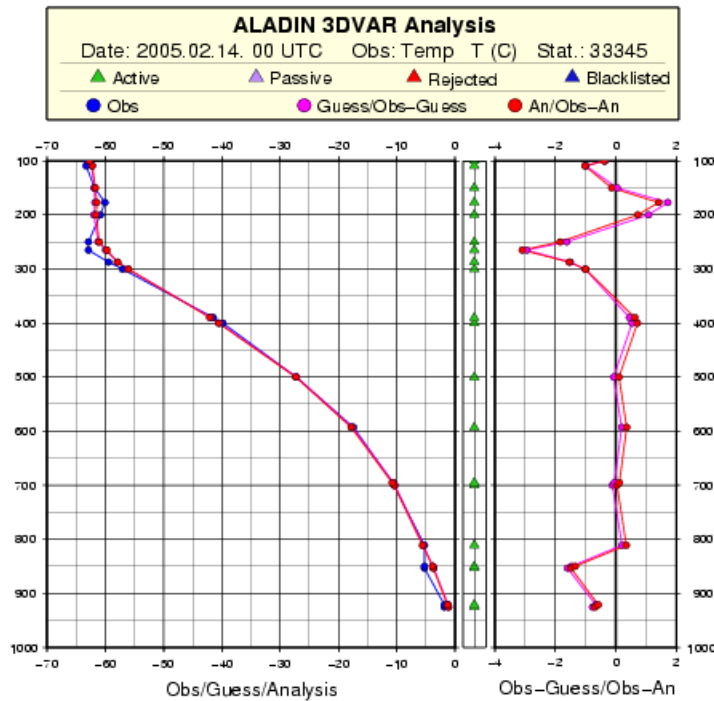


Figure 9 : Profiles of different quantities (obs, guess, analysis, obs-guess, obs-analysis) for a given analysis at the location of a radiosonde observation. The status of the observations is also indicated.

### 5.2.6. Conclusions and Outlook

According to the experiences at HMS, the local ALADIN assimilation can be beneficial in the everyday forecasting especially concerning the precipitation events and the 2m temperature, in the short range up to 24 hours. However, there is no common improvement for all variables and even some degradation for some variables (high level humidity analysis and forecast, mean sea level BIAS) was noticed in the objective scores compared to the dynamical adaptation, for the concerned periods. This will probably motivate the HMS team for trying to improve the system. We are looking forward to continue to include other new types of observations in the assimilation in the near future (ATOVS/AMSU-B, MSG wind, wind profilers) and to recompute the background error covariance matrix using the "Ensemble method". For longer term even further observation types are considered to be included (SEVIRI radiances, T2m and RH2m from SYNOPs), and the testing and possible application of the so-called  $J_k$  term or "variational blending" is also foreseen as well as experimentations with 3D FGAT.



### 5.3.2. Improvement of the falling process

The main weakness of the original scheme lies in the semi-Lagrangian handling of the falling of rain and snow. The treatment of evaporation and collection processes is not correct and the auto-conversion process is applied at the beginning of the time-step, which give an unrealistic 3D field of precipitating water.

A semi-Lagrangian algorithm for the falling of rain and snow may be regarded as a simulation of the evolution of the Probability Density Function (PDF) of the age of droplets. The meaning of "age of droplets" is "since how long does the droplet fall?". If the falling speed is known this is equivalent to "which level does it come from?". Philippe Lopez tried to answer the second question without completely taking into account his significance. The main idea is to consider at each level a PDF of the age of the droplets. In this context the falling process is just a shift of the PDF along the time axis. Droplets which become older than the time-step stay at the current level. All the processes can be described in this framework. For auto-conversion, which is a continuous process during the time step, an equi-partition is applied. For collection and evaporation, a partition proportional to the initial precipitating water content is made. In the code, the PDF can be described by an array. Due to the variable thickness of the vertical levels this array should have a size larger than the number of vertical levels. It is necessary to move at least by one box in the array when the droplets fall from one level. It seems more interesting to use the vertical axis for temporal description. The link between both is the vertical falling speed. The variable thickness of the levels impose to compute the time equi-partition in term of level thickness.

Using the average constant bulk values for vertical speed, each model layer is advected backward in time from  $t + \Delta t$  to time  $t$ , where  $\Delta t$  denotes the time step. The location of the layer at time  $t$  is fully determined by its top and bottom altitudes,  $Z_{top}$  and  $Z_{bot}$  respectively. Let us first number model layers starting from 1 at the top to N at the bottom, and let us denote  $Z_h$  the altitude of model half-levels (numbered from 0 at the top to N at the surface). These notations are illustrated by Figure 3.

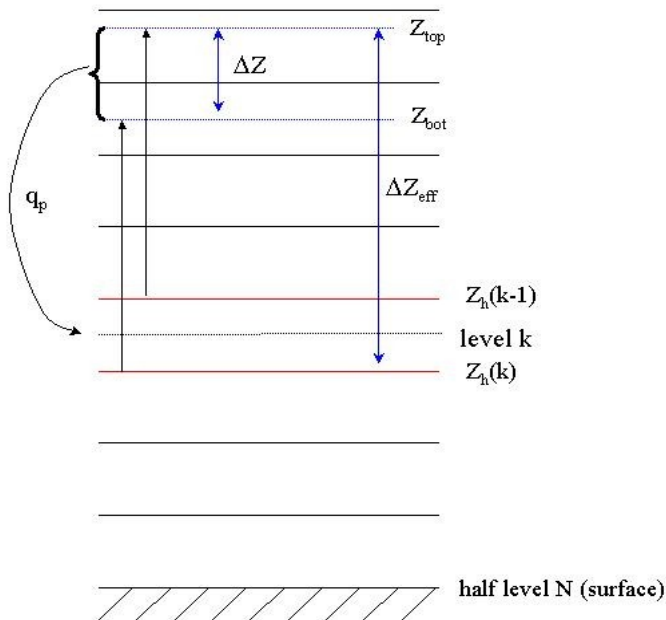


Figure 3: Visualisation of the notations used in the semi-lagrangian calculus.  
Except for level k only half levels are shown

The vertical distance representing the place from which droplets are able to cross the current level  $k$  during the time step is :

$$\Delta Z_{eff} = \sum_{j=1}^k \Delta Z_{eff}(j)$$

with :

$$\Delta Z_{eff}(j) = \max[0, \min(Z_{top}, Z_h(j-1)) - Z_h(j)]$$

If  $w(j)$  is the falling speed of the precipitation at level  $j$ , the total time necessary to cover this distance is :

$$\tau = \sum_{j=1}^k \frac{\Delta Z_{eff}(j)}{w(j)}$$

This can be written :

$$\tau = \Delta t + \frac{\Delta Z_{eff}(k)}{w(k)}$$

The meaning is that  $\tau$  is the sum of the time-step plus the time necessary to cross the current layer. A temporal equi-repartition of the content of precipitable water (liquid or solid) which comes from the auto-conversion process is needed (auto-conversion is continuous during the time step). The multiplication coefficient for the level  $j$  is the ratio of the time spent in level  $j$  by the total time  $\tau$  :

$$\left( \frac{\Delta Z_{eff}(j)}{w(j)} \right) / \tau$$

At each level  $j$  between 1 and  $k$  the content of precipitable water is then modified using the following formula:

$$q_p(j, t) = q_p(j, t) + [q_{auto}(k) \rho(k) \Delta Z(k) \Delta t] \frac{\left( \frac{\Delta Z_{eff}(j)}{w(j)} \right)}{\tau} \frac{1}{\rho(j) \Delta Z_{eff}(j)}$$

where  $q_{auto}(k)$  is the auto-conversion flux, coming from Kessler (1969) formulation.

Then, as in Lopez (2002) we compute the effective average precipitation content that crosses model layer  $k$  during one time-step:

$$q_p^{eff}(k) = \frac{1}{\rho(k) \Delta Z(k)} \sum_{j=1}^k \rho(j) \Delta Z_{eff}(j) q_p(j, t)$$

The effective precipitation content  $q_p^{eff}$  serves as an input to both the collection and the evaporation equations (6)-(9) of Lopez (2002). After computation of the precipitation, evaporation and collection rates ( $q_{evap}(k)$  and  $q_{coll}(k)$  respectively), at each level between 1 and  $k$ , the precipitating water content is again modified:

$$q_p(j, t) = q_p(j, t) \left[ 1 + \frac{q_{coll}(k) - q_{evap}(k)}{q_p^{eff}(k)} \right]$$

Finally the precipitating water content at level  $k$  at time  $t + \Delta t$  is computed following Lopez (2002) :

$$q_p(k, t + \Delta t) = \frac{1}{\rho(k) \Delta Z(k)} \sum_{j=1}^k \rho(j) \Delta Z(j) q_p(j, t)$$

where

$$\Delta Z(j) = \max[0, \min(Z_{top}, Z_h(j-1)) - \max(Z_{bot}, Z_h(j))]$$

For a better understanding,  $\Delta Z = \sum_{j=1}^k \Delta Z(j)$  is shown in Figure 3.

The effective precipitation content  $q_p^{eff}(k)$  is also recomputed with the new values of  $q_p(j, t)$  in order to determine the flux of precipitation  $F_p(k)$  at the half-level  $k$ . The precipitation flux is the difference between the effective precipitation content and the precipitation content which stays at level  $k$  :

$$F_p(k) = \frac{\rho(k) \Delta Z(k)}{\Delta t} (q_p^{eff}(k) - q_p(k, t + \Delta t))$$

### 5.3.3. Results

#### x Results with the Single Column Model (SCM)

Some tests have been done in the SCM, in particular with the EUROpean Cloud Systems (EUROCS) stratocumulus case. The EUROCS project used observations of stratocumulus off the coast of California during FIRE I (Hignett 1991 ; Duynkerke and Hignett 1993). For more information about EUROCS stratocumulus case see Duynkerke et al (2004). The forcing required to simulate the case has been coded in the SCM by Blazenka Vukelic and Jean-Marcel Piriou. These experiments were made more for technical tests than in a scientific goal. All the same the results are interesting.

The results are shown on Figure 4. The result for the operational scheme is very close to that shown in Duynkerke et al (2004). The main evolution in the operational model since the experiment made for this article is the use of a new cloudiness scheme from Xu and Randall and the use of the old version of the radiation code of the ECMWF (instead of ACRANEB). One can notice that there is a large impact of a change of the time-step with the operational scheme. The simulations with Lopez are better, but not perfect. Amongst other things there is a too small diurnal cycle, but the impact of a change of the time-step is very small. The Lopez microphysics scheme is prognostic, if there is no cloud condensate in the initial file the cloudiness is equal to zero during the first time-step. With a complex radiation scheme called with a frequency of one hour, the cloudiness seen by the model is equal to zero during the first hour of the simulation. This is shown on Figure 4, the liquid water path decreases during the first hour of the simulation and grows, as it is necessary, afterwards.

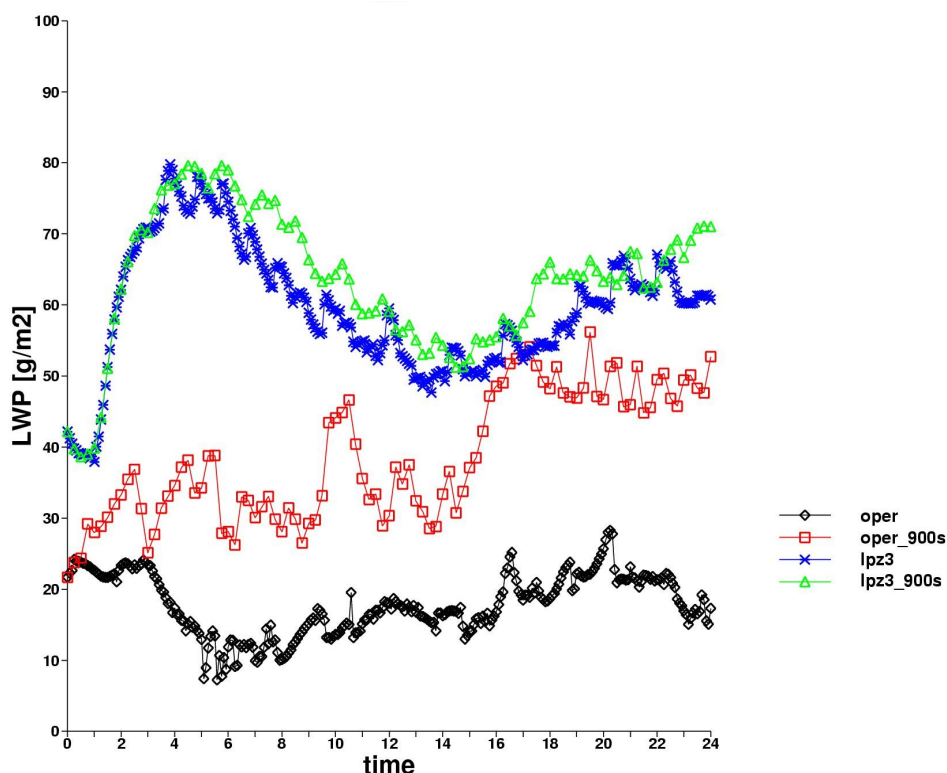


Figure 4: Liquid Water Path (LWP) during a 24 hour simulation of EUROCS stratocumulus. In black operational scheme with a time-step of 300s, in red operational with a time-step of 900s, in blue Lopez scheme with 300s and in green Lopez scheme with 900s.

During our first tests with the Lopez scheme in the SCM, we observed an instability, an oscillation from one time-step to the other one (not shown). We found that this instability can be corrected by the use of the diffusion of conservative variables. The modifications of ACDIFUS needed to compute diffusion of conservative variables has been coded in the SCM by Pascal Marquet from the GCM team.

However, with the last version (CY29T2) of the scheme this behaviour disappeared, and we did not succeed in reproducing it. We thus do not know which is its origin. Anyway, the use of the diffusion of conservative variables seems to be more coherent insofar as liquid and ice cloud water are used as prognostic variables.

### x Tests in 3D with ALADIN

A 3D simulation of a case of strong precipitations over Corsica has been presented in Bouysse et al. (2005). One of the known weaknesses of ALADIN is to simulate too strong orographic precipitations in some situations. It seems that with the new scheme the results are better, with less precipitation windward and more precipitations on the sea leeward Corsica. With another situation, over Austria, this aspect can be shown more precisely.

This situation occurred in November 2000 over Austria. Many thanks to Thomas Haiden and Christoph Wittmann (ZAMG) who proposed to simulate this case and provided a reference map, from rain gauge observations (Figure 5). In fig. 6a, the result of a simulation with the present operational physics is shown. One can see that the precipitations are overestimated windward mountains and underestimated (close to 0 m) leeward. On the simulation with the new scheme it is clearly shown that the precipitations are reduced over the highest tops. On a zoom (Figs. 7A-b), one can see that, linked to the reduction of precipitations over the mountains, some precipitations occur in the valley, which gives an overall more realistic field.

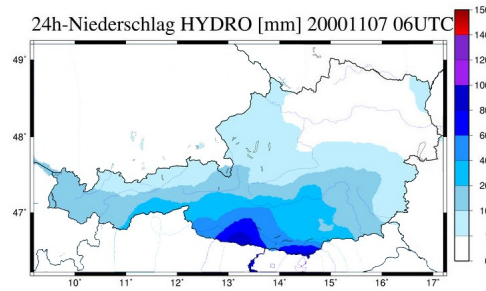


Figure 5 : 24 hours accumulation of observed precipitations over Austria for the 7 November 2000 case (from ZAMG)

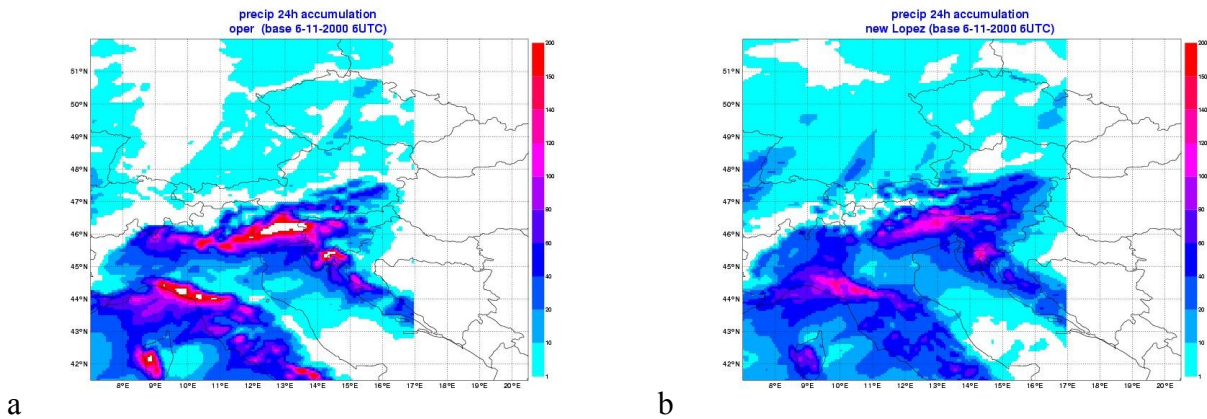


Figure 6 : 24 hours accumulation of precipitations over Austria . a : present operational scheme b : Lopez scheme  
Accumulations larger than 200mm are not shown

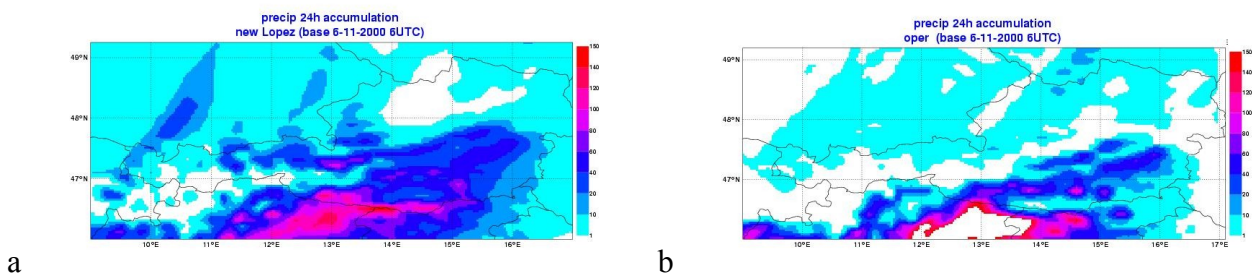


Figure 7 : Same as Figure 6 but zoom over Austria. a : present operational scheme b : Lopez scheme

An important question is : What is the mechanism which gives this behaviour to the new scheme ? Two experiments were made to try to answer the question. In the first one advection of the new prognostic variables was not performed, in the second one advection was performed on cloud variables but not on rain and snow. On Fig. 8a the cumulative precipitations field of the first experiment is shown. It is very closed to the operational result. The main mechanism to explain the behaviour of the new scheme seems to be the advection, it transports cloud water content and precipitations behind the mountains. On Fig. 8b the result from the second experiment is shown. The impact of the advection of precipitations is clearly highlighted. Contrary to certain generally accepted ideas, the advection of precipitations seems to be necessary to have a realistic forecast. Of course, many other experiments will have to be carried out to check these results.

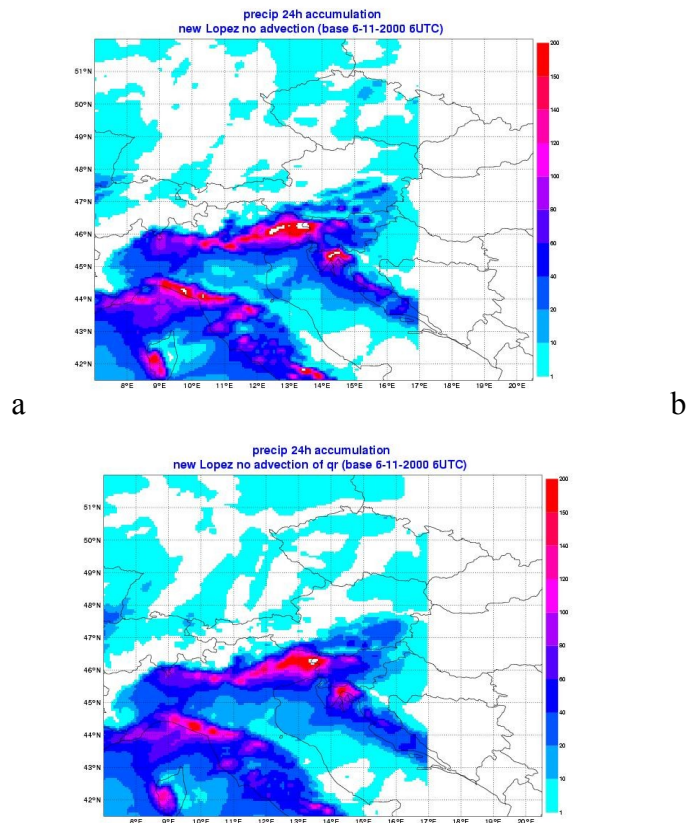


Figure 8 : Impact of advection. a : No advection (neither of cloud variables nor of precipitations) . b : Advection of cloud water (and ice) but no advection of rain and snow

### x Tests with ARPEGE

Validation forecasts have been performed with the modified Lopez scheme and the diffusion of conservative variables, all the other parameterizations (deep and shallow convection, radiation, subgrid scale orography, surface) being unchanged. All these results are described in Bouyssel et al. (2005).

#### 5.3.4. Conclusion

This article describe the last improvements made on the Lopez's prognostic large scale cloud and precipitation scheme. The main part is a rewriting of the lagrangian falling process. With the new algorithm the treatment of evaporation and collection processes is correct and the autoconversion process is now continuous during the time step. With these modifications the parametrisation seems to be more stable. Another interesting result is the impact of advection on strong orographic precipitation. The behaviour of the Lopez scheme is better than the operational one and it seems that this behaviour is a consequence of the advection of cloud condensate (liquid and ice) and precipitation (rain and snow). The validation will continue and focus on 4D-Var assimilation experiments. Some sophistications would be interesting, such as a better treatment of the precipitation melting and a separation of precipitating water in rain and snow, but the priority is more likely the implementation of a moist turbulence scheme taking into account the prognostic liquid and ice water contents, a work made jointly with the ARPEGE GCM team.

### 5.3.5. References

- Bouyssel, F., Y. Bouteloup and P. Marquet, 2005 : Toward an operational implementation of Lopez's prognostic large scale cloud and precipitation scheme in ARPEGE/ALADIN NWP models. *HIRLAM mini-workshop on convection and clouds*, Tartu, 24-26 January 2005 (<http://hirlam.knmi.nl/>)
- Duynkerke, P. G. And P. Hignett, 1993: Simulation of diurnal variation in a stratocumulus-capped marine boundary layer during FIRE. *Mon. Weather Rev.*, **121**, 3291-3300.
- Duynkerke, P. G., S. R. De Roode, M. C. Van Zanten, J. Calvo, J. Cuxart, S. Cheinet, A. Chlond, H. Grenier, P. J. Jonker, M. Kohler, G. Lenderink, D. Lewellen, C.-L. Lappen, A. P. Lock, C.-H. Moeng, F. Muller, D. Olmeda, J.-M. Piriou, E. Sanchez and I. Sednev, 2004: Observations and numerical simulations of the diurnal cycle of the EUROCS stratocumulus case. *Q. J. R. Meteorol. Soc.*, **130**, 3269-3296.
- Gerard, L., 2005: Adaptations to ALADIN of the Lopez microphysical package. *ALADIN Newsletter*, **27**, 131-134.
- Hignett, P., 1991: Observations of the diurnal variation in a cloud-capped marine boundary layer. *J. Atmos. Sci.*, **48**, 1474-1482.
- Kessler, E., 1969: On the distribution and continuity of water substance in atmospheric circulation. *Atmos. Meteor. Monograph*, **32**, 84 pp.
- Lopez, P., 2002: Implementation and validation of a new prognostic large-scale cloud and precipitation scheme for climate and data-assimilation purposes. *Q. J. R. Meteorol. Soc.*, **128**, 229-257.
- Smith, R. N. B., 1990: A scheme for predicting layer clouds and their water content in a general circulation model. *Q. J. R. Meteorol. Soc.*, **116**, 435-460.
- Xu, K.M. and D. Randall, 1996: A semi-empirical cloudiness parameterisation for use in climate models. *J. Atmos. Sci.*, **53**, 3084-3102.

## 5.4. Testing the new sub-grid scale orography representation on bura cases: *D.Drvar, I.Stiperski, M.Tudor, V.Tutiš.*

### 5.4.1. Summary

The operational forecast of ALADIN model is satisfactory for the wind field, although the wind speed is sometimes overestimated. A modified subgrid-scale orography representation was introduced and tested. The envelope was removed and, to compensate for the loss of volume, changes in gravity wave drag parametrization were introduced. New orography representation resulted in slight enhancement of upstream and general decrease of downstream wind speed, as well as reduction of mountain wave amplitude.

### 5.4.2. Introduction

#### x Envelope or not?

Representation of unresolved orographic effects is a difficult problem in numerical models, because of the large spectrum of processes involved. In the past few decades, the representation of subgrid-scale orography has been attempted by different means. One of the methods is the enhancement of terrain by adding an envelope (see Wallace et al., 1983), while another one uses parametrization of gravity-wave drag and lift. In ALADIN, both methods are implemented.

Although the envelope method is proved to give a better representation of the airflow over and around mountain ranges, it has limitations. The envelope artificially increases the mountain height, and therefore gives excessive precipitation on the windward side, stronger katabatic winds in the lee and overestimated amplitude of the mountain waves (see Bougeault, 2001). Because of the exaggerated terrain height, numerous measurements from the stations situated below the envelope are systematically rejected in data assimilation. Furthermore, studies of local behaviour of the ECMWF model near Pyrenees (Lott, 1995) and Alps (Clark and Miller, 1991) have shown that mountain drag is underestimated, and cannot be adequately substituted with the envelope. For these reasons, in a number of NWP models, the envelope has been suppressed, and the gravity wave-drag parametrization tuned to compensate for the lack of volume.

#### x Experiments

The operational model results (AL25T1) are compared to the results from an experimental version of ALADIN, without the envelope and with the new gravity-wave-drag parametrization. In the operational model, envelope is obtained by adding the standard deviation of the sub-grid-scale orography to the mean height. Removing the envelope actually means lowering the mountain peaks as well as the valleys (see Fig 1). The difference is largest in the areas where the orographic variability is highest, e.g. on the mountain slopes.

With the reduction of the mountain volume, the pressure drag decreases, and has to be compensated by parametrization. The pressure drag is addressed by its two components: the lift (perpendicular to the flow), and the drag (parallel to it). In the experiment, the orographic lift is activated and gravity-wave drag is tuned.

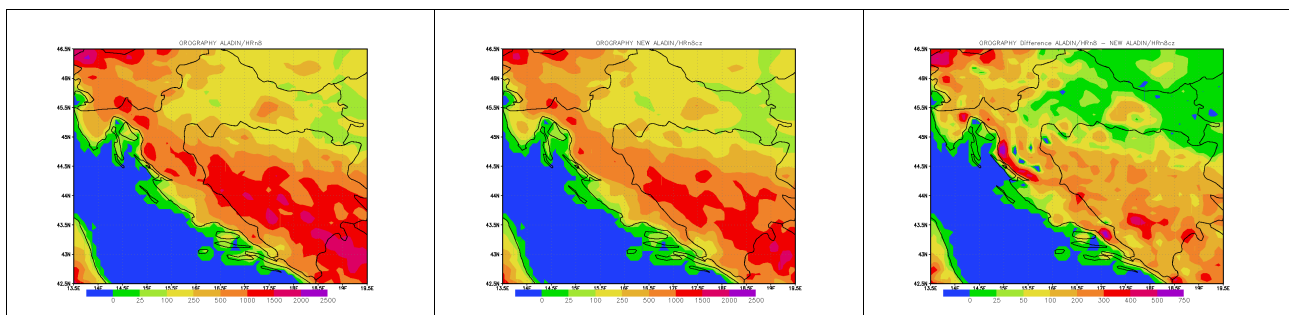


Figure 1. Orography in the operational (left) and experimental (centre) model version, and their difference (right).

## x Bura cases

One of the most interesting atmospheric features of the eastern Adriatic is orographically induced and forced bura wind. It is the outbreak of cold continental air over the Dinaric Alps, and its onset and intensity are strongly dependent on the wavelength and height of the orography. Therefore, an alternative version of ALADIN with the new sub-grid scale orography representation is tested on three bura cases.

Firstly, a case with generally weak bura was considered (3rd November 2004), when the drainage of air through the mountain-passes was induced by the pronounced difference in the air-mass characteristics in the inland and coastal part of the region. In addition, two extreme events of synoptically induced gale-force bura along the Adriatic coast (24th December 2003 and 13th November 2004) are studied.

### 5.4.3. Results

#### x Weak bura

In the case of locally forced bura, blocking in the windward side of the mountain in the operational model is clearly seen (Fig 2), while the new version allows the drainage of the cold continental air to start earlier leading to weaker winds.

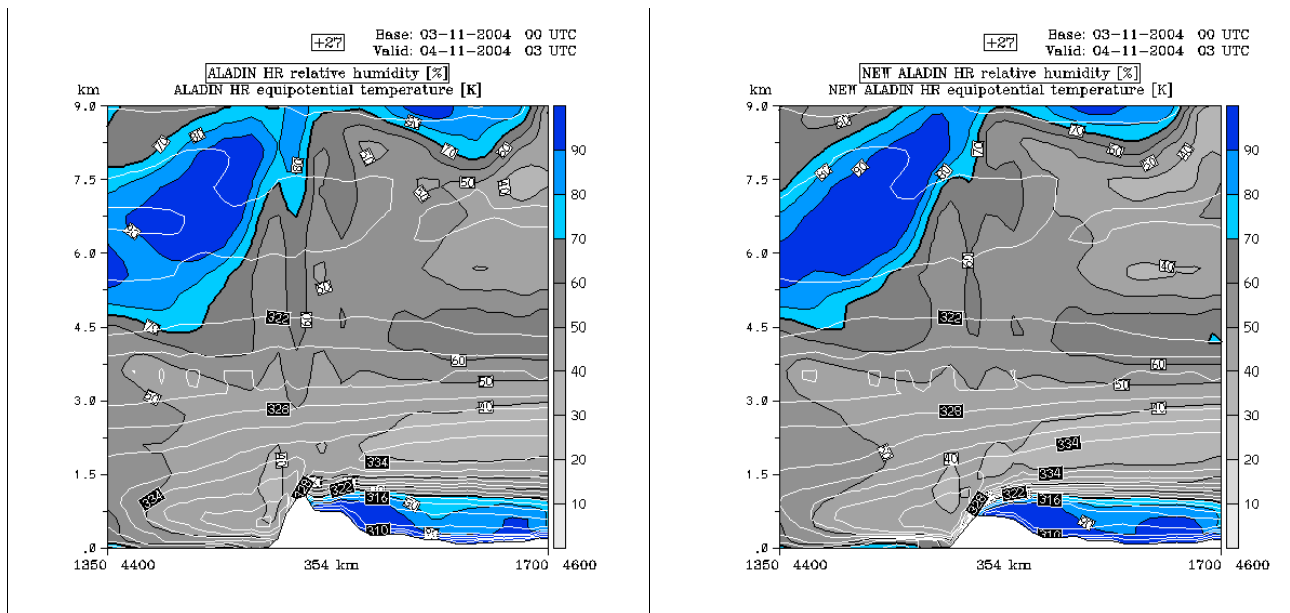


Figure 2. Vertical cross-sections perpendicular to the coastline from (13.5E, 44N) to (17E, 46N) of the modelled relative humidity with equivalent potential temperature in the operational (left) and experimental model version (right), 27 hours forecast starting from 00 UTC 3rd November 2004.

#### x Strong bura

In cases with severe bura, the most obvious feature of the experiment results is the increase of the 10m wind speed on the windward and its even more pronounced decrease on the leeward side (Fig 3). The reason for this is found in the reduction of the mountain range height and the slope angle on one hand, and the increase of the pressure drag related to the orographic lift on the other hand. Due to the removal of the envelope, the pressure gradient across the coastal mountains is reduced. Moreover, the relative difference between the high peaks and low valleys is smaller, hence the canalised structure of the wind is less pronounced. However, there is no significant change in the wind direction.

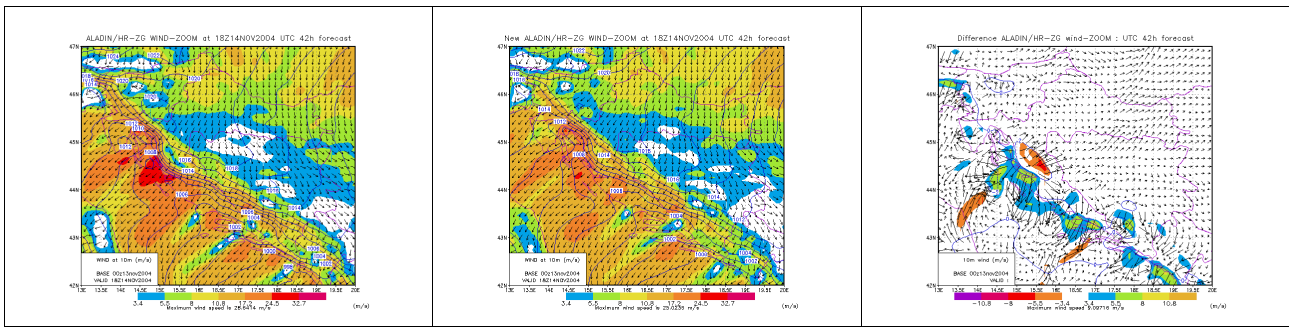


Figure 3. 10m wind in the operational (left) and experimental (centre) model version, and their difference (right), 42 hours forecast starting from 00 UTC 13th November 2004.

### x Severe bura

In the results of the operational model version, it is found that the artificially enhanced orography results in over-amplified mountain waves and unrealistic wave breaking (Fig 4). The lee wave reflects off the ground, therefore the wind maximum in the lee is closer to the surface, corresponding to the results found in the horizontal 10m wind fields. Results also show a pronounced orographically induced humidity maximum (cloudiness) near the mountaintop. As expected, in the experimental version the wave structure is smoothed. There is a more pronounced downstream momentum transfer leading to the different distribution of vertical motion induced by the obstacle. Therefore, the humidity maximum near the mountain peak is somewhat decreased, while the one in the middle troposphere is more pronounced and closer to the mountain.

### 5.4.4. Conclusion

Removal of the envelope and changes in the gravity-wave-drag parametrization result in stronger winds on the windward and generally weaker winds on the leeward side of the obstacle, as well as the reduction of the mountain wave amplitude.

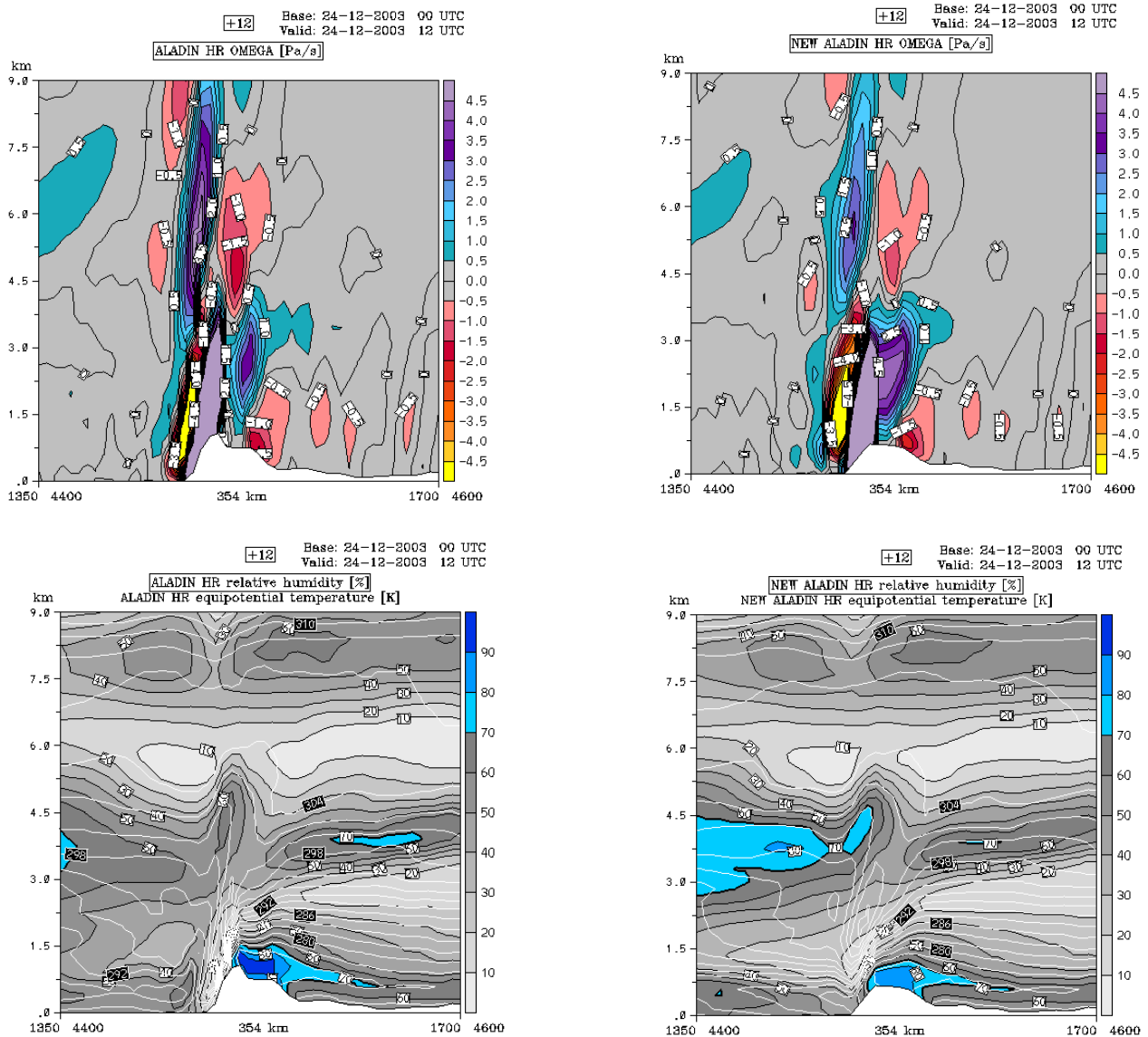


Figure 4. Vertical cross-sections perpendicular to the coastline from (13.5E, 44N) to (17E, 46N) of the modelled vertical velocity (top) and relative humidity with equivalent potential temperature (bottom) in the operational (left) and experimental model version (right), 12 hours forecast starting from 00 UTC 24th December 2003.

### 5.4.5. References

- Bougeault, P., 2001: Sub-grid scale orography parametrizations, Proceedings, *ECMWF Key issues in the parametrization of subgrid physical processes*, 3-7 September 2001, pp.53-69.
- Clark, T.L., and M. J. Miller, 1991: Pressure drag and momentum fluxes due to the Alps. II: Representation in large-scale atmospheric models. *Quart. J. R. Met. Soc.*, **117**, 527-552.
- Ivatek-Šahdan, S., and M. Tudor, 2004: Use of High-Resolution Dynamical Adaptation in Operational Suite and Research Impact Studies. *Meteorologische Zeitschrift*, **13**, No. 2, 1-10.
- Lott, F., 1995: Comparison between the orographic response of the ECMWF model and the PYREX data. *Quart. J. R. Met. Soc.*, **121**, 1323-1348.
- Wallace, J. M., S. Tibaldi and A. J. Simmons, 1983: Reduction of systematic forecast errors in the ECMWF model through the introduction of an envelope orography. *Quart. J. R. Met. Soc.*, **109**, 683-717.

## **5.5. Dynamical downscaling of the ECMWF ERA-40 re-analyses with the ALADIN model: S. Kertész, G. Szépszó, E. Lábó, G. Radnóti, A. Horányi.**

### **5.5.1. Introduction**

The fine scale investigation of the climate of the last few decades was mainly focused on the surface parameters disregarding the upper-level or PBL parameters. This was the straight consequence of the fact that observations of high spatial and temporal resolution were only available at the surface level. Nevertheless, PBL level climate information is of great importance for better understanding the climate and climate change, and there are several economical aspects, as well (e.g. installation of wind power plants requires the exact knowledge of the wind climate in the lower 100-150 m layer of the PBL).

The above problem can be solved using the global re-analyses that have become available at large centres (ECMW, NCEP) in the recent years. These re-analyses were produced by applying advanced data assimilation systems for past periods, reconstructing the full three dimensional fields in a dynamically-physically consistent way. However, the spatial resolution of these data is rather coarse (grid distance is over 100 km) describing only the large-scale features and providing little information of the small scales, highly affected by the orography. Thus, an appropriate downscaling technique is required to achieve the desired fine-scale climate fields.

In our experiments, such a scheme was applied to produce a high resolution wind climate for Hungary for the lowest part of the PBL. Our goal was achieved with the dynamical downscaling of the ECMWF ERA-40 re-analyses using the ALADIN model. The dynamical downscaling was realized in successive steps with nested model integrations. As a result, the wind climate for Hungary on a 5 km grid and 7 vertical levels from 10 m up to 150 m, for a 10-year period (1992-2002) was produced. In this article, a brief overview of the downscaling procedure is provided, and the first results and their inter-comparison with the available observations are presented.

### **5.5.2. The ERA-40 re-analysis**

The ERA-40 (ECMWF Re-Analysis) project started in 2000 to produce global re-analyses for the 1957-2002 period with 6 hour of temporal resolution (Simmons and Gibson, 2000). All the available observations including both in-situ and remote-sensing measurements were taken into account. The basic analysed variables included not only the conventional meteorological wind, temperature and humidity fields, but also stratospheric ozone and ocean-wave and soil conditions. The re-analyses were produced on a T159 horizontal spectral resolution (nearly 125 km) and 60 vertical levels (up to 65 km height), using the 3D-FGAT data assimilation technique with 6 hourly frequency throughout the period, supplemented by intermediate 3-hour forecasts. The results are available in the ECMWF MARS database.

### **5.5.3. The downscaling technique**

The dynamical downscaling of ERA-40 data was performed for a Hungarian domain of 5 km resolution for the period between January 1, 1992 and August 31, 2002. As the difference between our target resolution (5 km) and the ERA-40 resolution (~125 km) was quite significant, it was not obvious how many intermediate integration steps were needed to reach the optimal result. From a practical point of view, a single nesting and a double nesting solution were considered. The Slovenian colleagues, who were also working on the downscaling of ERA-40 data, carried out some experiments that indicated that double nesting gave better performances. Thus, two nested ALADIN integration steps were included at 45 and 15 km resolutions, respectively. In the final step ALADIN dynamical adaptation (DADA), developed for wind and precipitation (Žagar and Rakovec, 1999), was applied to reach the desired 5 km resolution (Fig.1). The applied DADA included a 30-minute quasi-adiabatic integration to reduce the interpolation errors, and to adapt the wind field to the high resolution orography. This configuration used only physical parametrization packages relevant to the near-surface wind fields (e.g. vertical turbulent diffusion, gravity wave drag). The dynamical downscaling consisted of the following integration, pre- and post-processing

steps (for each step AL15 was used):

1. As a first step - naturally - the ERA-40 global data had to be downloaded from the ECMWF MARS database. Considering the line width at that time this was a rather slow procedure and lasted for several months.
2. In the next step the raw global data (in GRIB format) was interpolated into a domain of 45 km resolution covering approximately the former LACE domain (see Fig.1). This step started with the run of configuration 901 to convert GRIB to FA format and was followed by configuration 927.
3. In the first dynamical downscaling step, the ALADIN model was run on the 45 km resolution domain, using the fields produced in the previous step as LBCs.
4. In the second dynamical downscaling step, the ALADIN model was run on a 15 km resolution domain that covered only a smaller Central-European area (see Fig.1). The LBCs in this case were provided by the forecasts of the previous - 45 km resolution - step.
5. In the last step, DADA was applied to the results of the 15 km resolution runs to achieve the desired 5 km horizontal resolution over a Hungarian domain (see Fig.1). The results of DADA was then post-processed by Full-Pos to derive fields on 10, 25, 50, 75, 100, 125 and 150 m height levels.

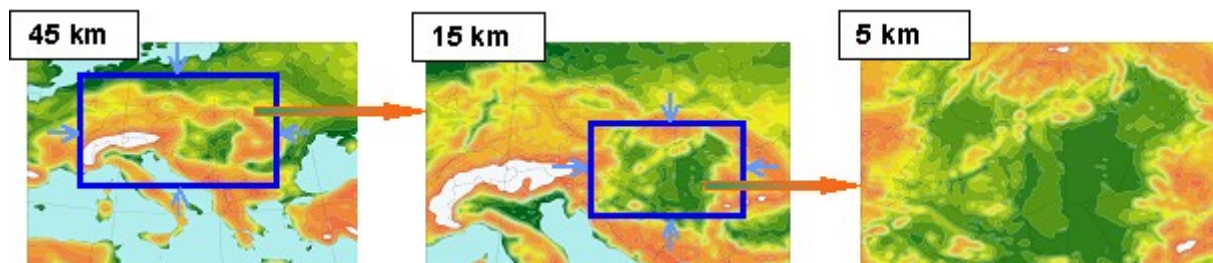


Figure 1. The steps of the dynamical rescaling using nested domains with increasing resolution.

While the coupling of the 45 km resolution runs with the ERA-40 data was quite obvious, it was not the case for the 15 km and 5 km resolution runs. The decision on the length of the individual integrations was not straightforward either. Regarding this question, two aspects were to be considered: if we want to use the re-analysis information as frequently as possible, then, short integration times seem to be optimal, while to avoid spin-up longer integration times should be used. Based on the Slovenian colleagues' experience, even 3 or 6 hour forecasts can be used to produce correct wind climate information. However, at a later stage, we would also like to generate precipitation climatology, and for precipitation, it is better to use longer forecasts (even beyond 12 hours). All things considered, the following configuration has been chosen (see Fig. 2):

- The integration on both the 45 and 15 km resolutions was started from 00 UTC on each day of the investigated period and lasted for 36 hours.
- To avoid spin-up only time-steps between 12 and 36 hours of the 45 km resolution runs were used as LBCs for the 15 km resolution runs.
- The LBCs for the first 12 hours for the 15 km resolution runs were provided by the 24-36 hour forecasts of the 45 km run started on the day before.
- The 5 km resolution DADA runs were coupled by the 12-36 hour forecasts of the 15 km resolution model runs.

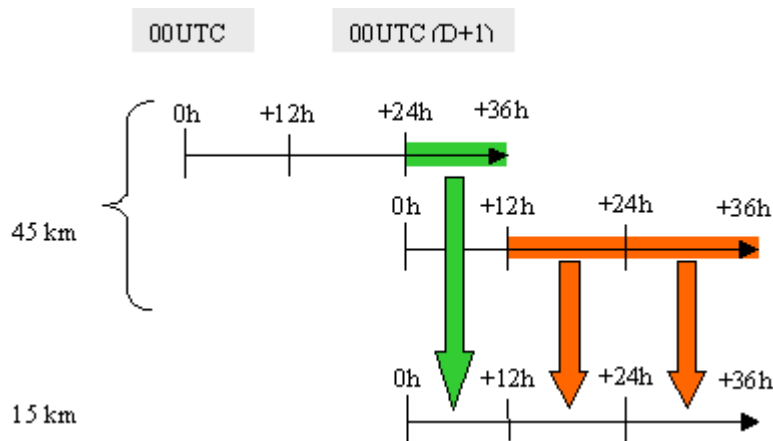


Figure 2. The coupling scheme between the nested 45 km and 15 km resolution ALADIN runs.

#### 5.5.4. Preliminary results

Up to now, only a limited evaluation and verification of the computed wind climate has been performed. The 6 hourly wind fields were used to create average wind speed maps for each investigated levels (see Fig.3). It can be seen on the maps that the wind maximum appears in the North Transdanubian region. At the 100-150 m height, the average values exceed even 7 m/s. The spatial distribution of the wind speed is in good accordance with two other wind climate maps produced at HMS. The first map is valid for the 1971-2003 period, and the upper-level winds were derived with the logarithmic wind profile from a grid-based wind climate at 10 m, generated with statistical modelling. The second 5 km resolution map covers the 2003-2004 period and was derived by the dynamical adaptation of the operational ALADIN/HU (AL15 and AL28) forecasts.

Regarding the verification, unfortunately, observations were only available at 10 m for the investigated period. Figure 4 shows the difference between the observed and computed average 10m wind speed values for 19 Hungarian locations. It can be seen from the figure that the dynamical downscaling usually overestimates the average wind speed. Beside the average wind, the wind direction distribution was also investigated. For most of the locations the computed wind direction distribution was in good accordance with the observations (see Fig.5), but there were also severe differences, especially in the vicinity of highly variable terrain.

The differences between the 10m measurements and the downscaled values can arise from at least three sources. Firstly, with dynamical downscaling, we produced wind data only every 6 hours, while the observed average is based on hourly measurements. Secondly, the applied 5 km resolution is obviously too coarse to describe the highly variable local orographic features that can greatly affect the wind field, because it only reflects the average features of a 5x5 km gridbox. Finally, both the ALADIN model and the ERA-40 re-analysis fields can be the source of a trivial error. At present, it is hard to assess the relative effect of the above error sources. Nevertheless, the forecast for upper levels is thought to be better than for 10 m since the effect of the local orographic structures becomes less significant with increasing height.

#### 5.5.5. Preliminary conclusions

The dynamical downscaling of the ECMWF ERA-40 re-analyses was performed with the ALADIN model, and a 5 km resolution Hungarian wind climate was derived for a 10-year period for the lowest 10-150 m layer of the PBL. The applied double-nesting technique combined with dynamical adaptation for wind proved to be effective, and resulted in realistic wind fields with a similar spatial distribution to wind climate fields derived with other methods. A preliminary verification was carried out for the 10m level. While the computed and observed wind direction distributions were quite similar in most of the cases, the average wind speed was overestimated at several locations. Due to lack of upper-level measurements, the verification of the upper level fields has not been possible, yet.

### **5.5.6. Future plans**

The more detailed evaluation and verification of the derived wind climate fields will be continued. We will compare the PDF of the observed and computed wind values for 10 m, and the wind speed distribution according to the direction will be also investigated. Some short term PBL wind measurements will be also included in the verification. Besides, the ERA-40 downscaling and wind climate investigation will be extended for the full 1957-2002 ERA-40 period.

### **5.5.7. References**

Simmons A. J., Gibson J. K., 2000: The ERA-40 Project Plan. ERA-40 Project Report Series,1  
Žagar M. and Rakovec J., 1999: Small-scale surface wind prediction using dynamic adaptation. *Tellus*, **51A**, 489–504.

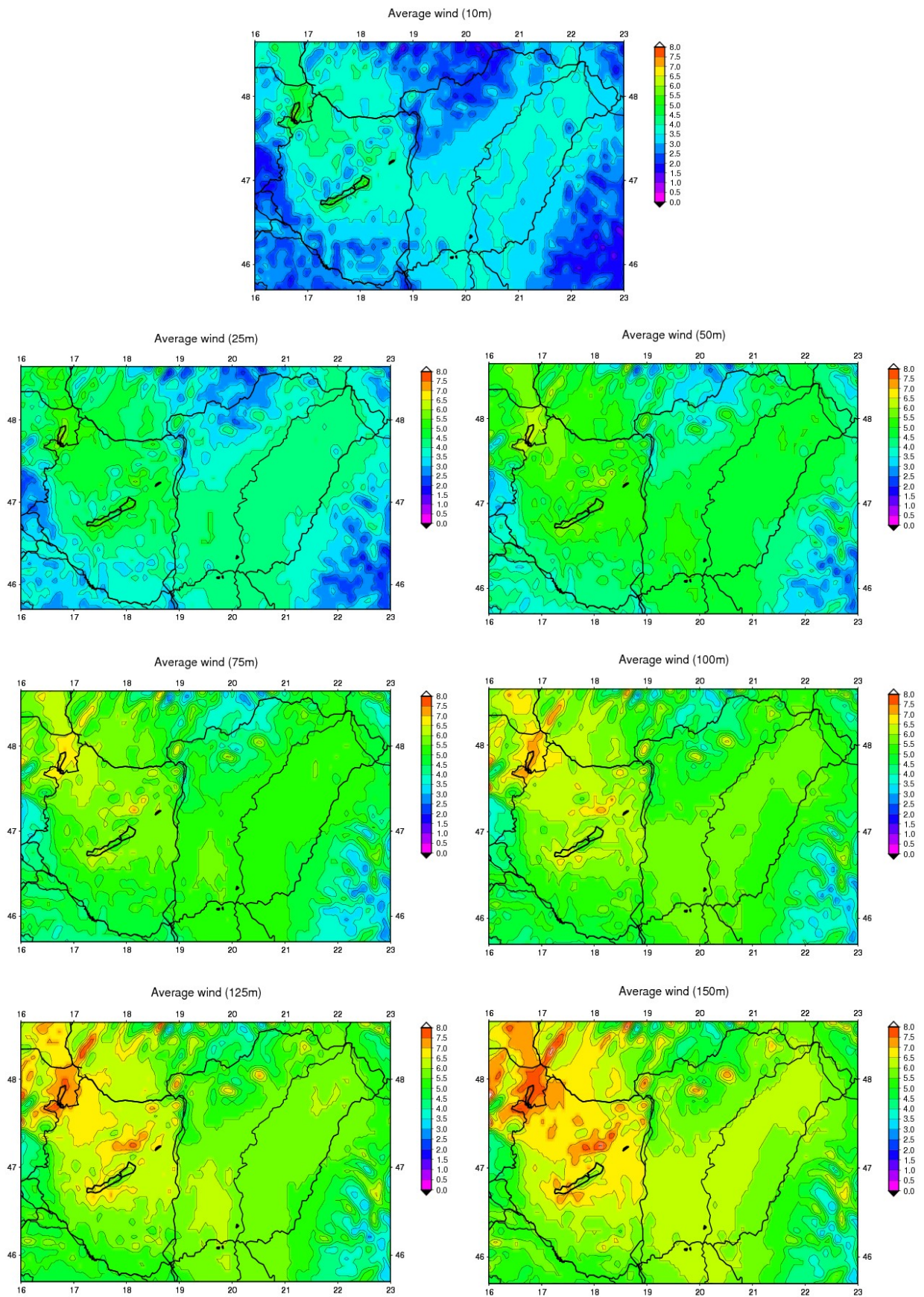


Figure 3. The average wind speed on different height levels between January 1, 1992 and December 31, 2001 derived from the dynamical downscaling of ERA-40 data.

Difference of the computed and observed average wind speed at 10 m

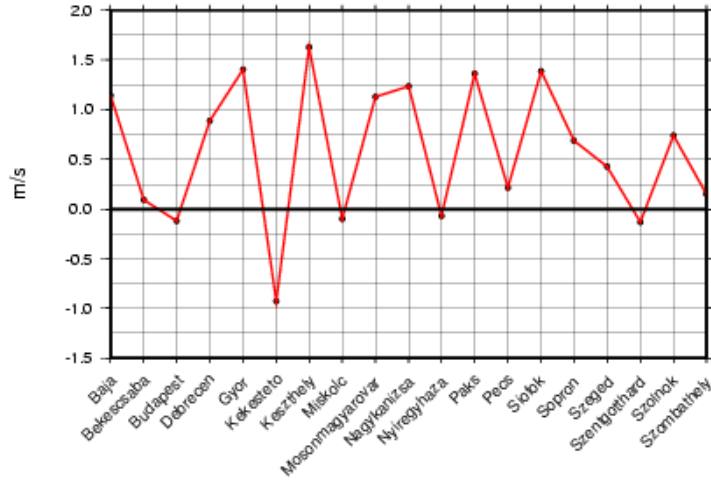


Figure 4. The difference between the computed and observed average 10 m wind speed for 19 Hungarian locations for the period between January 1, 1992 and December 31, 2001.

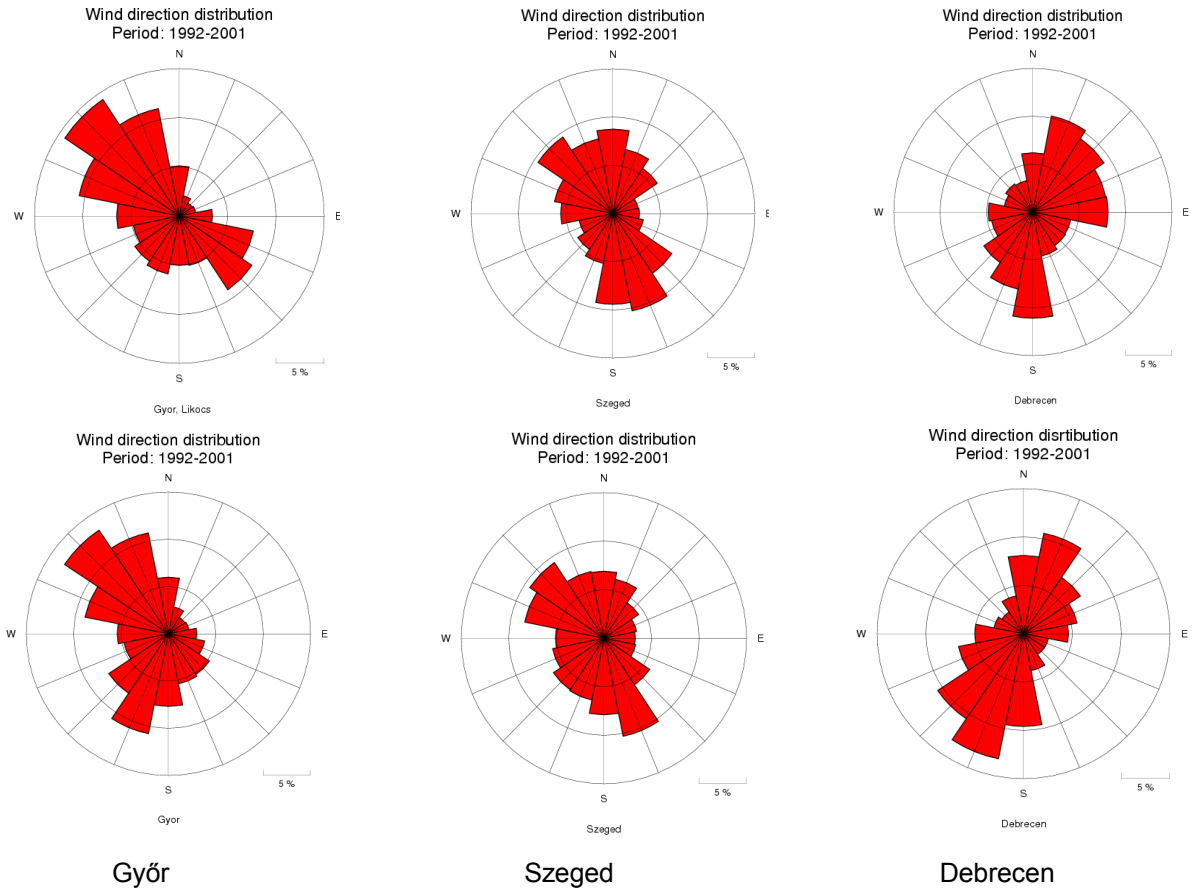


Figure 5. The computed (lower row) and observed (upper row) 10 m wind direction distribution for three Hungarian locations for the period between January 1, 1992 and December 31, 2001.

**5.6. Mesoscale overview of Lothar storm (26 december 1999): D. Raspaud, P. Arbogast, G. Hello, D. Lambert.**

**5.6.1. Summary**

The dynamics of the main growing phase of the 26 December 1999 storm is characterized by smaller horizontal and time scales than what is currently observed for mid-latitude cyclone developments. It seems therefore interesting to characterise the dynamical mechanisms using mesoscale simulations. This is done here using ALADIN simulations at 10km horizontal resolution. Then dynamical diagnoses are applied to the simulations in order to characterize mechanisms that are involved in the development of the storm.

**5.6.2. The ALADIN simulations of the Lothar storm**

The domain of the simulation is made such as the center of the domain corresponds to the location where the strengthening of the storm is maximum on the 25 of December at 21UTC. The simulation is starting on the 25 of December at 18UTC to end on the 26 of December at 06UTC. The period is covering the explosive development of the Lothar storm. The geographical domain is shown on the figure 1. Except from the geographical aspects, the configuration of the ALADIN model is the same as the one used currently in operation at Météo-France.

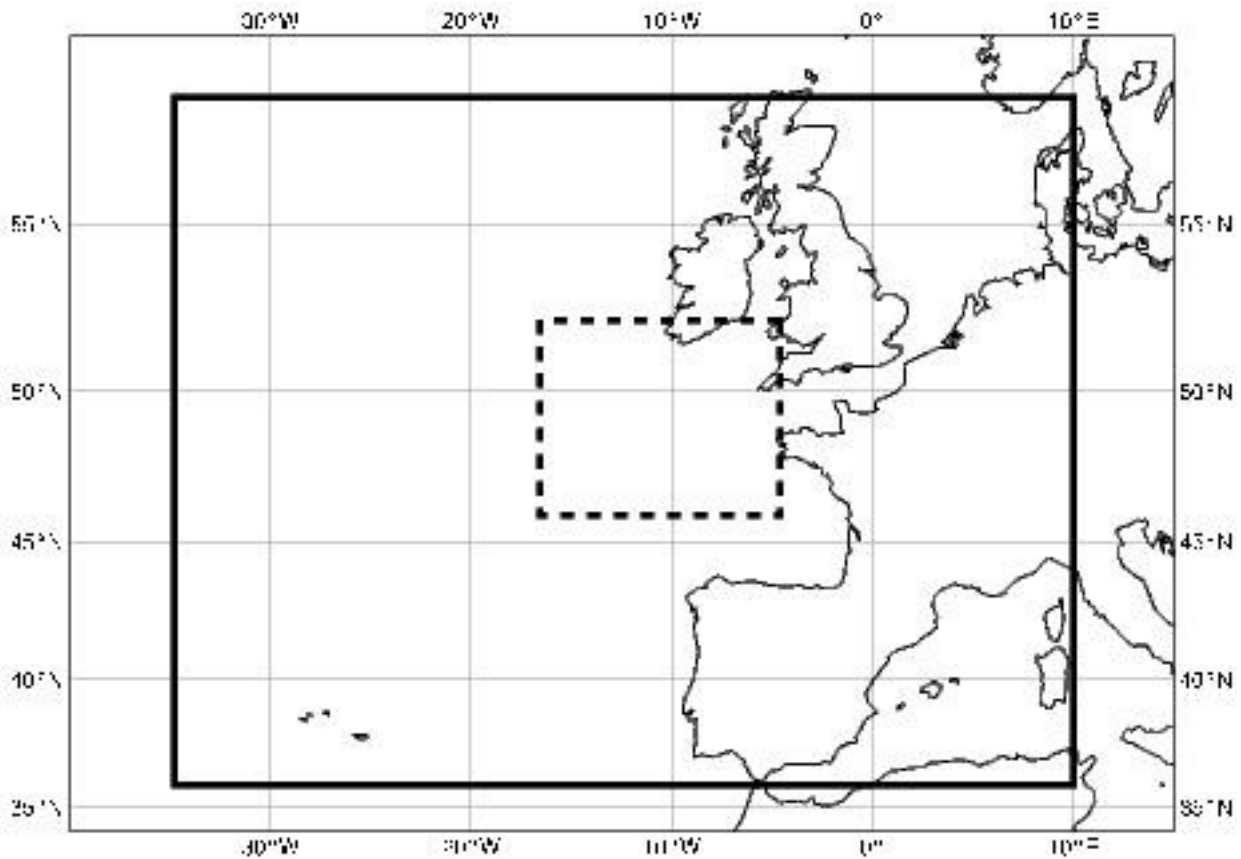


Figure 1: Geographical domain covered by the ALADIN simulations (in plain lines)

The upper level jet plays a major role in the development of the storm. It is well-simulated by the ALADIN model speaking in terms of location as well as in terms of depiction of its unusual intensity (Figure 2). The comparison of the ALADIN forecast is done when the cyclone is over the land on the 26 of December at 06UTC (Figure 2 bottom panel). The pressure field forecast by ALADIN (12 hours forecast) locates the surface cyclone on the west side of the Paris area. In reality, at this time the center of the storm is located a little more westerly on the normandy area. The value at the center given by the 12 hours forecast is of 976 hPa as the observed value is around

960 hPa. The low level winds given by the forecast show maximum values in the south part of the cyclone of  $27 \text{ ms}^{-1}$  which can be compared to the observed mean wind. In conclusion the ALADIN model forecast correctly the upper level dynamics and the location of the surface cyclone. The intensity of the deepening is not well forecast as it is also the case for the ARPEGE model.

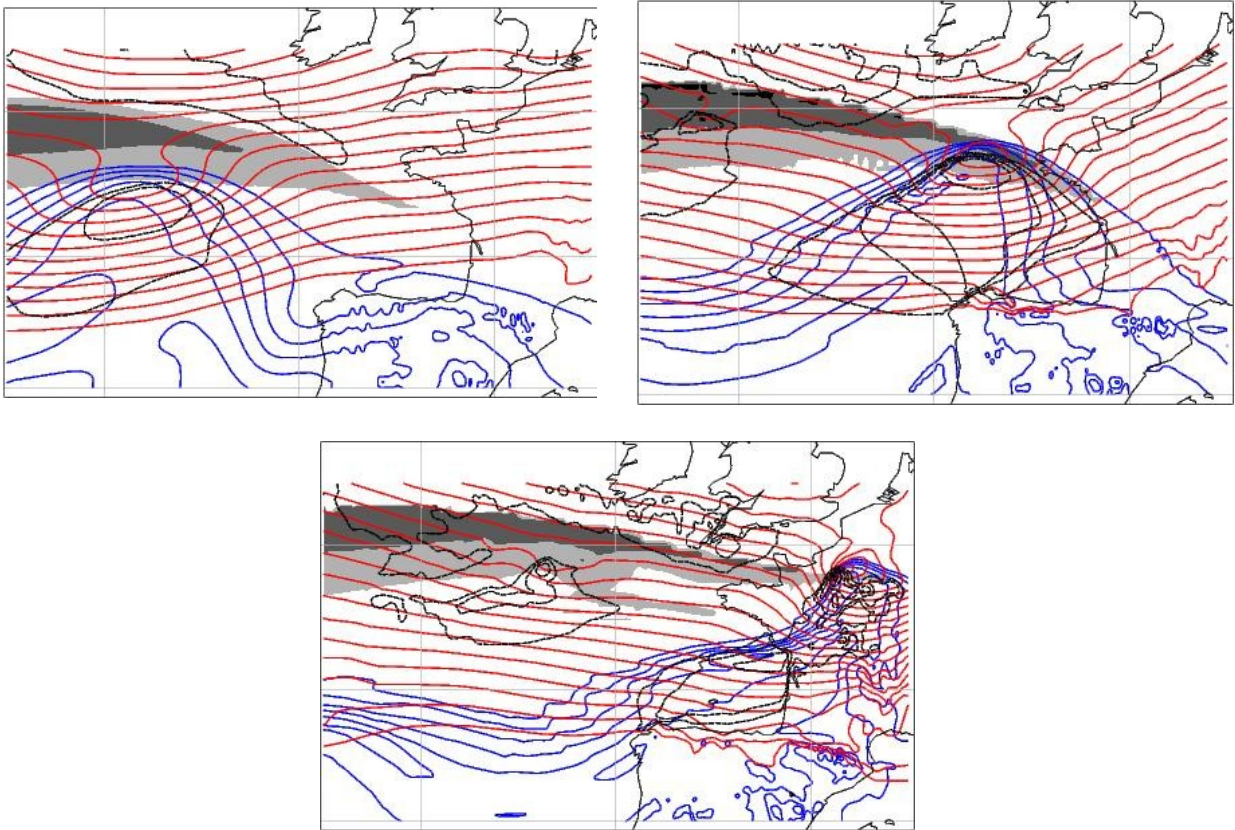


Figure 2 : ALADIN forecast. Upper left: analysis on the 25 of December 18UTC. Upper right: 6 hours forecast on the 26 of December 00UTC. Bottom: 12 hours forecast on the 26 of December 06UTC. In red, mean-sea-level pressure every 2 hPa for values lower than 1015 hPa. In blue  $\theta'_w$  (K) at level 850 hPa every 1K for values greater than 283K. In shading mode, the intensity of the wind, every 10 m/s for values greater than 80 m/s. The dot lines show the intensity of the low level wind at level 20 meters, every 25m/s for values greater than 17 m/s.

### 5.6.3. Results

#### x Energetics study

The first stage of this study is to split the model outputs into two parts: the first one is the time mean of the simulation over 12 hours (from 18UTC 25 December 1999 to 06UTC 26 December 1999) and the second part is the departure from this time mean. The first part will be called large scale environment whereas the second part may be associated with the storm itself. Then barotropic and baroclinic interactions between the storm and the large scale environment are studied using local energetic conversions.

To put on light barotropic interaction between the storm and its environment a superimposition of the deformation axis of the environment and the vorticity of the storm is shown at 23UTC 25 December 1999 (Figure 3, Left-hand side panel). If the wind associated to the large scale environment tends to make the vorticity maximum less elongated and more circular, i.e. the deformation axis is orthogonal to the main axis of the vorticity maximum, then the storm is able to extract some kinetic energy from its environment. Although the deformation field is not systematically orthogonal to the vorticity maximum main axis, the barotropic conversion has two maxima, the first one along the northern edge of the vorticity maximum and the second one along

the southern edge making the vortex more circular. Therefore the barotropic interaction between the vorticity maximum and its environment is one factor helping the cyclogenesis process.

The right-hand side panel of the Figure 3 suggests that baroclinic mechanisms dominate the growth of the storm. The baroclinic conversion displayed on the figure is proportional to  $\omega'\theta'$  where  $\omega$  is the vertical velocity,  $\theta$  the potential temperature and  $'$  denotes the departure from the time average. The magnitude of the local internal conversion maximum is about seven times the maximum of barotropic conversion showing the predominance of the baroclinic mechanisms for the growing phase of the storm.

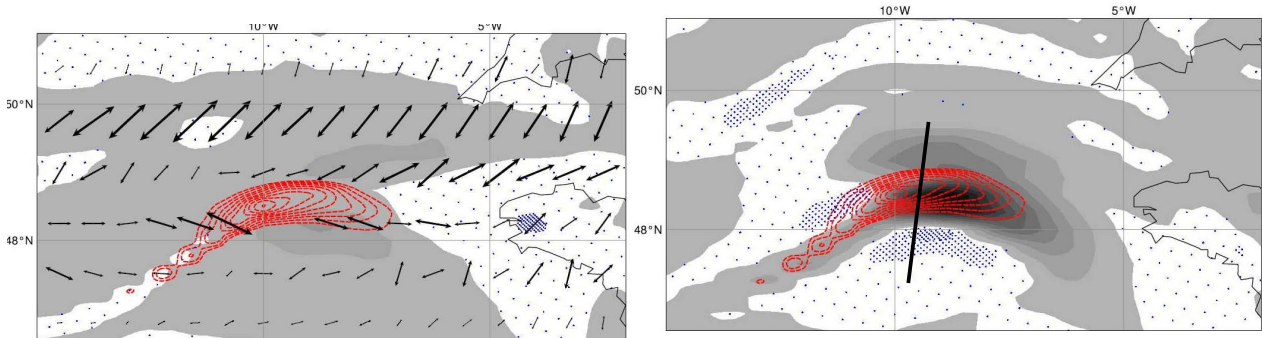


Figure 3: Energetic conversions at 23UTC 26 December 1999. Left: high-frequency relative vorticity associated to the cyclone (red contours every  $0.5 \cdot 10^{-5} \text{ s}^{-1}$  for values  $> 1.5 \cdot 10^{-5} \text{ s}^{-1}$ ), deformation associated to low-frequency wind field (the length of each arrow is proportional to the strength) and barotropic conversion (grey shading for value  $> 16 \text{ W/m}^2$ , blue shading for negative values). Right: same as left for the red contours, shading is for baroclinic conversion (maximum:  $110 \text{ W/m}^2$ )

### x Balanced vertical velocity diagnoses study

The vertical velocity field has two different origins: a dynamical one and a physical one. The dynamical mechanisms associated to the interaction of potential vorticity/potential temperature perturbations of finite amplitude embedded within a baroclinic environment (here a very strong and sharp jet stream) infer vertical velocity preserving the balance between the mass and wind fields. Such mechanisms are a key feature of baroclinic development. The physical mechanisms as latent heat release may also infer vertical velocity. After some balance assumptions -here the Alternative Balance (Davies-Jones, 1991) - it is possible to express the vertical velocity variable as solution of the following equation:

$$\mathcal{L}(\omega) = Q_{\text{dyn}} + Q_{\text{dia}}$$

where  $\mathcal{L}$  is a second-order partial derivative operator,  $Q_{\text{dyn}}$  is the baroclinic forcing function of the "q-vector" divergence and  $Q_{\text{dia}}$  is the diabatic forcing computed using the time tendency contribution of the physical parametrizations of the ALADIN physics. The dynamical vertical velocity is characterized by a dipole below the tropopause which is consistent with the classical configuration below a jet exit (Figure 4, left-hand side panel). The low-level vorticity maximum during its displacement towards the northeast will meet the ascending motion pattern. Then the deepening of the storm will be sustained by vorticity stretching.

However the diabatic contribution (Figure 4, right-hand side panel) presents features at the horizontal scale consistent with the cyclone itself and maximum four times the dynamical counterpart. The fact that the diabatically induced vertical velocity dominates the vertical velocity field supports the conclusion of Wernli *et al.* (2002). It may be inferred from this result that the forecast skill is not only determined by the initial conditions but also by a proper representation of subgrid scale physical processes.

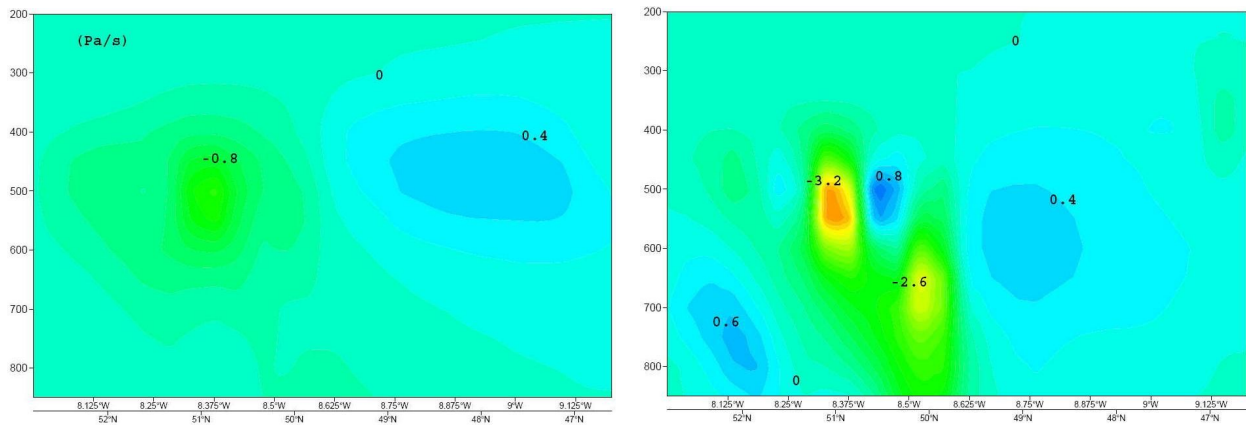


Figure 4 : 23UTC 25 December 1999. Vertical sections of dynamic (on the left) and diabatic (on the right) contributions to the vertical velocity field (in Pa/s) along the axis displayed on the previous figure. Green to red shading is for upward motion, cyan to blue for downward motion.

#### 5.6.4. References

- Davies-Jones, R., 1991: The frontogenetical forcing of secondary circulations. Part I: the duality and generalization of the Q vector. *J. Atmos. Sci.*, **48**, 497—509.
- Wernli, H., S. Dirren, M. A. Liniger and M. Zillig, 2002: Dynamical aspects of the life cycle of the winter storm 'Lothar' (24-26 December 1999). *Quart. J. Roy. Meteor. Soc.*, **128**, 405—429.

## 5.7. The sensitivity of the AROME simulations on the Gard case to synoptic forcing : D. Raspaud, P. Arbogast, G. Hello.

### 5.7.1. Summary

The Gard case is a case of a severe mesoscale convective event. The forecast skill for such an event at fine scale is known to be very dependent on the knowledge of the initial conditions (Ducrocq *et al.*, 2002). Therefore, the interaction between the synoptic forcing and the response of the mesoscale forecast is studied. The uncertainties in the initial and coupling conditions of the synoptic forcing are modelled by an ensemble system generated within the ARPEGE model. Then a "downscaling" is applied from the ARPEGE ensemble towards an AROME ensemble with an intermediate step using an ALADIN ensemble.

### 5.7.2. Methodology

#### x The ensemble

Several ensemble members are defined at synoptic scale (within the ARPEGE model) by the perturbations of the magnitude and/or the localisation of the key features of the synoptic scale dynamics at the initial stage of the simulations. These perturbations are computed by making corrections of the potential vorticity field that can be inverted in order to recover wind and temperature fields. Such a method is used currently at Météo-France in order to correct the initial conditions of a forecast (see Hello and Arbogast (2004) for a concrete application). Here, the tool is used in an unusual way, as the goal is not to correct an erroneous initial state but to model some kind of uncertainties at the synoptic scale. So a small ensemble of 8 members is built. The initial dispersion of the ARPEGE ensemble is shown in figure 1. The dispersion of the ensemble is a little bit greater than what would give a usual ensemble computed with singular vectors. But one can argue that the initial perturbations of this ARPEGE ensemble are not thought to optimally grow over a time period and thus can have greater values at initial time.

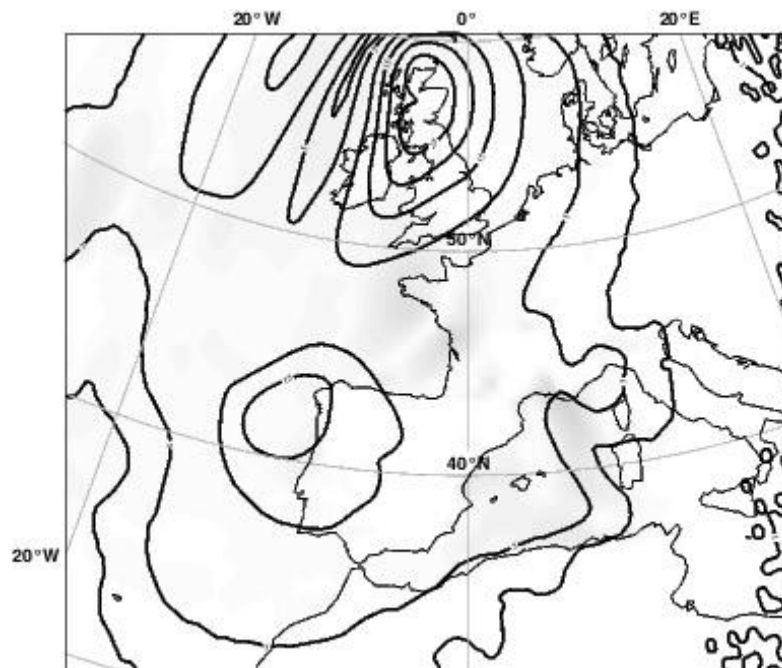


Figure 1: The characteristics of the ARPEGE ensemble on the initial state (08 of September 12UTC 2002). In plain lines, the standard deviation of the geopotential at 500 hPa (m) every 5 meters. In shading mode, the standard deviation of the intensity of the wind field at 950 hPa (maximum value of 2 m/s)

Then the ARPEGE model is run for a 18 hours forecast starting from the 8<sup>th</sup> of September 2002 at 12UTC. We obtain then 8 different forecasts. These forecasts are then used to initialize and couple the ALADIN model. The ALADIN model configuration used is the one currently in

operation at Météo-France. The ALADIN forecasts obtained are then used to initialise and couple the AROME model (at AROME nominal resolution i.e. 2.5 km, for details about AROME see in newsletters 25 and 27 the related articles). Figure 2 shows the nested models ALADIN and AROME.

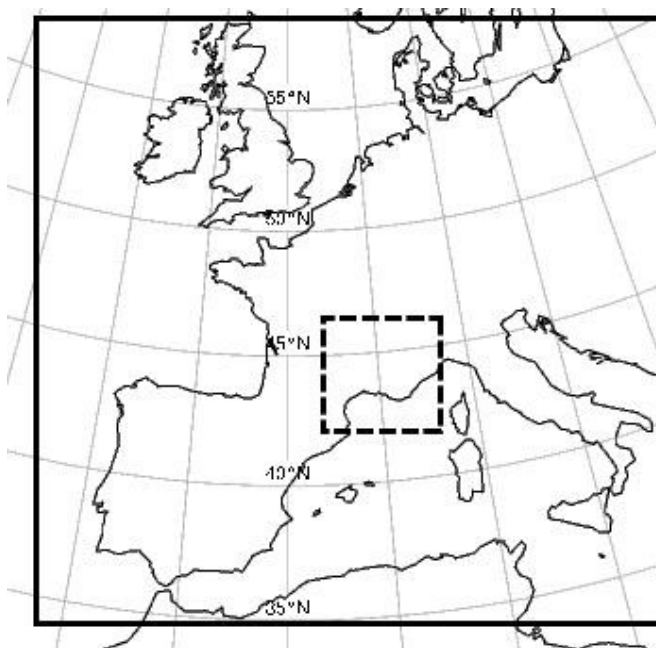


Figure 2: The nested ALADIN-AROME domains. The geographical domain covered by the ALADIN simulations is depicted in plained lines as the one covered by the AROME simulation in dashed lines.

### x The Gard case

This case has been thoroughly studied as it was a catastrophic flash-flood event over the South-East part of France. The reader can find more details on this case in Delrieu *et al.* (2004). The period that is considered in this study is starting on the 8 of September at 12UTC, to end on the 9 of September at 06UTC. On the 8 of September at 12UTC the convection has already started. The event is characterized by the large size of the area touched by heavy precipitation and also by important values of the cumulated rainfall: more than 300 mm of rain in 24 hours over the 'Gard' area (figure 3).

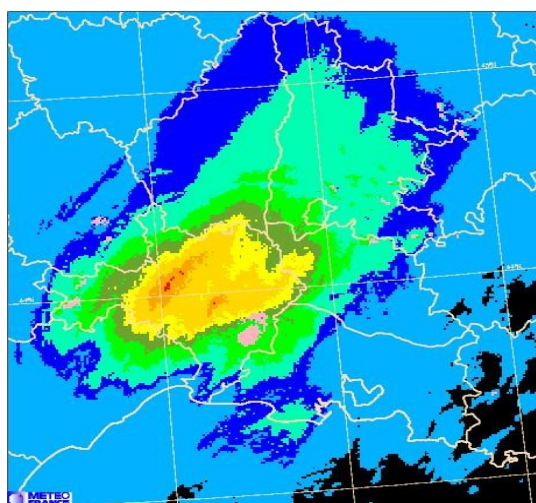


Figure 3: Cumulated rainfall over the Gard region in 24 hours from the 8 of September 12UTC to the 9 of the September 12UTC. In light green values between 50 and 100 mm, in khaki values between 100 and 150 mm, in yellow values between 150 and 200 mm, in light orange values between 200 and 300 mm, in dark orange values between 300 and 400 mm and in red values between 400 and 500 mm.

### 5.7.3. Results

#### x The ALADIN ensemble

The dispersion of the ensemble at the regional scale is examined with the help of the standard deviation of the geopotential field at 500 hPa and of the intensity of the wind field at 950 hPa. This dispersion is considered after 18 hours of forecast (figure 4).

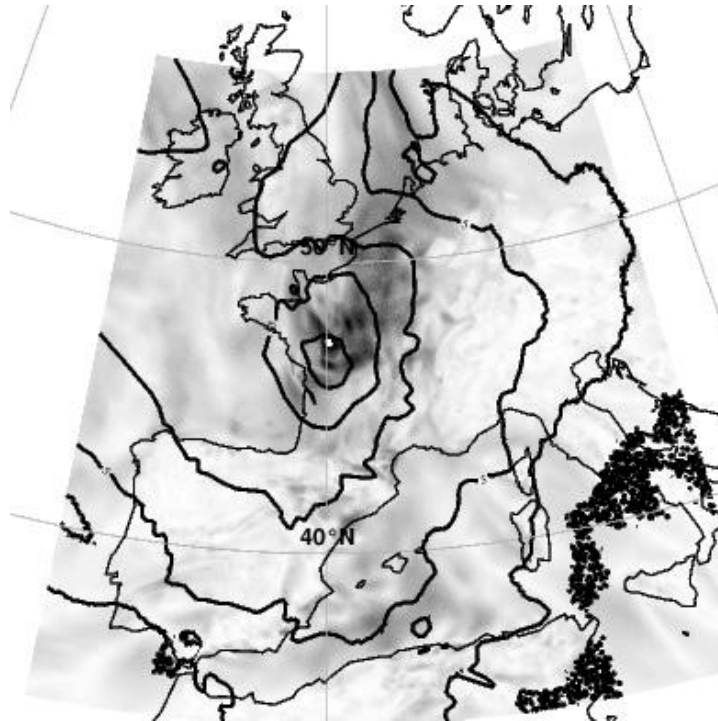


Figure 4: The dispersion of the ALADIN ensemble after 18 hours of forecast. In contouring mode is displayed the standard deviation of the geopotential at 500 hPa every 5 meters. In shading mode the standard deviation of the wind field at 950 hPa is displayed (black is for 6 m/s).

The ALADIN ensemble amplified the dispersion given by the ARPEGE ensemble especially for the low level wind. Apart from that fact, the location of the maximum of dispersion is the same as the one depicted by the ARPEGE ensemble, on the Northern part of France, and is related to a front that crossed this area during the night of the 8<sup>th</sup> of September.

#### x The AROME ensemble

The dispersion of the regional ensemble is furthermore amplified in the AROME ensemble. The standard deviation of the ensemble for the wind field on the AROME domain reaches its maximum value of 6 m/s in many places with important geographical extent as this value is not reached in the same area, as with the ALADIN ensemble. This increase could be due to a downscaling effect together with the impact of the convection, which is explicitly described at the AROME scale, on the low-level wind. Figure 5 shows the cumulated rainfall of the different AROME forecasts from the 8<sup>th</sup> of September 12UTC to the 9<sup>th</sup> of September 06UTC. The first remark is that the location of the event is the same on each simulation. In the reality, this event was located more south and east over the 'Gard' area (figure 3). So, the AROME ensemble was not able to catch correctly the localisation of the event. This can be due to the fact that the dispersion of the synoptic ensemble is not large enough, considering this specific aspect (only 8 members and the perturbations are done on too few features of the ARPEGE analysis) and, that this specific aspect may also be sensitive to finer scale forcing that can not be present in the ARPEGE ensemble. The second point that can be infer from figure 5 is, that the experiments are very different, considering

the intensity and the geographical location of the event. For example, there is more than 150 mm on 18 hours as a maximum difference inside the ensemble. This last point shows the extreme sensitivity of the strength of this event to the skill of the initial condition at synoptic scale.

#### **5.7.4. References**

Delrieu, G., V. Ducrocq, E. Gaume, O. Payratre, H. Andrieu, P. Ayrat, C. Bouvier, L. Neppel, M. Livet, M. Lang, J. Parent-du-Châtelet, A. Walpersdorf and W. Wobrock, 2004: The catastrophic flash-flood event of 8-9 September 2002 in the Gard region: a first case study for the Cévennes-Vivarais mediterranean hydrometeorology observatory. *J. Hydrometeor.*, **6**, 34-52.

Ducrocq, V. , D. Ricard, J.-P. Lafore and F. Orain, 2002: Storm-scale numerical rainfall prediction for five precipitating events over France: on the importance of the initial humidity field. *Wea. Forecasting*, **17**, 1236-1256.

Hello, G. And P. Arbogast, 2004: Two methods to correct the initial conditions applied to the storm of the 27 December 1999 over southern France. *Meteorol. Appl.*, **11**, 41-57.

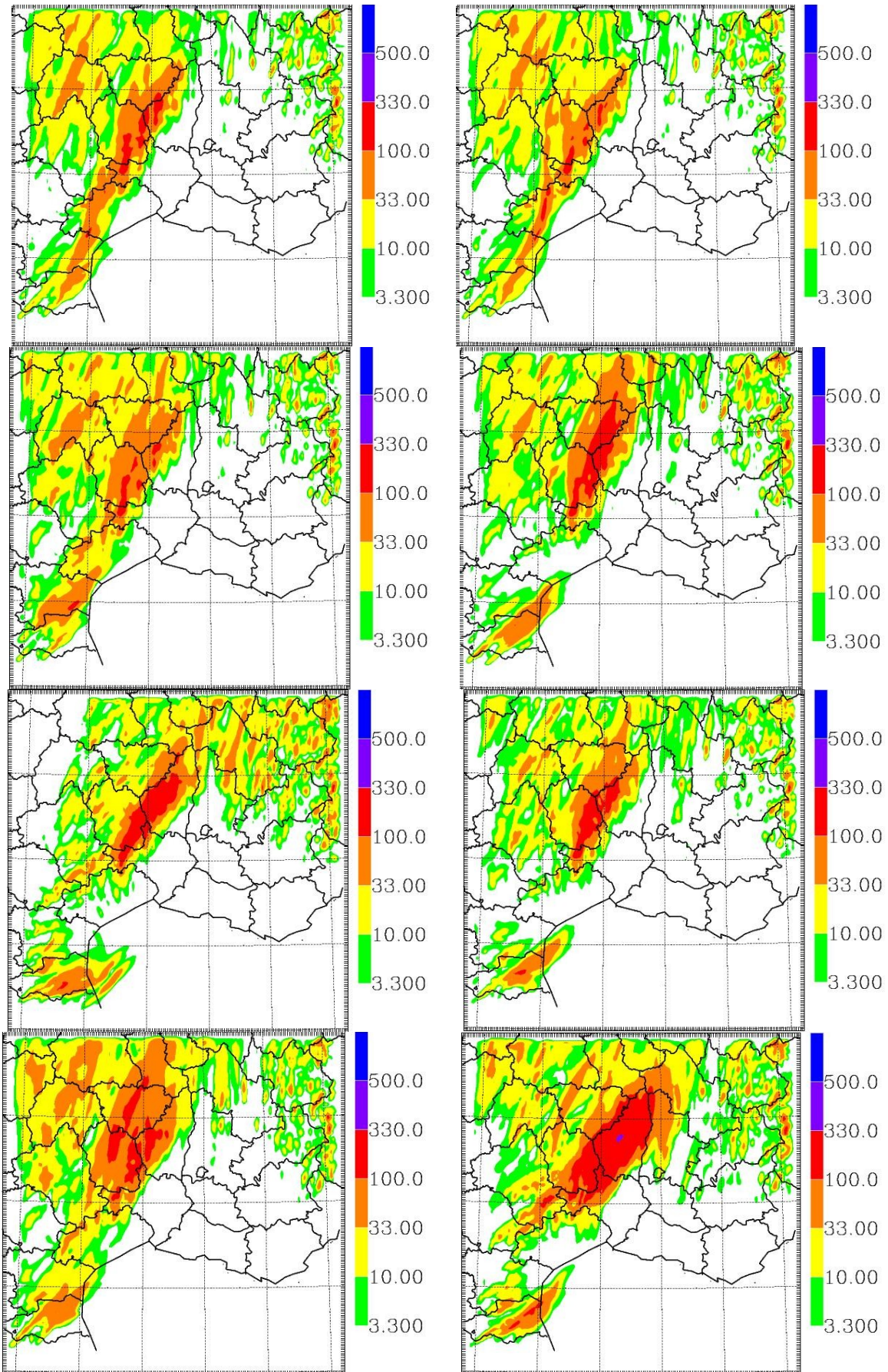


Figure 5: Cumulated rainfall over the 18 hours forecast starting from the 08 of September 12UTC. The panels are showing the different AROME forecasts of the ensemble.

## 5.8. Testing radiation and cloudiness parameterization: *M. Tudor, I. Stiperski, D. Drvar.*

### 5.8.1. Summary

In cases of stable atmosphere with low-level inversion and low cloudiness or fog, the operational version of the ALADIN model does not predict enough low cloudiness and consequently the diurnal cycle of the 2m temperature is too pronounced. Different cloud schemes and cloud-overlap assumptions play a more important role in the 2m temperature prediction than the modifications in the radiation scheme.

### 5.8.2. Introduction

For the cases of stable atmosphere with low-level inversion, low cloudiness and fog, the operational ALADIN model does not predict the diurnal pattern of the surface temperature nor the low cloudiness well. Although the model initially recognizes the existence of the temperature inversion and an almost saturated state of the atmosphere adjacent to the ground, the cloudiness scheme is usually unable to diagnose either low-level cloudiness or fog. Consequently, radiation scheme heats the ground and breaks the inversion, making the situation even worse.

### 5.8.3. Methods

There are several radiation schemes available in ALADIN, the currently operational one (Geleyn and Hollingsworth, 1979), FMR (Morcrette 1989) and RRTM (Mlawer et al. 1997). The first one is very simple and computationally cheap and may be used at every time-step. The other two are computationally expensive, so they could be called only every few hours.

The operational cloudiness parametrization results have been compared to the results from the scheme adapted from Xu and Randall (1996). Secondly, the operational radiation scheme has been enhanced (Bouyssel et al. 2003, Geleyn 2004) and the results have been compared to the one without the enhancements. In addition, the effect of different cloud-overlap assumptions and modified vertical profile of critical minimum, mesh averaged, relative humidity producing a cloud have been tested.

The operational cloudiness scheme diagnoses cloudiness in such a way that if a parcel is over-saturated the amount of diagnosed cloudiness depends on over-saturation (cloudiness ranges from 0.7 to 1.0). Therefore e.g. a 0.7 cloudiness allows part of the radiation through. Therefore, the surface cools more during the night and warms more during the day, giving pronounced diurnal pattern in surface temperature. In the morning this leads to the temperature rise due to heating, inversion breaking and eventual loss of cloudiness.

In the scheme adapted from Xu and Randall (1996) the over-saturated parcel has cloudiness equal to one. Therefore short-wave radiation is more efficiently reflected and longwave radiation is more efficiently absorbed. This helps to preserve the temperature inversion, fog and low stratus clouds.

If there are several layers of clouds with cloudiness less than one, the maximum overlap will vertically align these clouds in such a way that they will be on top of each other, leaving a part of the column without clouds permitting radiation transfer. On the other hand, randomly overlapped clouds produce more total cloudiness and reduce the cloud free area in the grid cell.

Random maximum is an intermediate method when maximum overlap is used for continuous cloud levels and random overlap when clouds are not continuous in the vertical.

### 5.8.4. Results and discussion

December 2004 has been characterized by long lasting fog in valleys inland. Results are shown for one run covering 2 days during that period. The 2m temperature varied very little during that period and showed no diurnal pattern.

The reference forecast (most similar to the operational one) is the experiment 1 (exp1). The use of random maximum overlap assumption when computing cloudiness significantly reduces the amount of clouds and even amplifies the diurnal variation of temperature. However, the introduction of the Xu-Randall cloudiness scheme gives more clouds and improves the 2m temperature forecast. Finally, the random overlap assumption produces even more clouds. Thus, the scheme with most clouds forecasts a surface temperature that is closest to the measured data.

The operational radiation scheme with Xu-Randall cloudiness parametrization and random overlap assumption produces the thickest low cloud layer, that reduces the night cooling and heating during the day. It still shows signs of diurnal variation but is closest to the measured data. Enhanced radiation increases the amplitude of the diurnal variation of temperature, which gives worse forecast in this case. It seems that the modification in the critical relative humidity profile does not play a significant role.

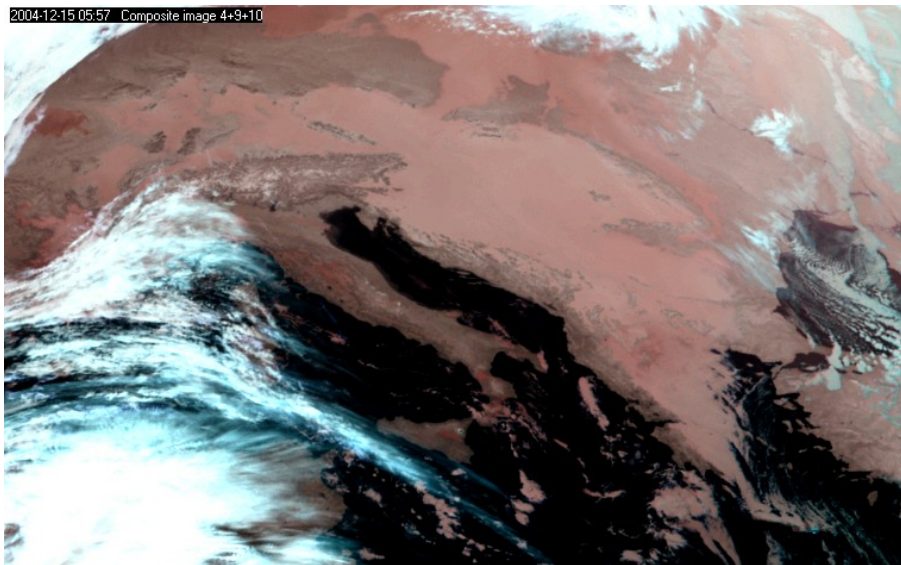


Figure 1. Meteosat-8 RGB composite of channels 3.9, 10.8 and 12.0  $\mu\text{m}$  for December 15th 2004, 06 UTC. Fog or low clouds over Southeastern Europe are clearly visible.

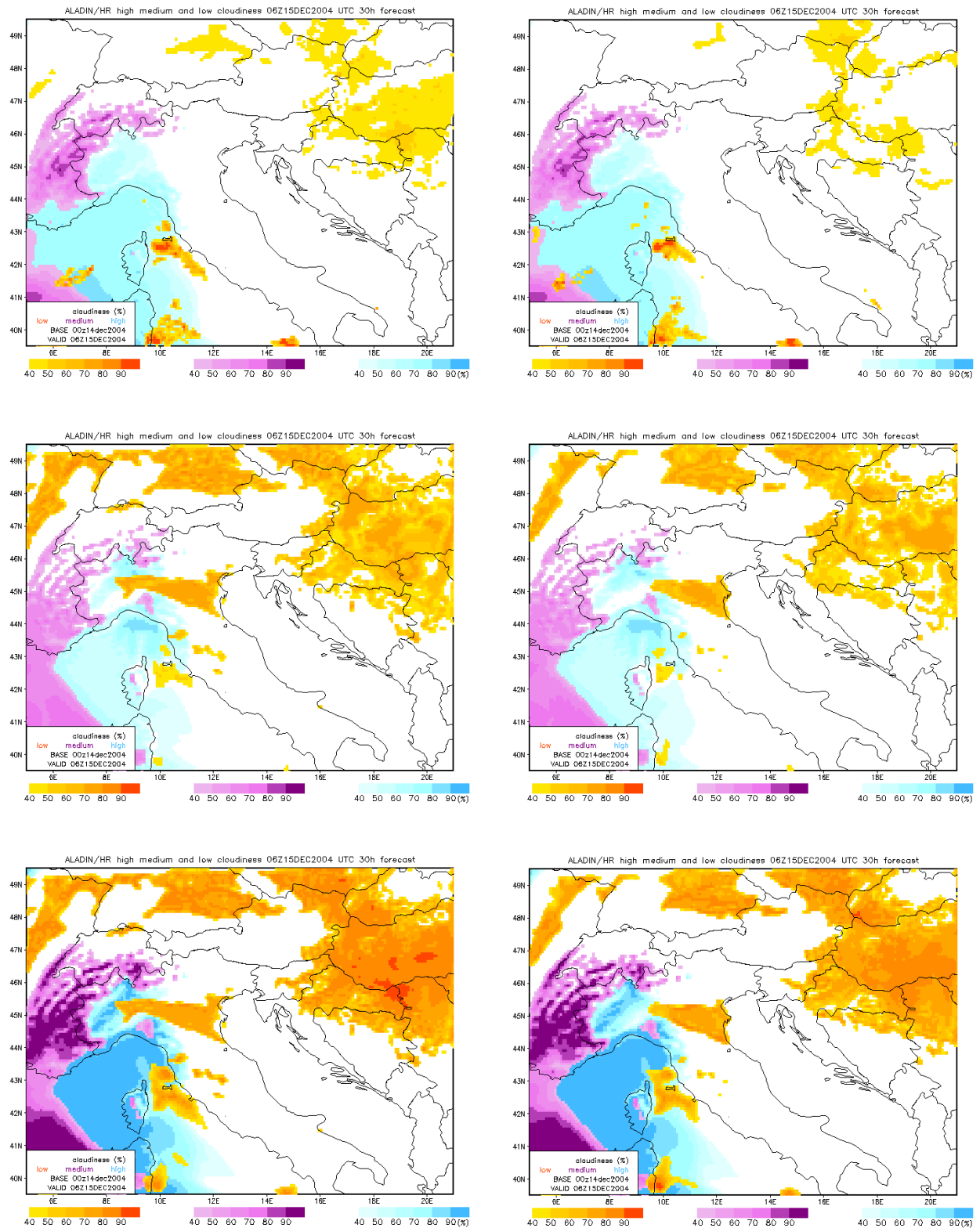


Figure 2. Low, medium and high cloudiness, with the operational (left) and NER (right) radiation scheme, operational critical relative humidity profile, cloudiness parametrization and random overlap (top row), random maximum overlap (second row), Xu-Randall cloudiness scheme and random overlap (bottom row), (only the modifications to the setup of the previous row are listed).

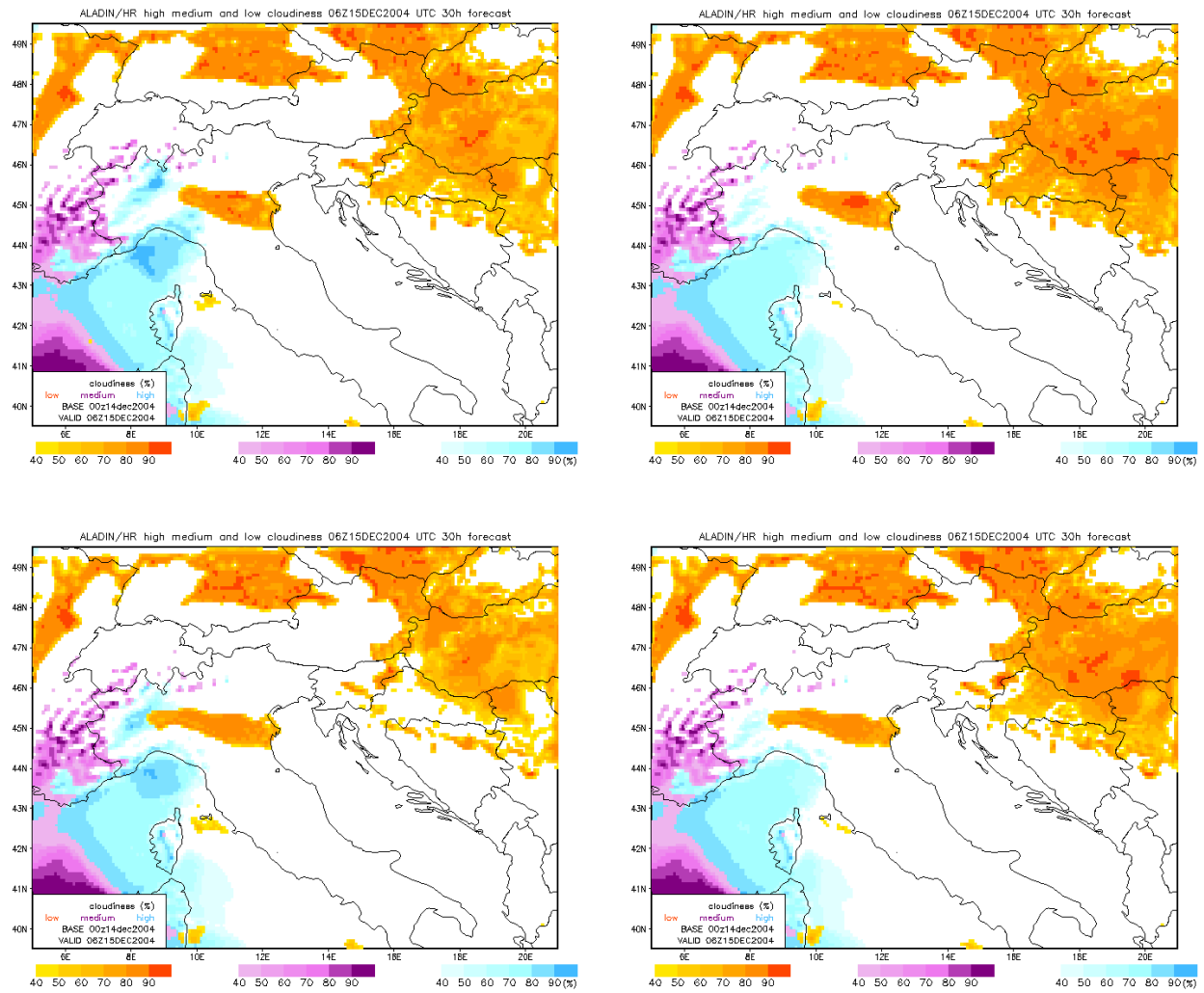


Figure 3. Low, medium and high cloudiness, with FMR radiation scheme called with 1 hr (top row) and 3 hr interval (bottom row), with maximum (left) and random overlap (right) and Xu-Randall cloudiness scheme, 30 hour forecast starting 00 UTC 14th December 2004.

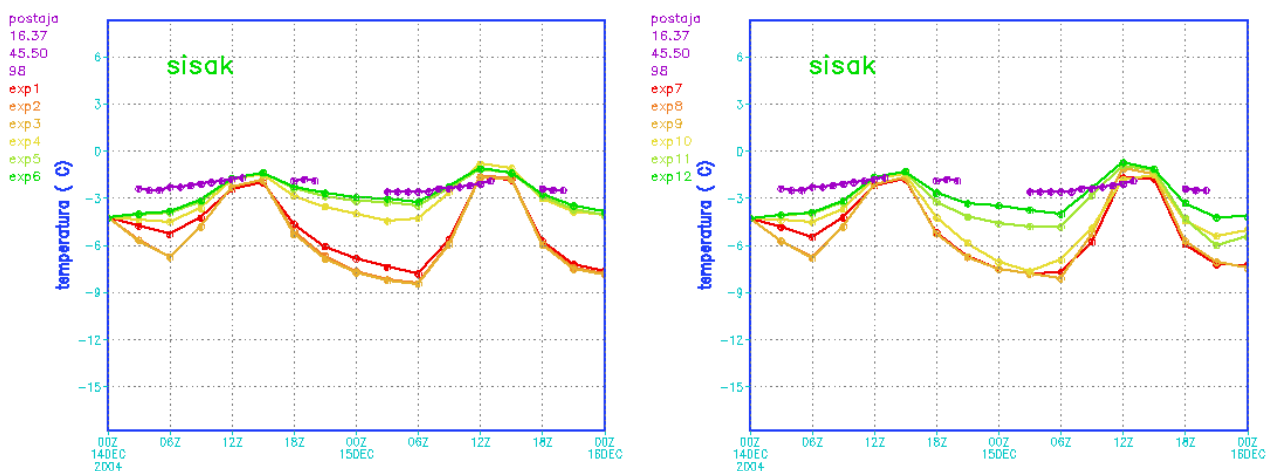


Figure 4. Comparison of the modelled 2m temperature evolution for 00 UTC run on 14th December 2004 with measured data from synoptic station with operational radiation scheme (left) and including NER (right), **reference, rand max, rm+new RH, XR cloud, random, old RH**.

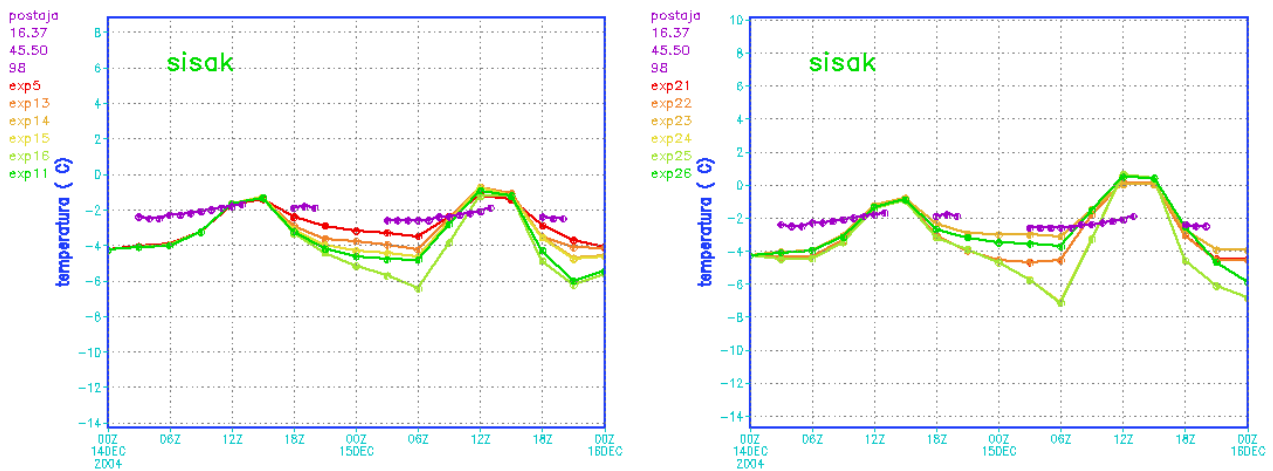


Figure 5. Comparison of the modelled 2m temperature evolution for 00 UTC run on 14th December 2004 with measured data from synoptic station with only parts of NER (left, **reference**, **LRMIX**, **LRPROX**, **LRSTAB**, **LRTDL**, **NER**) and FMR (right, **max**, **1hr**, **r-max**, **1hr**, **rand**, **1hr**, **max**, **3hr**, **r-max**, **3hr**, **rand**, **3hr** ).

### 5.8.5. Conclusion

Alternative versions of cloudiness and radiation schemes have been tested on a synoptic case marked by a strong temperature inversion, low cloudiness and fog in inland part of Croatia, that lasted for several days. The results show significant improvement in the low cloudiness and the surface temperature (2m AGL) diurnal pattern for certain configurations.

New relative humidity profile only slightly increases low cloudiness. Random maximum overlap significantly reduces the amount of clouds and amplified the diurnal variation of temperature when compared to the random overlap results. Xu-Randall cloudiness scheme gives more clouds and improves 2m temperature forecast. More sophisticated radiation schemes did not improve results.

Unsatisfactory model fog forecast has encouraged a study of alternative radiation and cloudiness schemes combined with different cloud overlap assumptions. The parameterization of cloudiness seems more important than the radiation parameterization for better forecast of 2m temperature.

## **5.9. Testing the New Semi-Lagrangian Horizontal Diffusion Scheme: Martina Tudor, Ivana Stiperski, Dunja Drvar, Vlasta Tutiš and Filip Vana.**

### **5.9.1. Summary**

The main role of the horizontal diffusion schemes in numerical models nowadays is to remove the information without forecast value and the energy accumulated due to finite truncation of a model spectrum, hence acting as a numerical filter. However, during intensive cyclogenesis, especially over steep surfaces, the physical horizontal diffusion should not be neglected. A stable and efficient non-linear horizontal diffusion, based on the control of the degree of interpolation needed for the semi-Lagrangian advection scheme, has been implemented in ALADIN. The results of several numerical experiments show a better simulation of a mesoscale Adriatic cyclone and upper troposphere cyclones and a beneficial impact on forecast of low cloudiness in anticyclones.

### **5.9.2. Introduction**

The main form of horizontal diffusion commonly used in NWP models is the numerical diffusion that acts as a numerical filter and selectively damps short waves. It is usually applied on model levels that often follow orography, so it is not purely horizontal. Physical horizontal diffusion is negligible for low horizontal resolution and requires computationally expensive nonlinear operator realistically describing physical processes.

The significance of the physical horizontal diffusion increases with horizontal resolution. Simultaneously, model levels become more tilted close to mountain areas, making the traditional numerical diffusion act more and more along the vertical. So the « horizontal » mixing often occurs between “the valley” and “the mountain top”. This feature of numerical diffusion is more pronounced in cyclogenetic areas surrounded by mountains, like Adriatic Sea surrounded by Dinaric Alps, Alps and Apennines. Simon and Vana (2004) have shown that physical horizontal diffusion should not be neglected when the horizontal component of the turbulent mixing is stronger than the vertical one. This could be in situations with strong horizontal wind shear, but also in statically stable situations.

### **5.9.3. Methods**

The operational ALADIN model is conducted with a 4th order numerical diffusion scheme. A new scheme has been developed by Filip Vana that controls the horizontal diffusion intensity using local physical properties of the flow and acting horizontally. In the semi-Lagrangian advection scheme, the origin point is found by interpolation. The interpolator characteristics (the degree of interpolation) depend on the local flow, yielding a horizontal diffusion based on physical properties of the flow. We will call this new scheme semi-Lagrangian horizontal diffusion (SLHD).

### **5.9.4. Results and discussion**

#### **x Adriatic cyclones**

The 00 UTC run 24 hour forecast starting 20<sup>th</sup> July 2001 produced a very intensive cyclone in the Adriatic. The position was good, but the intensity was overestimated. SLHD reduces the intensity of the cyclone at sea level as well as at 850 hPa and the forecasted 10m wind speed is reduced (fig.1).

It is important, however, to verify that this new scheme will not reduce the intensity of every small cyclone. On 6<sup>th</sup> May 2004, small but intensive cyclone quickly developed in the Adriatic and crossed it. Its intensity was predicted well, but the trajectory of the cyclone was more to the northwest. In this case, use of SLHD did not reduce the cyclone intensity, but shifted the system a bit in the northwestern direction (fig.2).

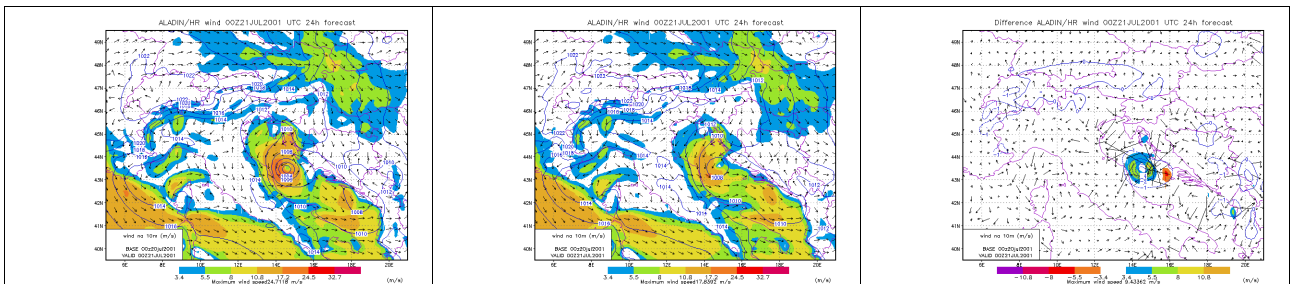


Figure 1. Mean-sea-level pressure and 10 m wind obtained with classical numerical diffusion (left), semi-Lagrangian horizontal diffusion (center) and their difference (right), 24 hour forecast starting from 00 UTC 20<sup>th</sup> July 2001.

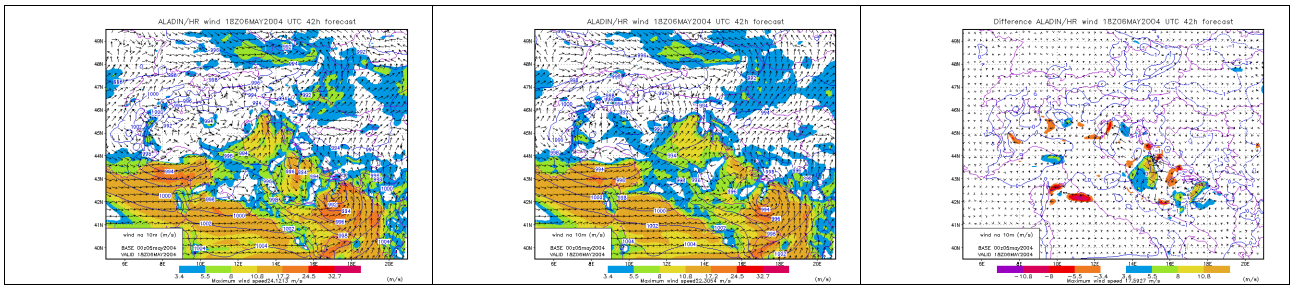


Figure 2. Mean-sea-level pressure and 10 m wind obtained with classical numerical diffusion (left), semi-Lagrangian horizontal diffusion (center) and their difference (right), 42 hour forecast starting from 00 UTC 5<sup>th</sup> May 2004.

### x Twin cyclones

24th January 2005, 00 UTC run produces twin cyclones, one above Tyrrhenian Sea and one in the Adriatic. The depth of the Tyrrhenian Sea cyclone was overestimated. Using SLHD, Tyrrhenian cyclone weakened and moved southwest while the Adriatic cyclone shifts inland.

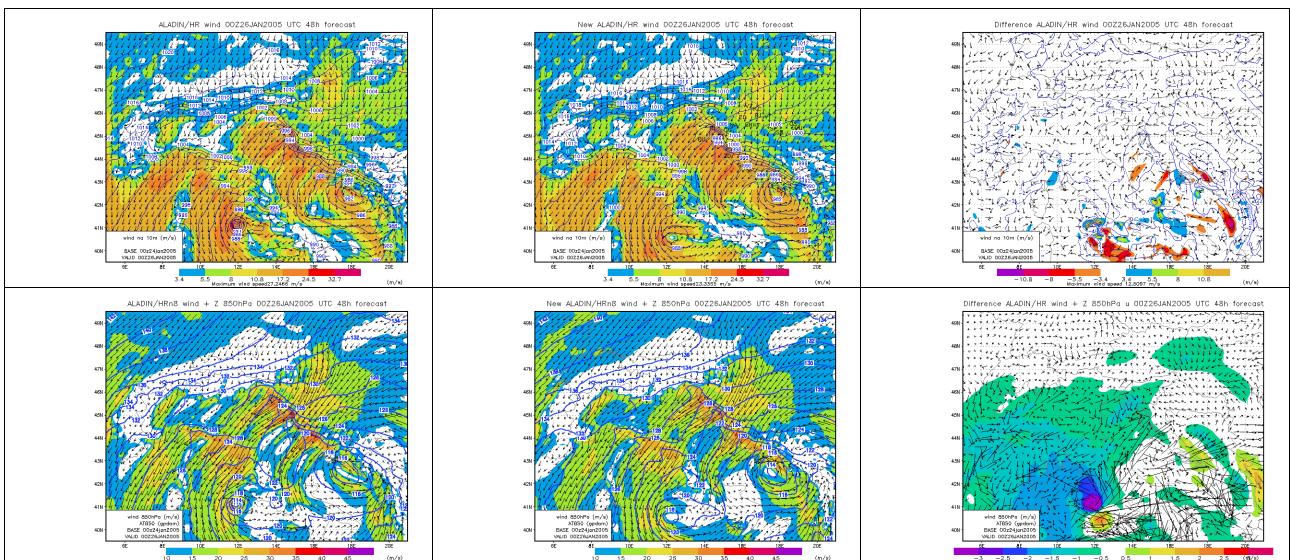


Figure 3. 10m wind and mean-sea-level pressure (top row) wind and geopotential at 850hPa (bottom row) obtained with numerical diffusion (left), SLHD (centre) and their difference (right), 48 hour forecast starting from 00 UTC 24th January 2005.

The results vary significantly depending on the type of the horizontal diffusion used in the coupling model. When the SLHD run is coupled to a purely numerical diffusion run, the Tyrrhenian Sea cyclone is much weaker.

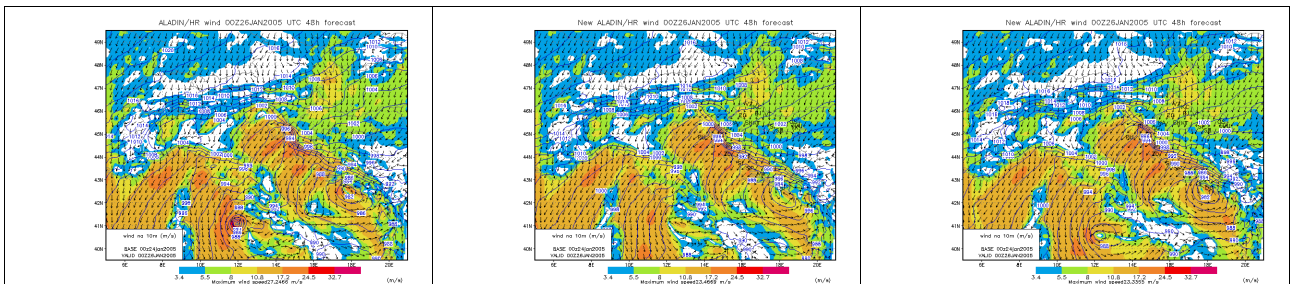


Figure 4. 10m wind numerical coupled to numerical diffusion (left), SLHD coupled to numerical diffusion (centre) and SLHD coupled to SLHD (right), 48 hour forecast starting from 00 UTC 24th January 2005.

### x Fog case

15th February 2004, Central Europe was under an anticyclone and most of the valleys were covered by fog. SLHD increases the amount of fog in Alpine valleys (border between Switzerland and Germany, and in Danube valley in Austria) since it reduces mixing between valleys and the air above.

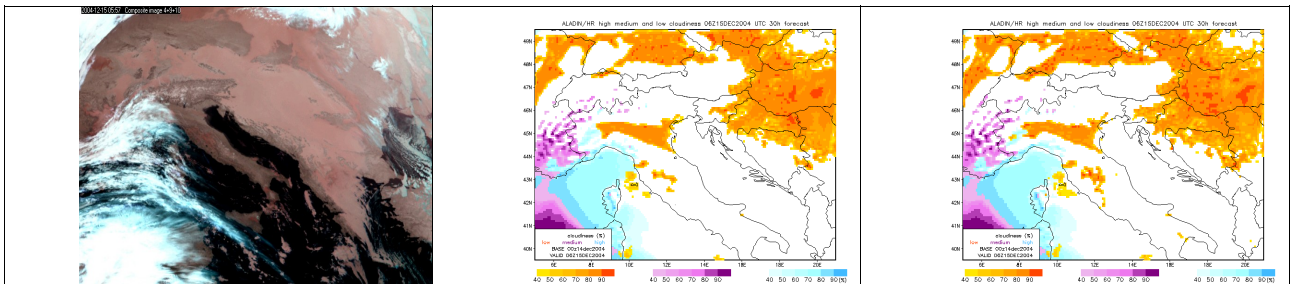


Figure 5. On the left is the Meteosat-8 RGB composite of channels 3.9, 10.8 and 12.0  $\mu\text{m}$  for December 15th 2004, 06 UTC. Low, medium and high cloudiness, numerical diffusion (centre) and SLHD (right), 30 hour forecast starting from 00 UTC 14th December 2004.

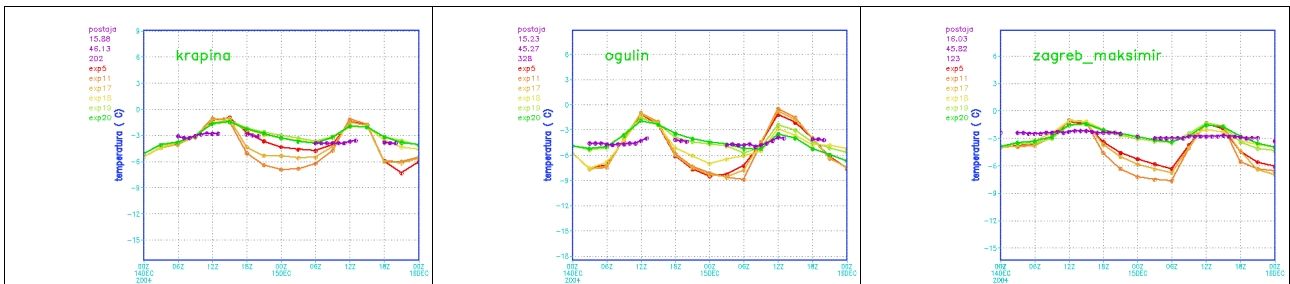


Figure 6. Comparison of the modelled 2m temperature evolution for 00 UTC run on 14th December 2004 with measured data from synoptic station (5-reference, 11-NER, 17-LRAUTOEV, 18-SLHD, 19-mean orography, 20-SLHD+mean orography).

### 5.9.5. Conclusions

Semi-Lagrangian Horizontal Diffusion (SLHD) shows beneficial impact on the reduction of the overestimated cyclone intensity, corrects the cyclone position while not altering a good intensity prediction and improves fog forecast in the valleys in an anticyclone.

## **5.10. High-resolution wind climatology from ERA-40: *M. Žagar, N. Žagar, J. Cedilnik, G. Gregorič, J. Rakovec.***

### **5.10.1. Summary**

The ALADIN model was used for downscaling of the ECMWF 40-years re-analysis dataset with a goal to produce a high-resolution wind climatology for Slovenia. In this paper results are presented concerning the quality of the obtained climatology. Overall, the downscaled wind climatology is regarded as useful. Characteristics of the observed wind climatology often appear to be controlled by terrain features of smaller scales than the resolution of the finest ALADIN configuration used, 2.5 km. Additionally, an investigation of the model's spectra in the temporal domain has been performed for various ALADIN configurations and compared to the observations. The investigation of the spectral power distribution has revealed that the applied 10 km ALADIN cannot realistically represent the sub-diurnal part of the spectrum in a complex terrain such as Slovenia.

### **5.10.2. Introduction**

The ECMWF 40 year re-analysis project (ERA-40) resulted in a consistent data-set of a climatologically meaningful length. Its horizontal resolution of one degree is, however, only sufficient for large-scale analyses. Downscaling methods have to be applied to produce higher resolution data containing the response of the large-scale flow to the local topography. This applies especially to the regions with complex topography as for example Slovenia. The ERA-40's predecessor, ERA-15, was previously used by Heimann (2001) to produce a wind climatology over the large Alpine area.

Our goal was to design, construct and evaluate the downscaling for the purpose of wind and precipitation climatology at a kilometre scale. Such a high-resolution climatology finds many applications, like road construction, pollution prevention, agrometeorological planning and not least the wind-energy harvest.

In this paper, we are presenting our approach, set-up of the simulations and the results in terms of 2.5km wind climatology. Additionally, we conducted research on the influence of the nesting strategy to the quality of the downscaled wind fields through comparison with local observations. Here not only the standard statistics is computed but we have also attempted to get a deeper insight into the model's ability to represent the mesoscale flow features. This is achieved by comparing modelled and observed energy spectra in the frequency domain. In this way we also assess stations' suitability for verification purposes, related to forthcoming evaluations of climate simulations and future climate scenarios.

### **5.10.3. The method**

ALADIN is a well-suited limited-area model for downscaling the ERA-40 data. The driving ERA-40 data provide synoptic-scale forcing through the lateral boundary conditions. Various surface forcings, coupled with a high-resolution dynamics in ALADIN provide the mesoscale flow features we are interested in.

The ERA-40 data resides on MARS archiving server at the ECMWF. Ten years of data at 6 hour intervals were retrieved and downloaded onto our local archiving server. These data were then used as an input to the IFS/ARPEGE configuration 901. The resulting ARPEGE global fields were then interpolated onto the mesoscale grid using configuration e927. The original design of our downscaling experiment, from which the actual wind climatology was obtained, was such that the resolution of this mesoscale grid was 30 km and the domain covered most of Europe (EU0 in Fig. 1). Following results of earlier studies (e.g. Qian et al., 2003) showing that for regional climate modelling reinitializing the model at certain frequency is advantageous over a continuous run, we chose to reinitialize the model every 2 days. The 10-year period 1991-2000 was broken into 60 hours long integrations with 12 hour overlap and ostracised the first 12 hours of each run. A 10 km nest was used next in the same fashion, initialized from and coupled with the 30 km run. Finally a

2.5 km dynamical adaptation for the wind field only (Žagar and Rakovec, 1999) was carried out on the 10 km fields every 3 hours. Obviously the kilometric scale has not been reached yet using ALADIN only. Dynamical adaptation to kilometre scale has not yet been tried because the required high resolution topographic database has not yet been constructed. Instead, we took an alternative path of a purely kinematic method, where the divergence of the wind field was minimised through iterations, controlled by only a few parameters, describing the atmosphere's resistance to vertical displacement. The Aiolos model (Focken et al., 1999) was used for this purpose. Some results of this model are shown to illustrate (im)possible improvement of dynamical modelling by a simplistic kinematic approach.

We have furthermore investigated the importance of the nesting strategy of ALADIN to ERA-40. For this purpose, we defined two additional domains, shown in Fig. 1. One is denoted EU1 and it includes 188x188 points at 10-km spacing while the second domain, denoted ALPS, contains 104x68 points at the same resolution as EU1. In this way the model results over Slovenia in these two simulations differ only in the distance from the lateral boundaries. In other words, the model tendency to develop its own solution should be better seen in the results of EU1, as opposed to strong controlling effect of the large-scale model due to vicinity of the lateral boundaries in ALPS. Besides standard statistical scores, we investigated the distribution of the spectral over temporal scales in different set-ups and compared it with these derived from observations.

#### 5.10.4. Results

##### x Average quantities

For comparing different model set-ups with observations we chose to present here six locations around Slovenia: Portorož, situated at an airport some two kilometres from the flat coast, Bilje near the exit of a valley at the pre-alpine transition, Murska Sobota in a flat land near the border with Hungary, Brnik airport at the northern edge of the Ljubljana basin, an exposed location Rogla, at the top of a 1500 m high wooded mountain, and Kredarica, located at a 2515 m high mountain observatory, partly shielded from north and west.

Figures 2-3 show the results of downscaling in three described configurations, ALADIN at 10 and 2.5 km and with a kinematic model, against the observed equivalent. It can be noted that the average wind power “punishes” model errors even more than the RMSE score, but also that the modelled average power can show reverse signal regarding the quality than that of the average speed. Not surprisingly the 10-km ALADIN performs well where the main topographic features affecting the flow (coast, flatland) are sufficiently well described at that horizontal resolution. Results are significantly improved when a higher resolution, 2.5km orography, is incorporated (e.g. at the mountainous stations). On the other hand, results of a kinematic model turned out to be rather difficult to interpret.

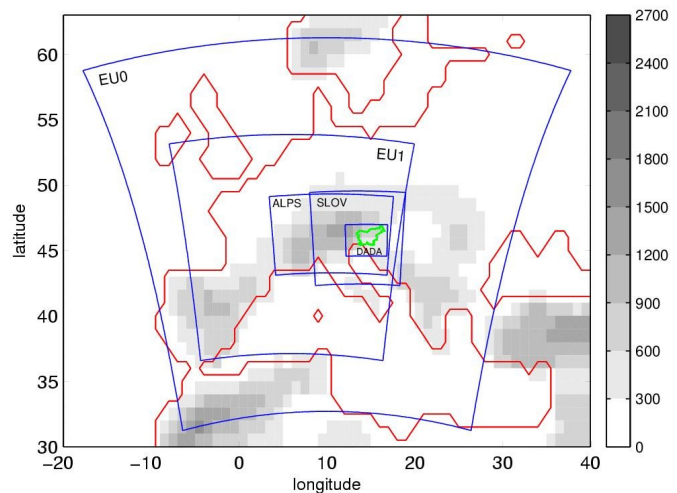


Figure 1. Geographical domains of different ALADIN setups, used for the climatology and the sensitivity studies.

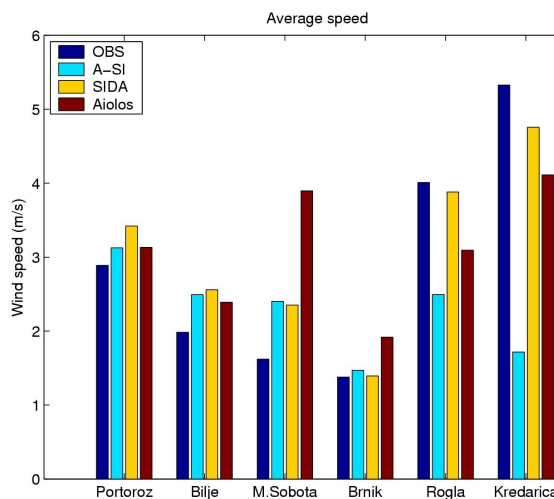


Figure 2: Comparison of the modelled wind speed to the observed one, at six stations.

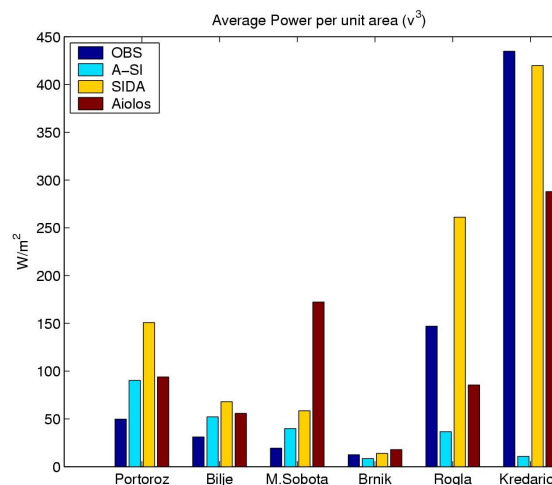


Figure 3: Average wind power (third momentum of the speed divided by the air density).

### x Energy spectra

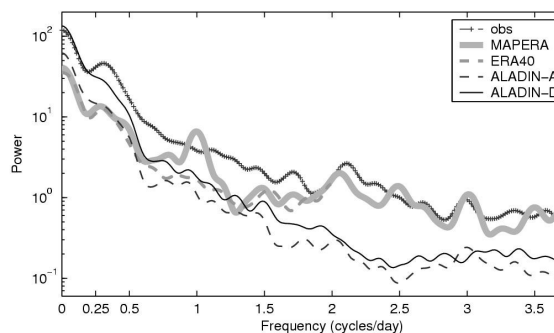


Figure 4: Modelled and observed spectra for the zonal wind component at Rogla.

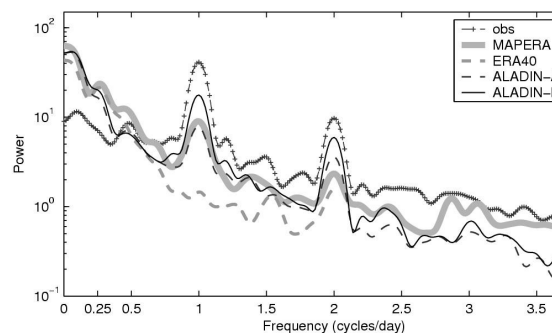


Figure 5: As Fig. 5 but for Portorož.

The spectral energy distribution in various temporal ranges (sub-diurnal, diurnal and longer-than-diurnal periods) should be as close as possible to the observed distribution. Figures 4-5 show the distribution in the temporal domain for two different locations, a mountainous one, Rogla (Fig. 5), and one at the coast, Portorož (Fig. 6). Domain ALADIN-ALPS was designed to include only the Alpine region and it is the smallest domain tested for downscaling. The dynamical adaptation nest (DADA) is driven by the ALPS simulation. Another included curve, denoted MAPERA, represents the best possible estimation of the observed state using the ECMWF re-analysis system during the MAP period (September-November 1999), for which comparison has been performed. The ALADIN spectra show that the model underestimates the spectral power in short temporal scales at Rogla. At Portorož, on the other hand, the model proves its capability to reproduce the diurnal and semi-diurnal peaks, related to the sea- and land-breeze circulation, especially after downscaling from 10 to 2.5 km. The underestimation of the subdiurnal power range is particularly noticed at the stations located in basins and lowlands (not shown). This remains to be further investigated.

### 5.10.5. References

Focken, U., Heinemann, D. and Waldl, H.-P., 1999: Wind Assessment in Complex Terrain with the Numeric Model AIOLOS - Implementation of the Influence of Roughness Changes and Stability, *Proceedings of the European Wind Energy Conference*, Nice, France, 01.-05.03.1999, 1173-1176

- Heimann, D., 2001: A Model-Based Wind Climatology of the Eastern Adriatic Coast. *Meteorol. Z.*, **10**, 5-16
- Qian, J.-H., Seth, A. and Zebiak, S., 2003: Reinitialized Versus Continuous Simulations for Regional Climate Downscaling. *Mon. Wea. Rev.*, **131**, 2857-2874
- Žagar, M. and Rakovec, J., 1999: Small-scale Surface Wind Prediction using Dynamic Adaptation. *Tellus*, **51**, 489-504.
- Žagar, N., Žagar, M., Cedilnik, J., Gregorič, G. and Rakovec, J., 2005: Dynamical Downscaling of ERA-40 for the Wind Climatology in the Mountainous Terrain. *Tellus A*, *under revision*.

## 5.11. Latent heat nudging: *J. Cedilnik*.

### 5.11.1. Summary

Latent heat nudging (LHN) is a method of forcing a NWP model with measured precipitation rates from radars. The aim is to improve analysis and short-range forecast of precipitations. The general idea of the scheme is to rescale the vertical profiles of latent heating using the ratio of observed and modelled precipitations. LHN is operationally used at the German and UK meteorological services.

A description of such a scheme applied in ALADIN is presented in this paper. The technique has generally a very small positive impact on model forecasts, which seems to last up to a few hours ahead.

### 5.11.2. Latent Heat Nudging procedure

LHN is a procedure where radar measured precipitation rates are used to modify latent heat profiles in the model. Model and measured precipitation rates are used to compute a weighted average according to distance from measurement point to radar. In such a manner a weighted value of precipitation rate is obtained. This weighted average may somehow be treated as precipitation analysis. For grid points far from radar, only the model value is used and closer to radar more stress is put on measured value and less on model. In our case there were three radars used: Fossalon (Italy), Kirbitzkögel (Austria) and Lisca (Slovenia). Weights for computing weighted precipitation values were computed according to the distance from the closest operational radar at the given time (at the time of nudging). The distances from all radars for the points in the model domain can be seen in Figure 1.

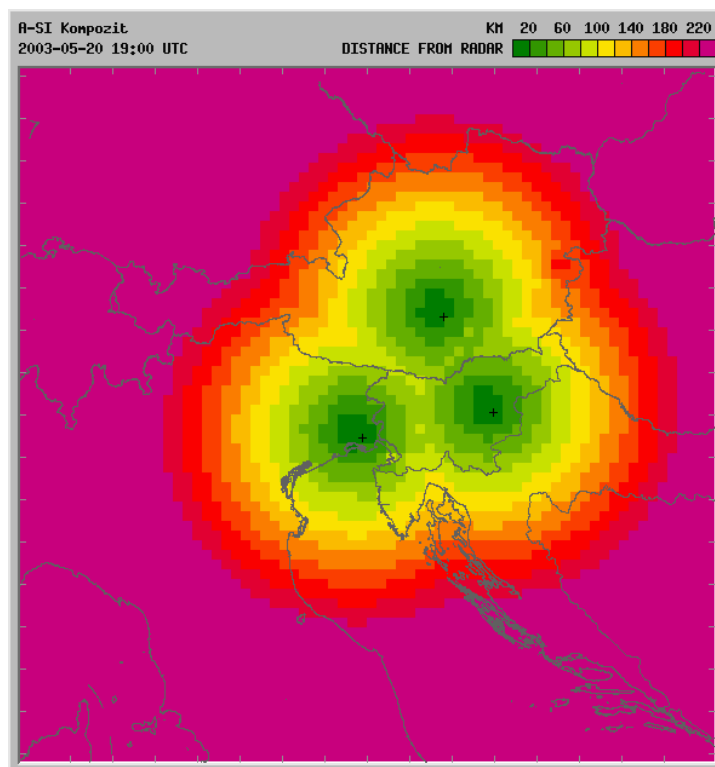


Figure 1 : Distances from three radars in the model domain area. These distances are used to compute weighted values of precipitation rate. The weights fall to zero at a distance of 120 km from the closest radar. In case of precipitation detected by more than one radar, only the value of the closest radar is used.

Radar measured hourly precipitation rates are interpolated in an eight times denser grid than the one used by the model and afterwards aggregated onto the model grid. The distance between two neighbouring grid points in the model grid is 11 km. In case of more radars detecting precipitation at the same grid point, the closest radar is used for computation of the weighted value. Such a

weighted value is then used to modify model heating rate profile due to latent heat release.

As mentioned, hourly radar precipitation fields were used as input data for LHN. The fields used at different time-steps in the model were linearly interpolated between two adjacent measurements, in the very same way as coupling fields on the boundaries are interpolated in time.

The value of the weighted average of precipitation rate is:

$$RR_{analysis} = w.RR_{radar} + (1-w).RR_{model} ,$$

where  $w$  is a weight depending on the distance from a radar (shown in Figure 1).

The model heating or cooling profile due to precipitation latent heat release is rescaled by the value obtained with weighted averaging of model and measured precipitation rates (as is described in the expression above). This is done by directly rescaling the temperature tendency profile, but only that part which is connected to latent heat cooling or heating. This is described by next relation:

$$\frac{\partial T}{\partial t}_{LHN} = \frac{\partial T}{\partial t}_{model} \cdot \frac{RR_{analysis}}{RR_{model}}$$

This works fine in cases when there exists precipitation in the model and there is precipitation detected by the radar in the same grid box.

However, in case when only the model is exhibiting precipitation and there is no precipitation detected by any of the radars, the heating rate profile in the model is set to zero.

In a reverse case, when the model is not producing any precipitation and some is detected by a radar, there are generally two possibilities. Either an idealized profile could be used or (as is done in our case) a climatological profile is applied. These profiles were derived from a one year control run of the same model without any precipitation assimilation procedure. Climatological profiles for four representative months are shown in Figure 2. Such a climatological profile is rescaled according to observed precipitation rate before it is applied in the model.

In general, there are two possible uses of LHN technique. One can be to use nudging for hindcasting with the aim of obtaining the best possible precipitation analysis. The more forecast-oriented usage is for nowcasting and very short range forecasting. In a hypothetical situation, a forecaster would, say at 12 UTC (after some precipitation had already occurred), rerun the ALADIN morning run using LHN till 12 UTC and see the impact. After the LHN period, the model is left as it was.

Another way of looking at this is that LHN is a simple initialization of precipitation which could provide a positive impact on scores up to some hours ahead.

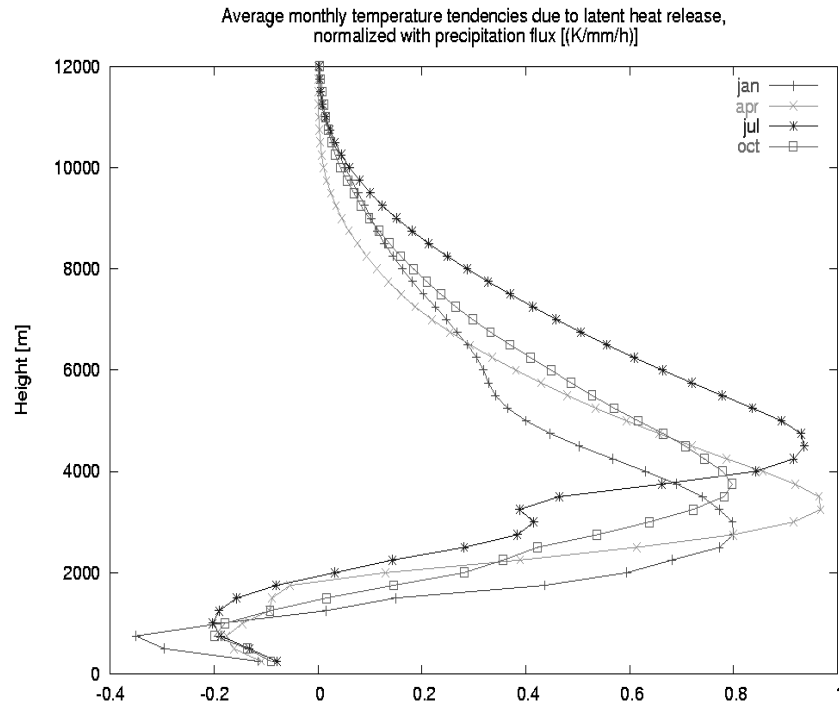


Figure 2 : Averaged monthly heating rate profiles due to latent heat release for 4 different months. These profiles were used as climatological profiles in case of no model precipitation (after being rescaled according to measured precipitation rate).

### 5.11.3. Validation - cases

The assimilation chain was applied to daily model runs throughout year 2002. Year 2002 was warmer than the 1961-1990 average (as is appropriate for climate trends). Precipitation amount in the western and southern parts of Slovenia (which receive more precipitation due to proximity of the coast and orography features) was greater than average. On the other hand there was less than average precipitation in the eastern part (where precipitation depends more on large-scale processes). This makes year 2002 a suitable choice for tests of LHN.

Results show that LHN may successfully replace typical precipitation patterns that occur in ALADIN (exaggeration of precipitation on the mountain ridges, also due to envelope orography). Such a case of successful use of LHN is presented in Figures 3 and 4. In Figure 3, LHN is applied as in a "climatological" sense (meaning that we are also using radar data, that is yet to be measured from model time point of view), whilst in Figure 4, LHN was only active up to +5 hours of forecast.

However, there are also many cases of deterioration of the forecast. This is especially true in cases when there is less precipitation measured by the radar than there is in the model, but the positioning might be alright. LHN tries to reduce the amount by repositioning the excessive amount of precipitation, but by doing this, it deteriorates the forecast. Figure 5 shows such an example from September 22, 2002. Even when applying LHN till +18 hours of integration time (18 UTC) (Figure 6) (in "climatological" or hindcast mode), the model still wrongly repositions the precipitation amount.

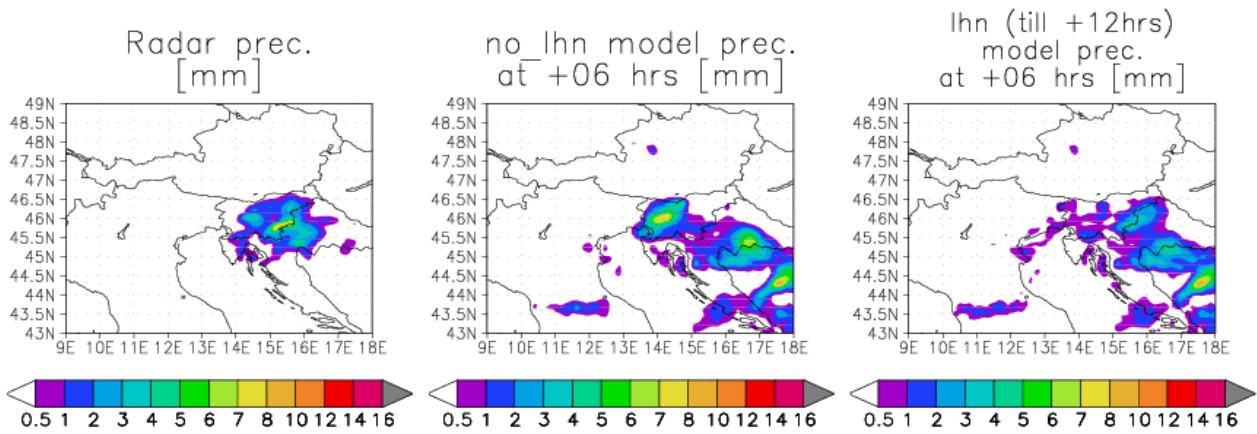


Figure 3 : Hourly accumulations of precipitation between 6 and 5 hours UTC for October 24, 2002. Left figure shows interpolated radar image (combination of three radars), the middle one shows the results of model control run (without LHN) and the image to the right is the LHN run, where nudging was performed till +12 hours of forecast (model was initialised at 00 UTC).

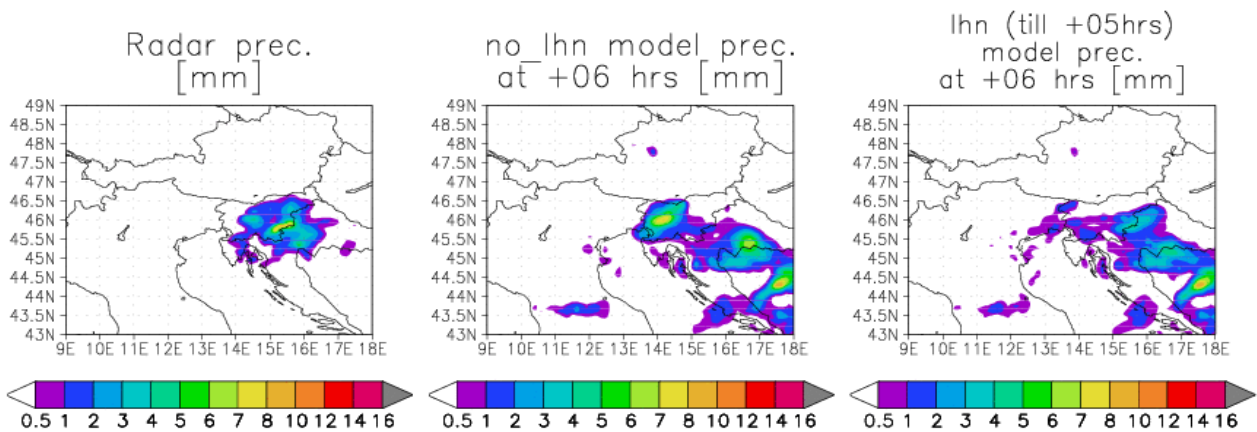


Figure 4 : Same as Figure 3, except that the LHN procedure stops at 5 hours UTC (+5hours of forecast).

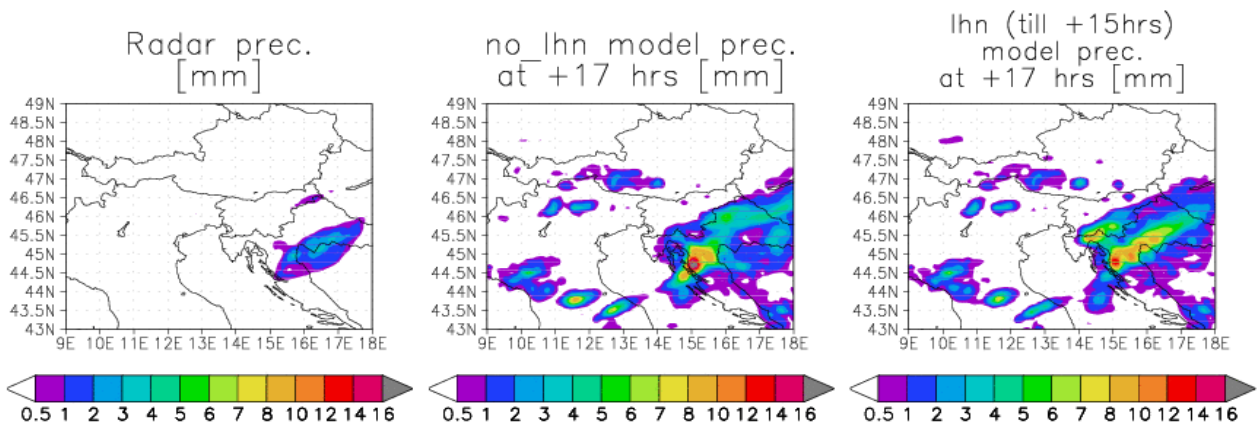


Figure 5 : Same as Figure 3, but for case on September 22, 2002, where nudging procedure was used till +15 hours (15 UTC). The hourly precipitation accumulation shown is between 17 and 16 UTC.

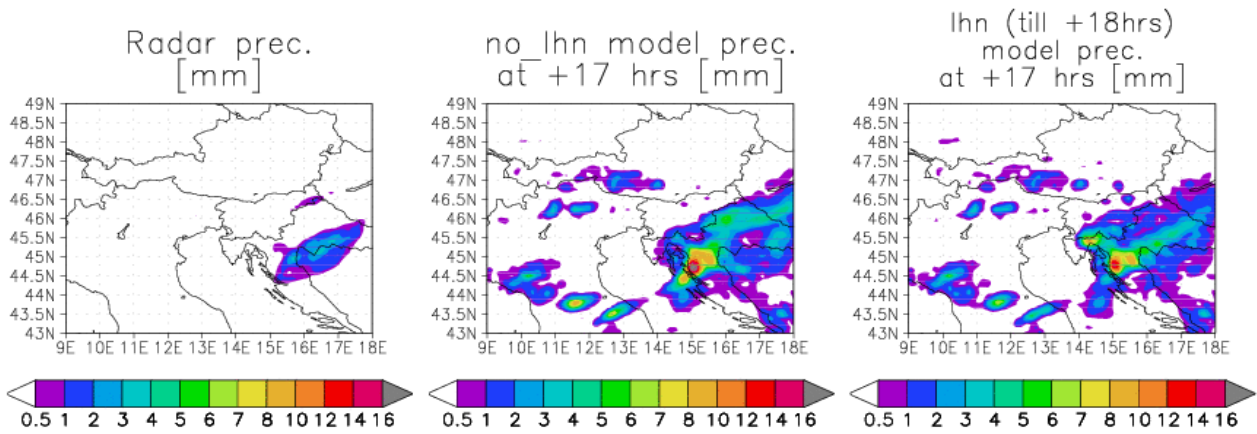


Figure 6 : Same as Figure 5, where nudging procedure was used till +18 hours (18 UTC). The hourly precipitation accumulation shown is between 17 and 16 UTC.

#### 5.11.4. Validation - scores

Calculation of average scores (e.g. equitable threat score) is very dependent on the threshold used for computing the scores.

When selecting a high threshold (1mm/h), the results for the first few hours after the end of the nudging process are slightly positive (Figure 7), but when using a 0.1 mm/h threshold the impact of LHN is even negative (Figure 8). This statistical verification was performed on the whole year of data (2002). Rain gauge measurements were used for that purpose. The model was initialised every day at 00 UTC and LHN was performed till +12 hours of forecast.

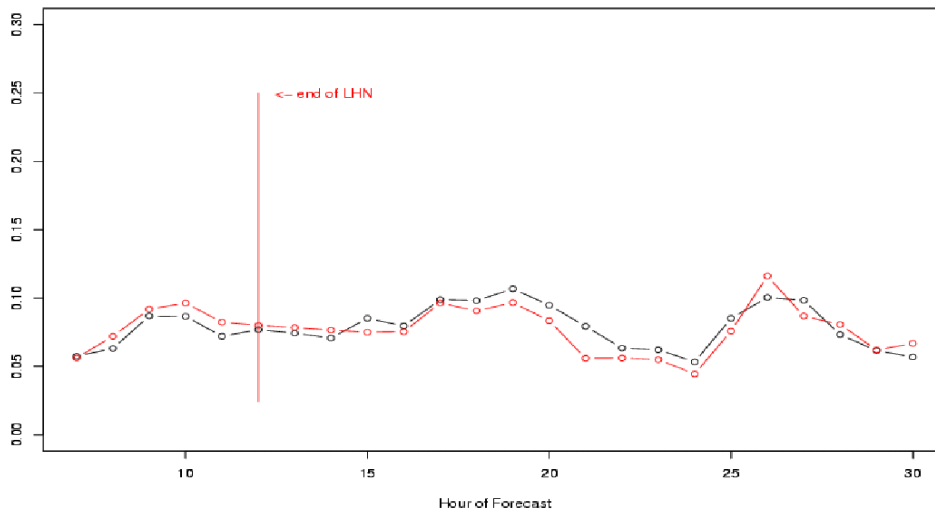


Figure 7 : Equitable threat score for 1 mm/h threshold for entire year 2002. The red line is with LHN, the black one without. The nudging was switched on till +12 hours.

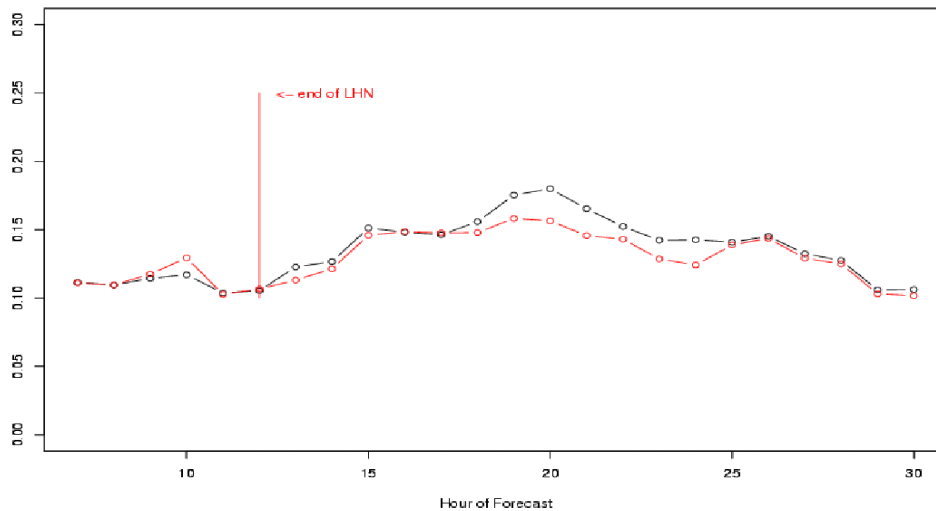


Figure 8 : Same as Figure 7, but for 0.1mm/h threshold.

### 5.11.5. Conclusion

After performing one year of experiments with LHN, we can conclude that there are some rather neutral impacts on precipitation forecast when using LHN.

It seems that LHN can be very strong in repositioning of the spatial pattern of precipitation (but not necessarily correctly). The impact of LHN occurs, when model is producing too much precipitation. In such a case, LHN is not capable of substantially reducing the amount, but is rather trying to move it around. We could say that LHN works better when rain is present in the model and detected by radar than in case when the radar shows (almost) nothing but there is a tendency for (convective) precipitation in the model.

This is confirmed by statistical scores results, where LHN is better with a higher threshold (when computing equitable threat score).

One might assume that LHN is not very suitable for convective processes since they are not resolved at this scale and thus using LHN with a higher resolution model would be much more beneficial. According to the German colleagues (via personal communication at the Bratislava June 2005 ALADIN workshop) the results of LHN are vastly improved when using prognostic cloud water, which is of course not the case in this experiment. They (the German meteorological service) are also using a much more sophisticated LHN technique, where they apply nudging only at the stage of cloud growth.

Another issue is that our domain was not adequately covered by radar observations. This radar "network" of three radars can not really compare to the one of DWD or UK Meteorological Office. The problem of such a small area of domain covered by radars is that the faster moving systems are only for a very brief time subjected to nudging.

## 5.12. ALADIN NORAF paralle suite based on 3D-VAR assimilation technique. Zahra SAHLAOU.

### 5.12.1. Data assimilation in the Moroccan numerical prediction model.

Morocco is among the pioneers in the ALADIN consortium who use data assimilation in a limited area model. It was valid for the ALBACHIR model and we try to keep the same interest for data assimilation methods with the ALADIN NORAF model. An optimal interpolation analysis (called CANARI) was used in the operational suite. Observations are provided by the local observation data base. However, the lack of a good conventional observation coverage directs us to the use of satellite observations. In this context, 3D-VAR seems to be a more appropriate data assimilation method than CANARI. Research work was carried out in this direction and finalized in a parallel suite with 3D-VAR data assimilation.

### 5.12.2. Description of the parallel suite.

The operational suite is described in the previous N27 ALADIN Newsletter.

Since November 2004, a parallel suite for ALADIN NORAF, based on 3D-VAR data assimilation technique, is running in Casablanca too. Four daily updates towards observations are performed at (00UTC, 06UTC, 12UTC, 18UTC) with an assimilation window of 6hours (long cut-off). A production run is performed once a day at 00UTC (called rAN). Observations used in this run are from a time window of 4.5 hours (short cut-off). Analysis steps are presented in figure 1.

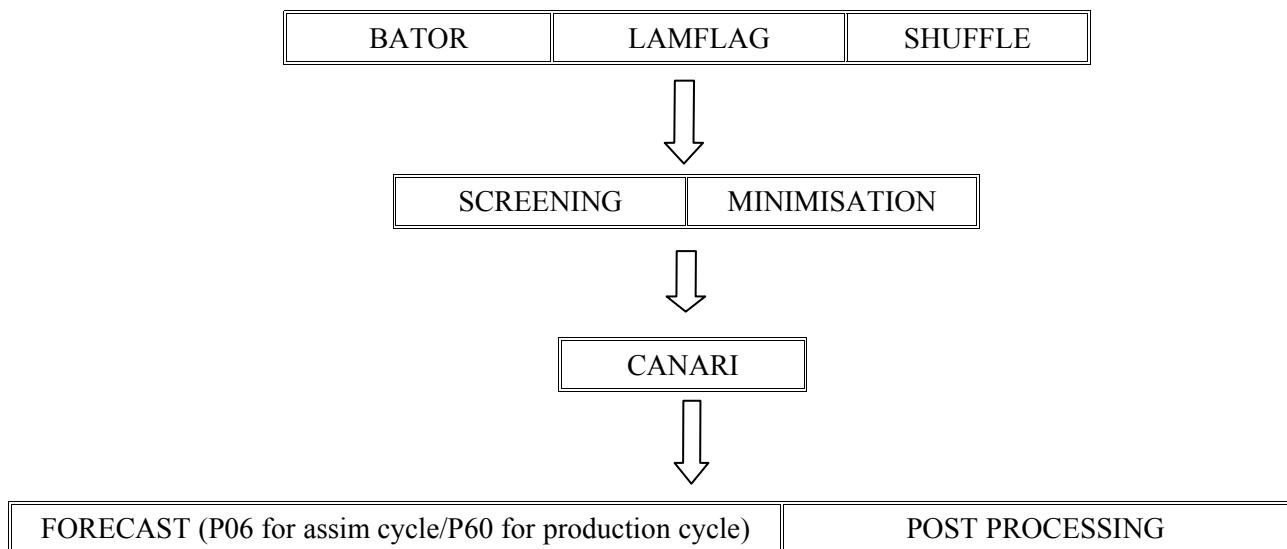


Figure 1. Steps of the parallel suite

Observation preparation : the ascii file of observations, provided by the local data base, is converted to ODB form by the script BATOR. Then LAMFLAG chooses observations inside of the model area and gives them a flag. SHUFFLE selects the flagged observations and splits the data base on many pools.

Upper air analysis: the observation control is performed by the screening to select observations in consistence with each other and with the guess. After this selection, we proceed to the minimisation of the cost function measuring the distance between observations and model.

Surface analysis: the surface analysis is done with an optimal interpolation method called

CANARI. The guess is the upper air analysis. The model fields produced by this step are the initial state for the forecast process.

As is shown in figure 1, the analysis is followed by an integration of the model. Forecast range is 6 hours for the assimilation cycle, to provide the guess for the next analysis. The production cycle has a forecast range of 60 hours.

### 5.12.3. Validation

Scores don't show a great impact of 3D-VAR compared to dynamical adaptation (4D-VAR ARPEGE analysis interpolated to the ALADIN grid). This is a result of the poor observation cover over the NORAF domain (see table below). Most of these observations are located in the northern part of the domain, a large part of which covers the Atlantic Ocean and the Sahara.

Observation type	rAN	r00	r06	r12	r18
SYNOP	667	707	827	964	798
AIREP	143	196	1114	1271	1127
SATOB	296	296	303	379	149
DRIBU	45	181	124	135	155
TEMP	37	37	7	37	6

TABLE 1. Observation statistics over the ALADIN-NORAF domain (2005-08-12)

Because of their high spatial resolution and temporal frequency, satellite data should be very useful and will be a good complement for conventional observation systems. A case study shows that AMSU-A<sup>1</sup> radiances from ATOVS have positive impact on temperature and geopotential forecasts.

Differences of bias (vs ARPEGE analysis) between simulation with and without AMSU-A radiances are shown in figure 2.

We can see a positive impact on the temperature field over the Sahara and an other positive centre over Atlantic Ocean in front of western African coasts.

Regarding the geopotential field, there is a large reduction of forecast bias (12 mgp) due to the assimilation of AMSU-A data.

The injection of AMSU-A raw radiances in the assimilation system have also an impact on humidity forecast (not shown). In fact, the tropical moisture is better simulated, whereas there is an overestimation of the humidity over Portuguese western coasts associated to a synoptic perturbation.

More OSE<sup>2</sup> experiments should be realised to better understand the effect of satellite data on the model performance, but we can already suggest that AMSU-A raw radiances seem to be beneficial over areas where there is a lack of conventional observations (ocean and Sahara).

Concerning surface analysis, a study was realised to qualify the impact of CANARI. Results (see figure 3) show that for both cycles with and without CANARI for surface analysis, the forecast scores are very similar. So it was concluded that the step of surface analysis could be avoided (reduce the computation time) without real harm to the forecast quality.

1 ATOVS Microwave Sounder Unit-A

2 Observing System Experiment

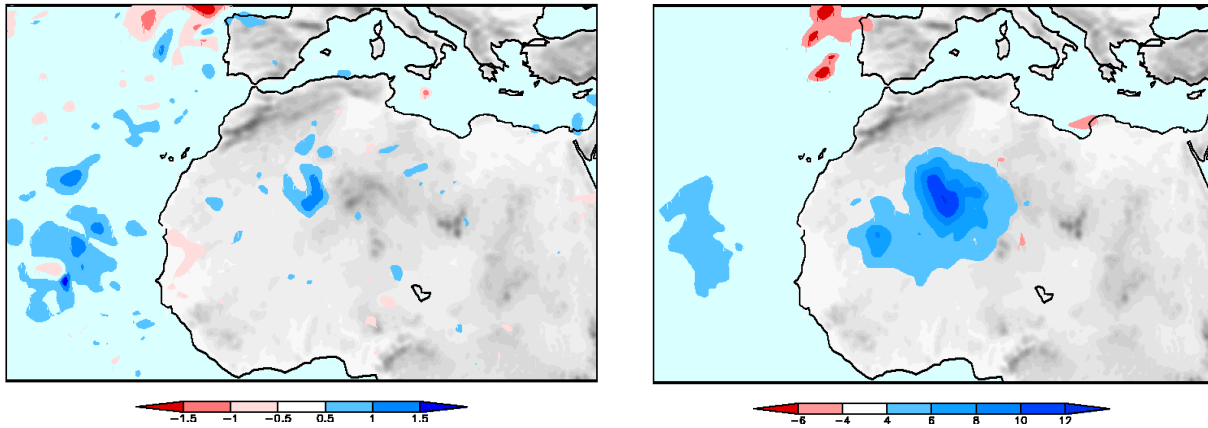


Figure 2. 24 hour forecast scores for temperature (left) and geopotential (right) at 700hPa level. Blue areas mean positive impact and red ones correspond to negative impact

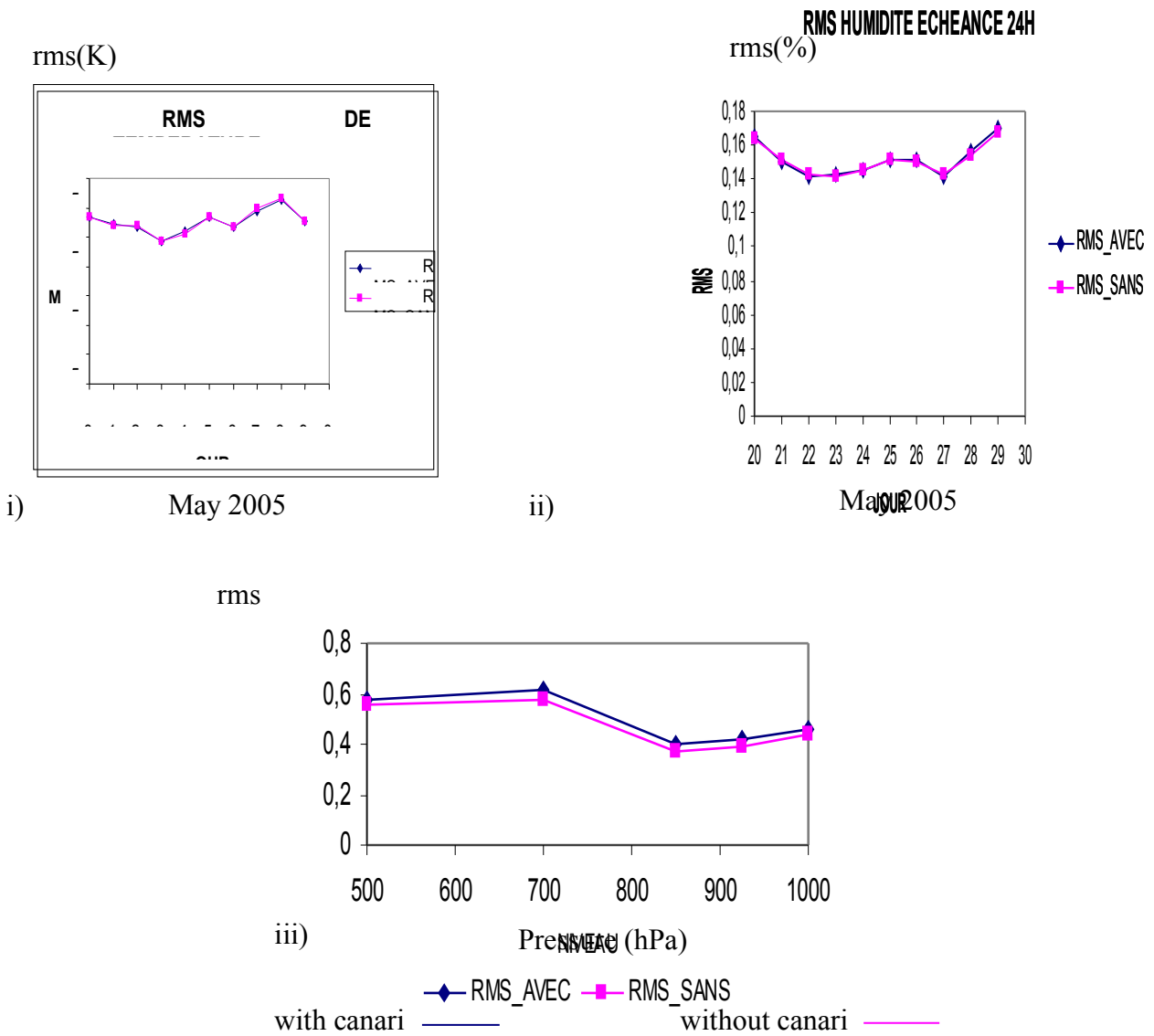


Figure 3. Temporal evolution of root mean square error (rms) of 24 forecast for i)T2m and ii)HU2m versus synoptic observations and iii)vertical profile of geopotential rms versus ARPEGE analysis. Blue line for experiment with CANARI and red line for experiment without CANARI

#### **5.12.4. Conclusions and future work**

The 3D-VAR parallel suite is the achievement of an earlier work on variational data assimilation methods for LAM models. Before a 3D-VAR operational suite, more tests and validations should be performed.

First, we need to carry out more OSE experiments with radiances (AMSU-A, AMSU-B, SSML...). Running 3D-VAR without satellite data will just cost more with no real improvement on model quality.

On the other hand, there are some on going studies about the background error covariance matrix (f-plane, ensemble-based Jb). The most appropriate method will be chosen for the operational suite.

Some of ALADIN countries use a blending technique to create the initial state for the model. In ALADIN NORAF, it is planned to use the blended field as a guess for 3D-VAR analysis. This method is called blendvar and preliminary studies shows that this will be beneficial.

#### **5.12.5. References**

- Hdidou.F, Sahlaoui.Z, 2004 : WMO Progress Report on Numerical Weather Prediction 2003.  
Rajel, Tilioui, Hdidou.F, Sahlaoui.Z , 2005 : Analyse de surface dans ALADIN NORAF. Internal report.

## 6. PUBLICATIONS

**6.1. Haiden T. and C. D. Whiteman: Katabatic Flow Mechanisms on a Low-Angle Slope: Vol. 44, No. 1, pp. 113–126. Journal of Applied Meteorology. <http://www.ametsoc.org>**

### ABSTRACT

Momentum and heat budget equations for katabatic flows on sloping surfaces are revisited. Terms in these equations are evaluated using wind and potential temperature data from four tethered-balloon data collection systems on a 3-km line running down a 1.6° slope at the foot of the Oquirrh Mountains in Utah's Great Salt Lake valley. The analyses focus on the development with downslope distance of the katabatic flow and the associated negatively buoyant layer under synoptically undisturbed conditions. With strong ambient stratification, the katabatic flow shows little variation between sites, suggesting a state close to local equilibrium. When the ambient stratification is weaker, the acceleration of the katabatic flow between two tethered sites is systematically larger than what would be predicted based on observed buoyancy. Comparison of observed flow direction with the local topographic gradient indicates that slope curvature, associated with small deviations from the basically planar slope, may be responsible for the anomalous increase. It is concluded that the cross-slope homogeneity of the flow, which is assumed in simplified katabatic flow models, may be significantly disturbed even on slopes that appear to be planar to the observer.

**6.2. Whiteman C. D., T. Haiden, B. Pospichal, S. Eisenbach, and R. Steinacker: Minimum Temperatures, Diurnal Temperature Ranges, and Temperature Inversions in Limestone Sinkholes of Different Sizes and Shapes: Vol. 43, No.8, pp. 1224–1236. Journal of Applied Meteorology. <http://www.ametsoc.org>**

### ABSTRACT

Air temperature data from five enclosed limestone sinkholes of various sizes and shapes on the Hetzkogel Plateau near Lunz, Austria (1300 m MSL), have been analyzed to determine the effect of sinkhole geometry on temperature minima, diurnal temperature ranges, temperature inversion strengths, and vertical temperature gradients. Data were analyzed for a non-snow-covered October night and for a snow-covered December night when the temperature fell as low as -28.5°C. A surprising finding is that temperatures were similar in two sinkholes with very different drainage areas and depths. A three-layer model was used to show that the sky-view factor is the most important topographic parameter controlling cooling for basins in this size range in near-calm, clear-sky conditions and that the cooling slows when net longwave radiation at the floor of the sinkhole is nearly balanced by the ground heat flux.

**6.3. Guidard V., C. Fischer, M. Nuret and A. Dzedzic:**

Evaluation of the ALADIN 3D-VAR with observations of the MAP campaign. Meteorology and Atmospheric Physics. <http://www.ametsoc.org>

**6.4. Bénard P., J. Masek, and J. Vivoda:**

Stability of Leap-Frog Constant-Coefficients Semi-Implicit Schemes for the Fully Elastic System of Euler Equations. Case with Orography. Mon. Wea. Rev., vol 133, n° 5, pp 1065-1075. <http://www.ametsoc.org>

**6.5. Deckmyn A., and L. Berre:**

A wavelet approach to representing background error covariances in a limited area model. Mon. Wea. Rev., vol 133 n°5 pp 1279-1294 <http://www.ametsoc.org>

**6.6. Pailleux, J. et J.-F. Geleyn:**

La prévision numérique du temps. La Science au présent, édition 2005, Encyclopaedia Universalis, pages 236-247. <http://www.universalis.fr/>, rubrique "La Science au présent".

**6.7. Geleyn J.-F., P. Bénard and R. Fournier:**

An general-purpose extension of the Malkmus band-model average equivalent width to the case of the Voigt line-profile., Q.J.R.M., Vol.13X, pp xxx-xxx. <http://www.royalmetsoc.org/>

**6.8. Fischer C., T. Montmerle, L. Berre, L. Auger and S.E. Stefanescu:**

An overview of the variational assimilation in the ALADIN/France NWP system: (submitted) to Q.J.R.M., <http://www.royalmetsoc.org/>

**6.9. Belo Pereira M. et L. Berre:**

The use of an Ensemble approach to study the Background Error Covariance in a Global NWP Model. (Accepted) Mon. Wea. Rev. <http://www.ametsoc.org>

**6.10. Berre, L., S. E. Sttefanescu and M. Belo Pereira:**

A formal and experimental comparison between an ensemble estimation of limited area model error statistics and two other error simulation methods. Submitted to Tellus. <http://www.blackwellpublishing.com/>

**6.11. Gérard, L. and J.-F. Geleyn:**

Evolution of a subgrid deep convection parameterisation in a Limited Area Model with increasing resolution. Q.J.R.M., Vol. 131 Number 610, July 2005 Part B pp. 2293-2312 . <http://www.royalmetsoc.org>

**6.12. Soci C. , C. Fischer and A. Horanyi:**

Sensitivity of high resolution forecasts using the adjoint technique at the 10 km scale in revision for MWR." <http://www.ametsoc.org>

**6.13. Stefanescu, S. E., L. Berre and M. Belo Pereira:**

The evolution of dispersion spectra and the evaluation of model differences in an ensemble estimation of error statistics for a limited area analysis. Submitted to Mon. Wea. Rev. <http://www.blackwellpublishing.com/>

**6.14. Žagar N., M. Žagar, J. Cedilnik, G. Gregorič and J. Rakovec:**

Dynamical Downscaling of ERA-40 for the Wind Climatology in the Mountainous Terrain. *Tellus A* ,2005, under revision.

